

ECGrecover: a Deep Learning Approach for Electrocardiogram Signal Completion

Alex Lence*

Ahmad Fall*

Federica Granese*

alex.lence@ird.fr

ahmad.fall@ird.fr

federica.granese@ird.fr

UMMISCO, IRD, Sorbonne Université

Bondy, France

Joe-Elie Salem

Vanderbilt University Medical Center

Nashville, USA Clinical Investigation Center Paris-Est,
CIC-1901, INSERM, UNICO-GRECO Cardio-Oncology
Program, Pitié-Salpêtrière University Hospital, Sorbonne
Université
Paris, France
joe-elie.salem@aphp.fr

Blaise Hanczar

IBISC, University Paris-Saclay, University Evry

Evry, France

blaise.hanczar@univ-evry.fr

Jean-Daniel Zucker

Edi Prifti

jean-daniel.zucker@ird.fr

edi.prifti@ird.fr

UMMISCO, IRD, Sorbonne Université, INSERM, Nutrition
et Obésités; systemic approaches, NutriOmique, AP-HP,
Hôpital Pitié-Salpêtrière
Paris, France

ABSTRACT

In this work, we address the challenge of reconstructing the complete 12-lead ECG signal from incomplete parts of it. We focus on two main scenarii: (i) reconstructing missing signal segments within an ECG lead and (ii) recovering missing leads from a single-lead. We propose a model with a U-Net architecture trained on a novel objective function to address the reconstruction problem. This function incorporates both spatial and temporal aspects of the ECG by combining the distance in amplitude between the reconstructed and real signals with the signal trend. Through comprehensive assessments using both a real-life dataset and a publicly accessible one, we demonstrate that the proposed approach consistently outperforms state-of-the-art methods based on generative adversarial networks and a CopyPaste strategy. Our proposed model demonstrates superior performance in standard distortion metrics and preserves critical ECG characteristics, particularly the P, Q, R, S, and T wave coordinates. Two emerging clinical applications emphasize the relevance of our work. The first is the increasing need to digitize paper-stored ECGs for utilization in AI-based applications (automatic annotation and risk-quantification), often limited to digital ECG complete 10s recordings. The second is the widespread use of wearable devices that record ECGs but typically capture only a

small subset of the 12 standard leads. In both cases, a non-negligible amount of information is lost or not recorded, which our approach aims to recover to overcome these limitations.

CCS CONCEPTS

- Applied computing → Bioinformatics;
- Computing methodologies → Artificial intelligence.

KEYWORDS

ECG Data Analytics, Signal Reconstruction, Generative Models, Clinical Application

ACM Reference Format:

Alex Lence, Ahmad Fall, Federica Granese, Blaise Hanczar, Joe-Elie Salem, Jean-Daniel Zucker, and Edi Prifti. 2024. ECGrecover: a Deep Learning Approach for Electrocardiogram Signal Completion. In *Proceedings of ACM Conference (Conference'17)*. ACM, New York, NY, USA, 27 pages. <https://doi.org/XXXXXX.XXXXXXX>

1 INTRODUCTION

An electrocardiogram (ECG) is a diagnostic test broadly used to evaluate cardiac health. It is commonly performed by placing electrodes at specific locations on the patient's body to capture the heart's electrical signals. Each electrode records a distinct waveform. The *thoracic* electrodes (V1-V6) provide specific information about the heart's electrical signals in areas like the right and left ventricles, while the *limb* electrodes (I, II, III, aVR, aVL, aVF) offer insights into the heart's electrical signals in various directions, encompassing left-to-right, superior-to-inferior, and diagonal orientations [18]. Healthcare professionals can effectively diagnose and assess cardiac conditions by leveraging the combined information obtained from thoracic and limb electrodes. Indeed, certain diseases may manifest with varied expressions on an ECG depending on the specific lead

*Equal contributions.

Permission to make digital or hard copies of all or part of this work for personal or classroom use is granted without fee provided that copies are not made or distributed for profit or commercial advantage and that copies bear this notice and the full citation on the first page. Copyrights for components of this work owned by others than the author(s) must be honored. Abstracting with credit is permitted. To copy otherwise, or republish, to post on servers or to redistribute to lists, requires prior specific permission and/or a fee. Request permissions from permissions@acm.org.

Conference'17, July 2017, Washington, DC, USA

© 2024 Copyright held by the owner/author(s). Publication rights licensed to ACM. ACM ISBN 978-x-xxxx-xxxx-x/YY/MM...\$15.00
<https://doi.org/XXXXXX.XXXXXXX>

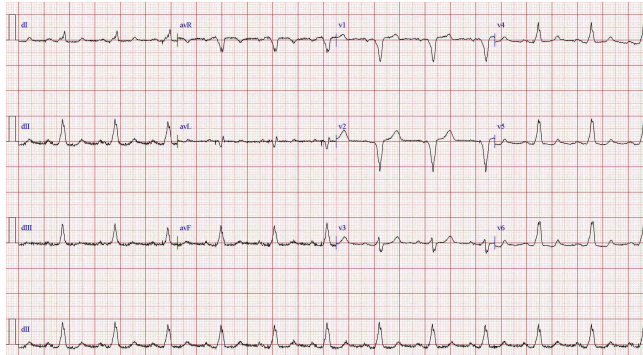


Figure 1: Example of 12-leads ECG recording. The machine has registered 10-second recordings for lead II and 2.5 seconds for the remaining leads (as in C3 in fig. 2).

under examination. For instance, when *myocardial infarction* occurs in the inferior part of the heart, it produces alterations on the ECG signal that are more visible in the leads II, aVF, and III¹.

While a comprehensive diagnosis of potential diseases requires all the leads (in most cases, 12), novel technological advancements have revolutionized how individuals monitor their health. Indeed, ECGs are frequently recorded using wearable devices designed to be worn for longer periods (in contrast with the classical clinical exam, which lasts 10-30 seconds). However, such devices measure only one or several leads in the best cases, e.g., certain smartwatches can record and transmit a single-lead ECG, equivalent to lead I [26].

Moreover, despite the ongoing shift towards AI and automated ECG analyses, many health establishments, particularly in developing countries, still rely on paper to record and store ECGs [28]. This poses obvious accessibility issues and makes computer analyses especially challenging. Indeed, paper-stored ECGs are inherently limited when compared with their raw counterparts. In the most common formats, each lead is only partially represented (i.e., only 2.5 or 5 seconds instead of the usual 10-second signal is printed). Although several tools exist [15] to digitize the ECG stored on paper, they cannot compensate for the missing signal. Relying on a partial signal for a medical assessment can lead to even more catastrophic consequences: intra-lead variability refers to changes within the same lead of the ECG. Specifically, QT alteration involves fluctuations in the duration of the QT interval. Analyzing a longer segment may provide a clearer picture of QT alteration and other subtle changes that might not be as evident in a shorter segment. For instance, conditions such as bradycardia or extra-systoles require practitioners to analyze more than three heartbeats to determine the presence of the pathology. The significance of QT alterations lies in its association with an increased risk of ventricular arrhythmia, including Torsades-de-Pointes (TdP), which can degenerate into potentially life-threatening ventricular fibrillation [6, 19, 23].

Consequently, reconstructing missing portions of an ECG signal, whether it involves an entire lead or part of it, is a challenging task with implications for both the medical field and computer science.

¹<https://ecgwaves.com/topic/localization-localize-myocardial-infarction-ischemia-coronary-artery-occlusion-culprit-stemi/>

To approach this problem comprehensively, we formally define it and address it from two perspectives: *ECG lead-reconstruction* and *ECG segment-recovery*. In ECG lead reconstruction, the objective is to reconstruct the 11 missing leads using the complete trace of one lead. For ECG segment recovery, the goal is to recover the full signal of 10 seconds for all the leads from only partial segments. Our strategy begins by understanding how the partial signal appears in real-life situations. In Figure 1, an example is provided to illustrate what a 12-lead ECG recording looks like when utilized by clinicians. The names of the leads are indicated in blue, while the actual signals are in black. The recordings from the various leads are concatenated according to the standard 4-channels printing format (e.g., starting with lead I, followed by aVR, V1, and V4). Typically, a 10-second recording of lead II or I is also provided. Lastly, the initial one millisecond of each row serves for amplitude calibration. We utilize a masking approach involving specific masks to replicate real-life scenarios like those illustrated in Figure 1. Given a 12-lead ECG input, the masks are functions that return the same signal with a portion of it preserved and the rest replaced with randomly valued signals. For instance, the 4-channels format mentioned before corresponds to the mask C3 in Figure 2, where the portion of the signal retained is highlighted in green and is referred to as the *primer*.

Our methodology consists of developing a U-Net-like model, trained with a novel objective function, combining the mean squared error loss (which serves to guide the model to preserve the magnitude of the original ECG signal correctly) with the Pearson loss (which helps the model to maintain the same trend as the original signals). We named the final model *ECGrecover*. The model was trained on a (4498 ECG) real-life 12-lead, 10-seconds ECGs from a cohort of 990 subjects recruited at the Pitié-Salpêtrière Clinical Investigation Center [23]. During training, all the masks depicted in Figure 1 are applied to the training subset of the dataset. However, each mask configuration is evaluated separately to quantify its performance during testing. The main contributions of this work are therefore three-fold:

- (1) **We identified 17 realistic scenarios where ECG signals may be partially available.** Our analysis distinguishes between two primary challenges: reconstructing missing segments within an ECG lead and reconstructing the entire set of 12 leads from one single lead. In addition, a formal definition of the problem is provided (Section 2.1).
- (2) **We introduce ECGrecover, a model based on the U-Net architecture tailored for segment-recovery and lead-reconstruction tasks. ECGrecover is trained with a novel objective function combining mean squared error and Pearson correlation coefficient.** This approach ensures that the reconstructed signals match the original in amplitude and maintain fidelity to their waveform patterns, a crucial aspect for accurate ECG analysis and subsequent clinical applications (Section 2.2).
- (3) **In close collaboration with clinicians, we extensively evaluated ECGrecover on a dataset composed of real-life ECGs² [19, 23].** Besides considering classical distortion metrics,

²Code available at <https://git.ummisco.fr/open/2024-ecg-recover>.

this assessment was also focused on the model’s ability to preserve essential features of the ECG signal, including P, Q, R, S, and T waves. Our findings demonstrate ECGrecover’s effectiveness in maintaining the integrity of these signal components (Section 3).

1.1 Related works

Synthesizing ECG signals involves creating artificial waveforms that resemble real ECG patterns. Generally, ECG synthesis has been studied through the lens of data augmentation [20] aiming to augment the training dataset by generating ‘authentic’-like ECGs conditioned or not on heart disease, thereby to enhancing classifiers performances in arrhythmia predictions (e.g., [4, 7, 8]); to improve ECG quality assessment [33], and to improve ECG anomaly detection [16], among other applications. Existing techniques often involve training deep neural networks such as Variational Autoencoder (VAE) (e.g. [13, 25]), Generative Adversarial Networks (GAN) (e.g. [9, 30]), or CycleGAN (e.g [1]).

While these authors focus on synthetically generating ECG signals, they do not consider the ECG lead-reconstruction problem or the ECG segment-recovery problem, which can be viewed as a special case of the broader ECG synthesis problem.

ECG lead-reconstruction has been addressed in [2, 29], where the remaining leads are reconstructed from other leads (I, II, and V2). In [5, 14], the ECGs at limb leads (frontal electrodes) are used to generate the ones at the thoracic leads (precordial electrodes). Nonetheless, the aforesaid studies do not address the scenario where the reconstruction of the remaining leads is required when only a single lead is available, nor when the leads are partially recorded (less than 10 seconds). This is common when patients’ health is monitored using wearable devices that measure only lead I.

An interesting solution is proposed in [12], where the authors introduced EKGAN, a conditional GAN based on Pix2Pix [10], consisting of two generators and one 1D U-Net [22] discriminator, that tackles the reconstruction of 12-lead ECGs from one single-lead (lead I). Prior attempts in synthesizing multiple ECGs from a single-lead ECG were made in [24] where the authors proposed a GAN composed of a U-Net generator and a discriminator based on the PatchGAN [10] architecture. The model is designed to take 2.5-second ECG segments from lead I as input and reconstruct 2.5-second segments for any of the other leads. This means there are 11 different models, each tailored for reconstructing the ECG segment of a specific lead from the input derived from lead I.

It is worth noting that in both [12] and [24], the experimental data comprise 10s ECG recordings at 500Hz. However, the evaluation is conducted on different databases: a private one for [12] and PTBXL [27] along with a second dataset [32] for [21, 24].

Finally, a naive technique for the ECG segment-recovery problem involves copy-pasting the available signal to fill-up the missing segments, as suggested by Badilini et al. in [3].

2 METHODS

In this section, we first formally define the problem of ECG reconstruction. Subsequently, we introduce ECGrecover, our proposed approach, and provide real-life cases of partial ECG we analyze. In Table 1, the list of the symbols used throughout this article.

Table 1: Table of symbols

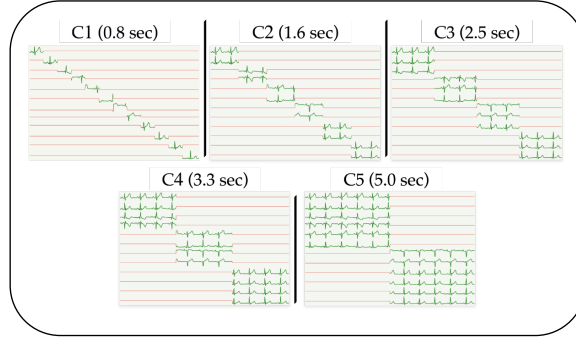
Symbol	Definition
L	Number of leads in ECG
N	Length of the ECG
$\mathcal{X} \subset \mathbb{R}^{L \times N}$	Valid (and complete) multi-lead ECG
$\tilde{\mathcal{X}} \subset \mathbb{R}^{L \times N} \setminus \mathcal{X}$	Incomplete multi-lead ECG
$f_\theta(\cdot)$	Model parameterized by θ
$\hat{\mathbf{x}} \equiv f_\theta(\mathbf{x})$	Reconstructed multi-lead ECG
$\mathbf{x}_l, \tilde{\mathbf{x}}_l, \hat{\mathbf{x}}_l \in \mathbb{R}^{1 \times N}$	ECG signal at lead l
$\mathbf{x}_{ln}, \tilde{\mathbf{x}}_{ln}, \hat{\mathbf{x}}_{ln} \in \mathbb{R}$	ECG value at lead l and point n
$\mathcal{L}_{\text{MSE}}(\cdot)$	Mean Squared Error loss
$\mathcal{L}_{\text{Pearson}}(\cdot)$	Pearson loss
r_{lj}	Sample correlation coefficient (i.e., Pearson correlation coefficient) between lead l and j

2.1 Problem formulation

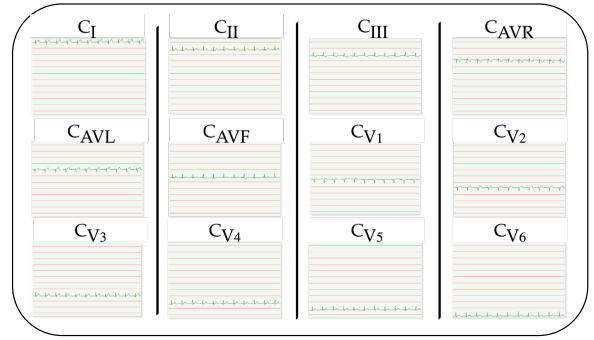
Let $X \sim P_X$ be the random variable (r.v.) for which we have realization $\mathbf{x} \in \mathcal{X} \subseteq \mathbb{R}^{L \times N}$, where $L \in \mathbb{N}$ represents the number of leads and $N \in \mathbb{N}$ the length of the signal in terms of time points. In particular, we will refer to \mathcal{X} as the set of *valid* ECGs, meaning they make sense in clinical terms. In this specific context, we say that an ECG is valid if it is also *complete* meaning that, for all $l \in \{1, \dots, L\}$ and $n \in \{1, \dots, N\}$, $\mathbf{x}_{ln} \neq 0$, where \mathbf{x}_{ln} indicates the specific data point at lead l and time point n within the ECG matrix while \mathbf{x}_l denotes the ECG vector of N time points at lead l . We call it *incomplete* otherwise, and we denote the set of incomplete ECGs as $\tilde{\mathcal{X}} \subset \mathbb{R}^{L \times N} \setminus \mathcal{X}$.

We aim to develop a model capable of inferring the missing portions of incomplete ECG, whether these are specific segments within leads or entire leads themselves. To achieve this goal, we employ a data-driven approach, training a generative model on masked data to simulate real-life configurations where specific segments (or leads) of the signal are missing: in Figure 2 for each of the twelve leads, the green segments denote the available segments, i.e., the *primer*, while the red segments denote the part of the ECG that needs to be reconstructed. Specifically, in Figure 2a, we present configurations with contiguous primers varying in overall signal coverage and lead: primers of 0.8s in C1, primers of 1.6s in C2, primers of 2.5s in C3, primers of 3.3s in C4, and primers of 5.0s in C5. In Figure 2b, we depict configurations where the full leads must be reconstructed.

The configuration, which is the most considered in the literature, is C1, where given the full trace of the first lead, the goal is to reconstruct the remaining ones [12]. Although in reality, the ECG acquisition machines record the whole signal (12-lead 10-seconds), most of this signal is lost when it is stored in paper ECG format. For instance, some recording machines may capture six leads for 5.0 seconds, as illustrated in C5, or they might record three leads for a shorter span of 2.5 seconds, as in the case of the C3 configuration (Figure 1). It is noteworthy to mention, that our problem definition comprehensively encompasses both *scenarii*: ECG segment recovery and ECG lead reconstruction, at a higher level of abstraction.



(a) Masks to simulate ECG segment-recovery.



(b) Masks to simulate ECG lead-reconstruction.

Figure 2: Masks applied to ECGs for simulating real-life incomplete ECGs. The green sections represent the *primers* – the portions of the signal available, while the red sections indicate the parts of the signal that need to be reconstructed. In 2a, the numbers in brackets specify the primers’ length.

2.2 Our proposed method

Formally, let $\mathcal{S}_M \triangleq \left\{ \mathbf{x}^{(i)} \right\}_{i=1}^M \sim P_X$ be a random realization of M i.i.d. valid ECGs according to P_X . Moreover, let \mathcal{K} be a countable set of indexes corresponding to each of the possible real-life data masks (e.g., as the ones we show in Figure 2). Finally, we let $\mathcal{G} \triangleq \{g_k : \mathcal{X} \rightarrow \tilde{\mathcal{X}} \mid k \in \mathcal{K}\}$ be the set of possible masking functions that, given a valid ECG, outputs an incomplete one. Our training set is defined as

$$\mathcal{D}_M \triangleq \{(g(\mathbf{x}), \mathbf{x}) \mid \mathbf{x} \in \mathcal{S}_M, g \in \mathcal{G}\}.$$

Given the parametric family of models $\mathcal{F} = \{f_\theta : \tilde{\mathcal{X}} \rightarrow \mathcal{X} \mid \theta \in \Theta\}$, where θ represents the model parameters, our learning algorithm aims to minimize the following objective function:

$$\min_{f_\theta \in \mathcal{F}} \sum_{(\tilde{\mathbf{x}}, \mathbf{x}) \in \mathcal{D}_m} \left[\mathcal{L}_{\text{MSE}}(\tilde{\mathbf{x}}, \mathbf{x}, f_\theta) + \alpha \cdot \mathcal{L}_{\text{Pearson}}(\tilde{\mathbf{x}}, \mathbf{x}, f_\theta) \right], \quad (1)$$

where α is the hyperparameter regulating the loss and

$$\begin{aligned} \mathcal{L}_{\text{MSE}}(\tilde{\mathbf{x}}, \mathbf{x}, f_\theta) &\triangleq \frac{1}{L \cdot N} \sum_{l=1}^L \sum_{n=1}^N (f_\theta(\tilde{\mathbf{x}})_{ln} - \mathbf{x}_{ln})^2 \\ \mathcal{L}_{\text{Pearson}}(\tilde{\mathbf{x}}, \mathbf{x}, f_\theta) &\triangleq \frac{1}{L} \sum_{l=1}^L \left(1 - r_{\mathbf{x}_l \tilde{\mathbf{x}}_l} \right), \end{aligned}$$

where $r_{\mathbf{x}_l \tilde{\mathbf{x}}_l}$ is the sample correlation coefficient for $(f_\theta(\tilde{\mathbf{x}}), \mathbf{x}) \equiv (\tilde{\mathbf{x}}, \mathbf{x})$ for the lead l , i.e.,

$$r_{\mathbf{x}_l \tilde{\mathbf{x}}_l} = \frac{\sum_{n=1}^N (\tilde{\mathbf{x}}_{ln} - \mu_{\tilde{\mathbf{x}}_l})(\mathbf{x}_{ln} - \mu_{\mathbf{x}_l})}{\sqrt{\sum_{n=1}^N (\tilde{\mathbf{x}}_{ln} - \mu_{\tilde{\mathbf{x}}_l})^2} \sqrt{\sum_{n=1}^N (\mathbf{x}_{ln} - \mu_{\mathbf{x}_l})^2}},$$

with $\mu_{\tilde{\mathbf{x}}_l} = \frac{1}{N} \sum_{n=1}^N \tilde{\mathbf{x}}_{ln}$ and $\mu_{\mathbf{x}_l} = \frac{1}{N} \sum_{n=1}^N \mathbf{x}_{ln}$.

The final cost function in Equation (1) accounts for the ECG’s spatial and temporal aspects. Specifically, \mathcal{L}_{MSE} is the mean squared error loss and ensures an accurate reconstruction of the ECG signal by capturing the average distance in amplitude between the reconstructed and the real signal. On the contrary, $\mathcal{L}_{\text{Pearson}}$ is the

Pearson loss, which promotes the preservation of specific linear relationships within the signal. A strong correlation (close to 1, in absolute value) signifies that the reconstructed signal varies similarly and simultaneously with the real one. In Appendix A.1, we detail the performance of the model in the validation set across various values of α , particularly focusing on the extreme cases: $\alpha = 0$, i.e., when the loss is exclusively based on \mathcal{L}_{MSE} , and $\alpha = \infty$, i.e., the loss is $\mathcal{L}_{\text{Pearson}}$ only.

Similarly to what has been done at training time, at testing time starting from T random realization of U i.i.d. valid ECGs according to P_X , we apply each of the mask in \mathcal{G} to create the pair of samples to test. In contrast to the training phase, our evaluation is performed separately for each set of samples generated according to the specific masks under consideration.

3 RESULTS

In this section, we evaluate the effectiveness of the proposed method, ECGrecover. We first outline the experimental setup, and then we discuss the results. Additional simulations and findings are provided in Appendix A for space reasons.

3.1 Experimental setup

3.1.1 Datasets. We utilized the Generepol dataset [23], comprising 10-second 8-lead ECGs sampled at 500Hz. Leads III, aVF, aVL, and aVR were computed from the eight other leads I, II, and V1-V6, following the common practice in the ECG literature [23].

The study was conducted at the Clinical Investigation Center of the Pitié-Salpêtrière Hospital from 2008 to 2012 in Paris, France, and involved 15 119 ECG recordings from 990 healthy subjects. These recordings were taken before and at 1, 2, 3, and 4 hours after administering 80mg oral sotalol dose, denoted as softT1, softT2, softT3, and softT4, respectively. To ensure data quality, two expert cardiologists curated the recordings. We refer to [19, 23] for further details about the acquisition process.

The raw dataset used for training denoted as \mathcal{S}_M in Section 2.1, comprises 4 498 ECG recordings. When augmented through the application of various masks as detailed in Figure 2, this dataset expands to a total of 76 466 samples. The original 558 ECG recordings

are augmented to 9 486 ECG for the validation set. Similarly, the testing set, initially consisting of 591 ECGs, is augmented to a total of 10 047 ECG.

3.1.2 Data preprocessing. We first min-max normalized the ECG data to a range of [-1,1]. For the preparation of our data, we followed a strategy close to [12]. In short, we applied bandpass filtering to the normalized data, using lower and upper cut-off frequencies of 0.05Hz and 150Hz, respectively, to eliminate noise such as baseline drift and improve signal quality. Finally, we down-sampled the original signal from 5000pts (500Hz) to 512pts (50Hz).

As described in Section 2.1, to mimic real-life cases of ECG with incomplete leads or segments, we considered the *scenarii* illustrated in Figure 2. For a given 12-lead ECG input signal, we initially segmented the signal following the different configurations at coordinates corresponding to the primers. Subsequently, to maintain the original dimensions of the signal, we completed the primers with random noise. This noise is generated from a continuous uniform distribution within the [0, 1] interval. This method introduces variability in the noise across samples, thereby realistically simulating the presence of missing signals. An illustration of how an ECG with incomplete leads or segments would appear after introducing random noise is shown in Figure 3 top.

3.1.3 Evaluation metrics. We assessed the effectiveness of the proposed approach from two distinct perspectives. Initially, we evaluated its reconstruction capability using standard distortion metrics employed in recent literature [12, 24]. These metrics measure the reconstruction error between the original and reconstructed signals, with lower values indicating better performance. Specifically, we employed the *root mean square error* (RMSE) and the *maximum absolute error* (MAE). Additionally, we utilized the *dynamic time warping* (DTW) as an alignment-based similarity measure to evaluate temporal alignment between the original and reconstructed signals, favoring lower values. The Pearson correlation coefficient (PCC) evaluates linear relationships between leads, with higher values indicating better alignment.

Subsequently, we examined ECGrecover ability to preserve crucial features of the ECG signal. In particular, we focused on preserving wave coordinates, including peaks, i.e., P, Q, R, S, T, as illustrated in Figure 9. We used the *neurokit2* python library for this task [17]. The results were evaluated by measuring the difference in seconds between the positions of the peaks in the original ECG and the reconstructed one, denoted as $\Delta-\pi$ (the lower, the better), where π represents one of the potential peaks of interest.

3.1.4 State-of-the-art methods. We compared ECGrecover with the most recent state-of-the-art (SOTA) methods for the ECG lead-reconstruction problem³. It's worth noting that, to the best of our knowledge, no existing methods address the ECG segment-recovery problem. We briefly introduce these SOTA as follows:

Pix2Pix [10]. A conditional generative adversarial network (cGAN), initially proposed for images, employs a 2D U-Net generator and a PatchGAN discriminator. Unlike traditional discriminators that classify the entire image as real or fake, PatchGAN evaluates the realism of small, overlapping patches within the image.

³No comparison could be made with Seo et al. (2022) [24] due to the unavailability of their code.

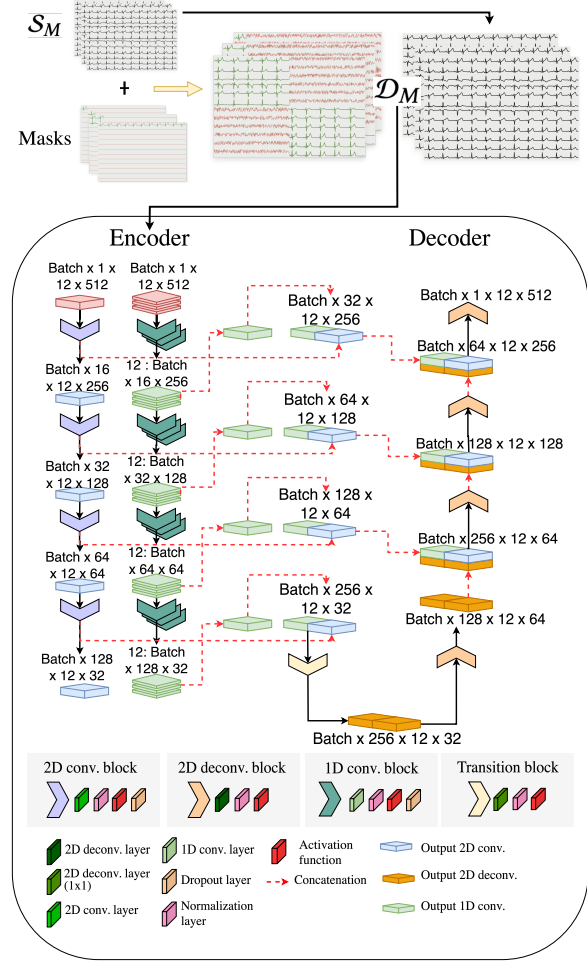


Figure 3: Training set and network architecture.

EKGAN [12]. A generative adversarial network (GAN) for the reconstruction, which is based on Pix2Pix augmented by an additional label generator and the use of a 1D U-Net discriminator instead of a PatchGAN discriminator.

CopyPaste. A naive-approach, which consists in replicating the primers throughout the signal to complete the ECG. This technique is notably implemented in Badilini et al. [3], a software used to digitize paper ECGs.

In their original paper, particularly in EKGAN, the focus is on the reconstruction of the 11 leads given lead I, corresponding to setting C_1 in Figure 2. Hence, the method was not initially designed for the ECG segment-recovery problem. Nevertheless, for completeness and fairness, we assessed all the methods performance across all the settings in Figure 2.

3.1.5 Model architecture and training procedure. We consider a U-Net like architecture [22], which is summarized in Figure 3. The encoder consists of two input branches one 2D and the other one 1D. On the one hand, the purpose of the 2D branch is to let the model learn inter-lead information of the signal. This branch is made of 4,

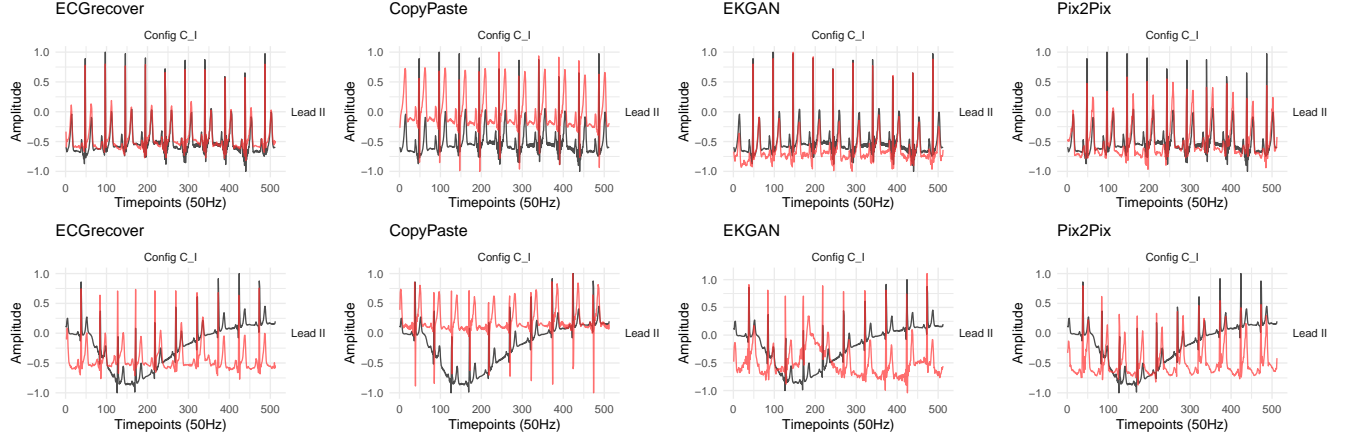


Figure 4: Lead II signal obtained with different approaches for C1. Reconstructed leads are in red, the original ones are in black. Top depicts a relatively clean ECG while Bottom, an noisy ECG with baseline wander

2D convolution blocks, each of them presenting a 2D convolution layer, batch normalization, a LeakyReLU (0.2) activation function, and dropout (0.2). On the other hand, the 1D branch provides the model to learn intra-lead characteristics. Similarly to the 2D branch, this one consists of 12×4 , 1D convolution blocks. The output of each block (1D/2D) is concatenated and then given to the decoder during the decoding phase.

The transition block consists of a 2D deconvolution layer, kernels of dimension (13, 3) with no stride, followed by batch normalization and a LeakyReLU (0.2) activation function. The output of the transition is fed into the decoder, which consists of 4, 2D deconvolution blocks. Each of them is composed of a 2D deconvolution layer, batch normalization, and LeakyReLU activation function (0.2). Each output of a deconvolution block is concatenated with the output (concatenated 1D/2D) of the symmetric convolution block. Finally, in the last 2D deconvolution block of the decoder, we use the Tanh activation function to have a signal between -1 and 1 as in the original normalized signal in the input.

We trained the model for 100 epochs with a batch size of 256. We also used the Adam optimizer with a learning rate of 0.01. The hyper-parameter α in Equation (1) was tuned by choosing values within the range (0, 1). The final value of α used for the experiments was fixed to 0.1 (cf. Appendix A.1).

3.2 Discussion

We now present the main experimental results to show the effectiveness of ECGrecover for both the ECG lead-reconstruction and the ECG segment-recovery problems. In particular, we first discuss the capability of our approach by considering the metrics in Section 3.1.3; then, we analyze the ability of the method to preserve important features of the ECG; finally, we assess how the reconstructed signal affects the inter-lead correlation. Further results are provided in Appendices A and B.

Specifically, throughout this section, we use the $C\bullet$ notation to indicate the input sample that, at testing time, has been masked according to the considered configuration \bullet . Therefore, we compare the reconstructed lead (for example, lead I from the ECG in output

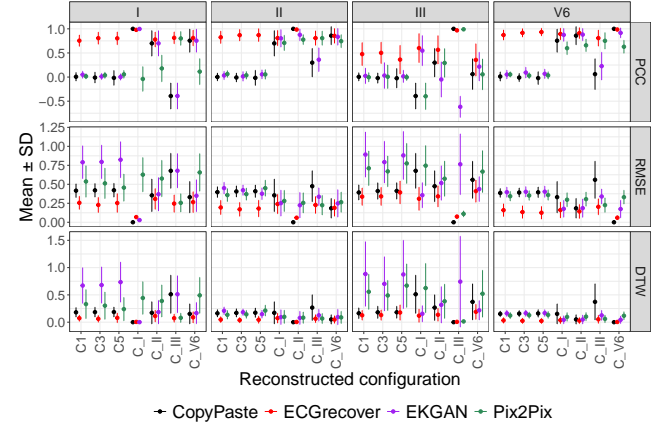


Figure 5: Performance of ECGrecover and the state-of-the-art methods in their reconstruction capabilities for the segment recovery problem (C1, C3, C5) and the lead reconstruction problem (C1, CII)

when the input sample was masked with the C1 configuration) with its original counterpart.

Figures 4 and 8 shows examples of lead II ECG reconstructions.

3.2.1 ECG segment-recovery and lead-reconstruction. Figure 5 presents an evaluation of our proposed method, ECGrecover, alongside benchmark state-of-the-art approaches, focusing on PCC, RMSE and DTW for the Generepol dataset. We relegate to Appendix B the complete sets of the results across all the 17 different scenarios in Figure 2 and all the 12 leads.

As for the ECG segment-recovery problem, in Figure 5, we specifically focused on the configuration C1 as it represents the scenario with primers of shorter duration (i.e., 0.8sec) where most of the signal needs to be reconstructed. Additionally, we analyze the settings C3 and C5 as they reflect real-life situations when digitizing paper

Table 2: The performance of ECGRecover and the SOTA in generating coherent ECG signal, which allows to compute the QT-interval computed as the difference with that calculated in the original signal (mean \pm standard deviation). This is evaluated before (Sot-) and after (Sot+) drug intake, for the segment-recovery (C_1 , C_3 , C_5) and the lead-reconstruction problem (C_I , C_{II}).

Lead	Δ QT distance (Sot-) (↓)				Δ QT distance (Sot+) (↓)			
	ECGrecover	EKGAN [12]	Pix2Pix [10]	CopyPaste	ECGrecover	EKGAN [12]	Pix2Pix [10]	CopyPaste
C_1	I 0.01 \pm 0.02	0.11 \pm 0.06	0.09 \pm 0.04	0.05 \pm 0.05	0.02 \pm 0.03	0.12 \pm 0.07	0.11 \pm 0.05	0.07 \pm 0.05
	II 0.01 \pm 0.01	0.12 \pm 0.06	0.08 \pm 0.04	0.04 \pm 0.04	0.01 \pm 0.03	0.15 \pm 0.07	0.1 \pm 0.05	0.06 \pm 0.07
	III 0.07 \pm 0.07	0.11 \pm 0.09	0.11 \pm 0.09	0.05 \pm 0.08	0.06 \pm 0.06	0.11 \pm 0.09	0.13 \pm 0.09	0.06 \pm 0.07
	V1 0.03 \pm 0.04	0.05 \pm 0.05	0.04 \pm 0.04	0.02 \pm 0.04	0.03 \pm 0.04	0.05 \pm 0.05	0.04 \pm 0.04	0.02 \pm 0.04
	V6 0.01 \pm 0.01	0.13 \pm 0.06	0.06 \pm 0.04	0.02 \pm 0.05	0.01 \pm 0.03	0.16 \pm 0.06	0.08 \pm 0.06	0.03 \pm 0.06
					0.01 \pm 0.03	0.07 \pm 0.05	0.09 \pm 0.05	0.03 \pm 0.04
C_3	I 0.01 \pm 0.01	0.05 \pm 0.04	0.08 \pm 0.04	0.02 \pm 0.03	0.01 \pm 0.02	0.10 \pm 0.06	0.07 \pm 0.04	0.03 \pm 0.04
	II 0.01 \pm 0.01	0.07 \pm 0.05	0.05 \pm 0.04	0.02 \pm 0.02	0.05 \pm 0.05	0.11 \pm 0.09	0.13 \pm 0.09	0.05 \pm 0.06
	III 0.06 \pm 0.07	0.11 \pm 0.09	0.10 \pm 0.08	0.04 \pm 0.06	0.02 \pm 0.04	0.04 \pm 0.05	0.03 \pm 0.04	0.02 \pm 0.02
	V1 0.03 \pm 0.03	0.04 \pm 0.04	0.04 \pm 0.04	0.02 \pm 0.03	0.01 \pm 0.02	0.13 \pm 0.06	0.07 \pm 0.05	0.03 \pm 0.04
	V6 0.01 \pm 0.01	0.10 \pm 0.05	0.05 \pm 0.04	0.02 \pm 0.03				
					0.01 \pm 0.03	0.04 \pm 0.04	0.05 \pm 0.04	0.02 \pm 0.02
C_5	I 0.01 \pm 0.02	0.03 \pm 0.02	0.03 \pm 0.03	0.01 \pm 0.02	0.01 \pm 0.02	0.07 \pm 0.06	0.04 \pm 0.04	0.01 \pm 0.02
	II 0.01 \pm 0.01	0.04 \pm 0.04	0.03 \pm 0.03	0.01 \pm 0.02	0.05 \pm 0.06	0.12 \pm 0.09	0.10 \pm 0.09	0.02 \pm 0.04
	III 0.05 \pm 0.06	0.09 \pm 0.08	0.08 \pm 0.08	0.02 \pm 0.04	0.02 \pm 0.03	0.03 \pm 0.05	0.05 \pm 0.04	0.01 \pm 0.02
	V1 0.03 \pm 0.03	0.04 \pm 0.04	0.05 \pm 0.04	0.01 \pm 0.02	0.01 \pm 0.02	0.09 \pm 0.06	0.04 \pm 0.04	0.02 \pm 0.02
	V6 0.00 \pm 0.01	0.05 \pm 0.04	0.02 \pm 0.02	0.01 \pm 0.01				
					0.01 \pm 0.03	0.01 \pm 0.03	0.02 \pm 0.04	0.01 \pm 0.03
C_I	II 0.01 \pm 0.01	0.01 \pm 0.01	0.01 \pm 0.03	0.01 \pm 0.02	0.06 \pm 0.07	0.07 \pm 0.07	0.09 \pm 0.07	0.09 \pm 0.07
	III 0.06 \pm 0.07	0.08 \pm 0.08	0.09 \pm 0.08	0.08 \pm 0.07	0.03 \pm 0.04	0.03 \pm 0.04	0.12 \pm 0.06	0.12 \pm 0.06
	V1 0.03 \pm 0.04	0.04 \pm 0.04	0.10 \pm 0.05	0.09 \pm 0.06	0.01 \pm 0.03	0.01 \pm 0.03	0.03 \pm 0.03	0.01 \pm 0.03
	V6 0.01 \pm 0.01	0.01 \pm 0.01	0.02 \pm 0.02	0.01 \pm 0.02				
					0.01 \pm 0.04	0.01 \pm 0.04	0.03 \pm 0.04	0.01 \pm 0.04
					0.08 \pm 0.09	0.11 \pm 0.08	0.08 \pm 0.07	0.09 \pm 0.07
C_{II}	III 0.09 \pm 0.10	0.09 \pm 0.08	0.08 \pm 0.07	0.08 \pm 0.06	0.03 \pm 0.04	0.03 \pm 0.04	0.09 \pm 0.06	0.12 \pm 0.06
	V1 0.03 \pm 0.04	0.04 \pm 0.04	0.09 \pm 0.05	0.09 \pm 0.05	0.01 \pm 0.02	0.01 \pm 0.03	0.02 \pm 0.03	0.01 \pm 0.03
	V6 0.01 \pm 0.01	0.01 \pm 0.01	0.02 \pm 0.02	0.01 \pm 0.01				
					0.01 \pm 0.02	0.01 \pm 0.03	0.02 \pm 0.03	0.01 \pm 0.03

ECGs. Regarding the ECG lead-reconstruction problem, we highlight in the table the configurations C_I as it is the one considered also in [12], and C_{II} because of its relevance in wearable device recordings and paper-stored ECGs, where Lead II, akin to Lead I, is predominantly captured. For each of the input masks, we tested the ability of the model to reconstruct the limb leads I, II, and III and the chest leads V1 and V6. Practitioners note that leads II and V1 contain the most information, while lead III contains the least.

Overall, ECGrecover consistently outperforms the SOTA, regardless of the chosen metric. As depicted in Figure 5, lead V6 emerges as the most straightforward to reconstruct, both in ECG segment-recovery (C_1 , C_3 , C_5) and ECG lead-reconstruction (C_I , C_{II}). Conversely, lead III proves to be the most challenging to reconstruct from the other leads. This can be explained by the perpendicular information that it captures relative to the other leads. In particular, while our method consistently delivers satisfactory results across all samples tested, competing methods exhibit greater variability (e.g., DTW values for EKGAN). Interestingly, the simple CopyPaste method yields reasonable results regarding RMSE and DTW. However, as seen from the PCC results, the method fails to preserve the linear relationships between the original and reconstructed leads, underscoring the method's limitations as the heart rhythm may vary through time, thus losing sync. This highlights the importance of evaluating the methods from multiple perspectives. Relying solely on traditional distortion metrics, primarily measuring spatial distances between signals, may lead to overly optimistic results. Referring to the comprehensive results in Figure 10, our analysis shows that, in contrast to ECGrecover, the competing approaches

EKGAN and Pix2Pix face significantly more challenges in the ECG segment-recovery task compared to the ECG lead-reconstruction task. On the other hand, the CopyPaste method struggles primarily with the lead-reconstruction problem. This outcome is not surprising as EKGAN and Pix2Pix were precisely designed for ECG lead-reconstruction, whereas CopyPaste, which essentially duplicates the signal across leads, performs poorly when the lead to reconstruct is less correlated with the primer lead in the mask.

Finally, we emphasize that in Appendix A.3, we conduct an additional evaluation of our proposed method using the PTB-XL dataset [27]. The results underscore that the effectiveness of ECGrecover is not confined to our Generepol dataset thereby demonstrating its applicability and robustness across different datasets.

3.2.2 On the QT distance preservation. An ECG visually represents the heart's electrical activity during a cardiac cycle. This cycle, which encompasses a single heartbeat, involves the heart filling with blood and then contracting to pump blood to the rest of the body. The standard ECG trace includes several key components, each corresponding to specific electrical events within the heart. As shown in Figure 9, the signal typically includes identifiable points corresponding to the start, end and peaks of the underlying waves P and T and the QRS complex. The intervals and segments between these components (QT distance, PR interval, etc.) also provide important information about the cardiac cycle's timing and electrical conduction through the heart. Understanding and evaluating these components helps diagnose a wide range of cardiac abnormalities and conditions [18].

In Table 2, we evaluate the methods' capacity to generate a signal that can be effectively analyzed. The performance is computed as the difference between the QT distance calculated in the reconstructed signals and the QT distance computed in the original signals (Δ -QT). Specifically, we segment each ECG into individual heart-beats by identifying the position of the R-peak within the original leads. Then, we isolate the specific spike by taking a window of 50 points around the R peaks—20 points before and 30 points after. For the detection of the peaks, we use the Neurokit library⁴, which supports the extraction of critical features from the ECG, such as P, Q, R, S, and T peaks, by utilizing advanced signal processing techniques. At each heart-beat, we identified the Q wave and the end of the T wave, allowing us to calculate the mean QT interval for each ECG.

The results in Table 2 are grouped w.r.t. Sot+ and Sot- true label, originally assigned to the ECGs. Indeed, as described in Section 3.1.1, in the Genepol study, participants were administered Sotalol, which is known to prolong the QT interval and sometimes modify the morphology of the T-wave, which makes the measurement of QT more challenging [19, 23]. The ECG recordings were taken before (Sot-) and after (Sot+) the drug administration.

Remarkably, our analysis did not reveal a significant performance difference of ECGrecover between the pre-sotalol and post-sotalol ECGs. The methods demonstrate consistent performance across various input masks and lead reconstructions. While ECGrecover consistently outperforms its competitors, the CopyPaste method occasionally achieves better results. The explanation lies in the inherent nature of the CopyPaste technique, which maintains beat information through direct replication. By duplicating each beat identically, the CopyPaste method inherently preserves the average QT distance, with a lower variability.

3.2.3 On the inter-lead correlation. We conclude the assessment of ECGrecover by analyzing the inter-lead correlation. Specifically, in Figure 6, the matrix entry at index (i, j) represents PCC between the j -th reconstructed lead and the j -th original lead, given that the input mask applied is C_i . Thus, the i -th row illustrates the model's effectiveness in utilizing the specific i -th lead's data to accurately reconstruct the remaining leads of the ECG. Conversely, the j -th column indicates which input mask most significantly guides the model towards a more accurate reconstruction.

Figure 6 highlights the strong correlation between leads V3, V4, V5 and V6. Lead III exhibits a lower correlation with the other leads. While surprising at first, given that lead III can theoretically be derived from leads I and II through Einthoven's triangle [18], this characteristic has also been observed in [11], where a similar analysis was conducted on a distinct dataset. Indeed, lead III captures a perpendicular view of the heart compared to the others.

Moreover, similar conclusions can also be found in [31], regarding lead V1. Indeed, Zhang et al. demonstrated that the absence of lead V1 could significantly affect the diagnostic accuracy of various deep neural network models. Their findings revealed a notably low correlation between lead V1 and the other leads, with PCC close to 0. This low correlation suggests that the information provided by lead V1 is substantially distinct from that of the other leads. Consequently, it is understandable that the mask C_{V1} in Figure 6 is the

⁴<https://neuropsychology.github.io/NeuroKit/>

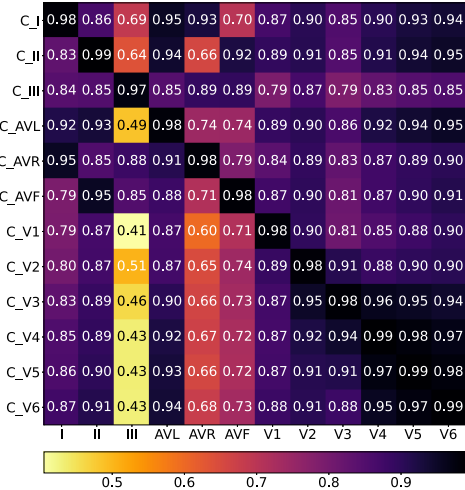


Figure 6: The matrix entry at index (i, j) represents PCC between the j -th reconstructed lead and the j -th original lead, given that the input mask applied is C_i . Analyzing the matrix row-wise provides insights into the model's capability to reconstruct the leads based on the specific input mask used. Conversely, examining the matrix column-wise reveals which input mask enables the model to reconstruct each particular lead most effectively.

most challenging to reconstruct. Noteworthy, PCC measures linear correlation, and if there are nonlinear relationships or complex dependencies between these leads, PCC may not fully capture such associations. Factors like noise, artifacts, or variations in individual physiology can also contribute to lower correlation values.

4 CONCLUSIONS AND FUTURE WORK

We tackled the problem of reconstructing the 12-lead ECG signal when only a partial subset of the signal is available. We proposed a U-Net-like model trained on a novel objective function, combining the classical mean squared error loss with the Pearson correlation. We extensively evaluated our method, ECGrecover, on a real-life ECG dataset comprising 15 119 ECGs. The comparison to recent state-of-the-art methods reveals the effectiveness of ECGrecover in recovering the missing signal, even in challenging cases such as the C_1 configuration, as quantified either with distortion metrics or by the preservation of QT segment or the QRS-complex.

The primary objective of this method is to enhance the comprehensive analysis of ECG data for clinicians. By utilizing the reconstruction capabilities of ECGrecover, we can significantly improve the readability of ECG traces, which can be determinant in diagnosing diseases. This advancement allows for a more detailed and accurate assessment of cardiac activity, facilitating better diagnostic decisions and patient care. Notably, the proposed approach is part of a larger translational research project, *DeepECG4u*⁵, which aims to improve patient care through automatic analyses of ECG based on AI.

⁵<https://anr.fr/Project-ANR-20-CE17-0022>

REFERENCES

- [1] Mohamed Amine Abdelmadjid and Mounir Boukadoum. 2022. Neural Network-Based Signal Translation with Application to the ECG. In *2022 20th IEEE International NEWCAS Conference (NEWCAS)*. IEEE, 542–546.
- [2] Hussein Atoui, Jocelyne Fayn, and Paul Rubel. 2010. A novel neural-network model for deriving standard 12-lead ECGs from serial three-lead ECGs: application to self-care. *IEEE transactions on information technology in biomedicine* 14, 3 (2010), 883–890.
- [3] Fabio Badilini, Tanju Erdem, Wojciech Zareba, and Arthur J Moss. 2005. ECGScan: a method for conversion of paper electrocardiographic printouts to digital electrocardiographic files. *Journal of electrocardiology* 38, 4 (2005), 310–318.
- [4] Jintai Chen, Kuanlun Liao, Kun Wei, Haochao Ying, Danny Z Chen, and Jian Wu. 2022. ME-GAN: Learning panoptic electrocardio representations for multi-view ECG synthesis conditioned on heart diseases. In *International Conference on Machine Learning*. PMLR, 3360–3370.
- [5] Younghoon Cho, Joon-myung Kwon, Kyung-Hee Kim, Joss R Medina-Inojosa, Ki-Hyun Jeon, Soohyun Cho, Soo Yoon Lee, Jinsik Park, and Byung-Hee Oh. 2020. Artificial intelligence algorithm for detecting myocardial infarction using six-lead electrocardiography. *Scientific reports* 10, 1 (2020), 20495.
- [6] Lia Crotti, Giuseppe Celano, Federica Dagradì, and Peter J Schwartz. 2008. Congenital long QT syndrome. *Orphanet journal of rare diseases* 3, 1 (2008), 1–16.
- [7] Tomer Golany, Gal Lavee, Shai Tejmar Yarden, and Kira Radinsky. 2020. Improving ECG classification using generative adversarial networks. In *Proceedings of the AAAI conference on artificial intelligence*, Vol. 34. 13280–13285.
- [8] Tomer Golany and Kira Radinsky. 2019. Pgans: Personalized generative adversarial networks for ecg synthesis to improve patient-specific deep ecg classification. In *Proceedings of the AAAI Conference on Artificial Intelligence*, Vol. 33. 557–564.
- [9] Debapriya Hazra and Yung-Cheol Byun. 2020. SynSigGAN: Generative adversarial networks for synthetic biomedical signal generation. *Biology* 9, 12 (2020), 441.
- [10] Phillip Isola, Jun-Yan Zhu, Tinghui Zhou, and Alexei A Efros. 2017. Image-to-image translation with conditional adversarial networks. In *Proceedings of the IEEE conference on computer vision and pattern recognition*. 1125–1134.
- [11] Utkars Jain, Adam A Butchy, Michael T Leaseur, Veronica A Covalesky, Daniel McCormick, and Gary S Mintz. 2023. Redundancy and Novelty Between ECG Leads Based on Linear Correlation. (2023).
- [12] Jinho Joo, Gihun Joo, Yeji Kim, Moo-Nyun Jin, Junbeom Park, and Hyeonseung Im. 2023. Twelve-Lead ECG Reconstruction from Single-Lead Signals Using Generative Adversarial Networks. In *International Conference on Medical Image Computing and Computer-Assisted Intervention*. Springer, 184–194.
- [13] VV Kuznetsov, VA Moskalenko, DV Gribanov, and Nikolai Yu Zolotykh. 2021. Interpretable feature generation in ECG using a variational autoencoder. *Frontiers in genetics* 12 (2021), 638191.
- [14] Jaehyeok Lee, Minkyu Kim, and Jungkuk Kim. 2015. Reconstruction of precordial lead electrocardiogram from limb leads using the state-space model. *IEEE Journal of Biomedical and Health Informatics* 20, 3 (2015), 818–828.
- [15] Alex Lence, Fabrice Extramiana, Ahmad Fall, Joe-Elie Salem, Jean-Daniel Zucker, and Edi Prifti. [n. d.]. Automatic digitization of paper electrocardiograms – A systematic review. 80 ([n. d.]), 125–132. <https://doi.org/10.1016/j.jelectrocard.2023.05.009>
- [16] Fangyu Li, Hui Chang, Min Jiang, and Yihuan Su. 2022. A Contrastive Learning Framework for ECG Anomaly Detection. In *2022 7th International Conference on Intelligent Computing and Signal Processing (ICSP)*. IEEE, 673–677.
- [17] Dominique Makowski, Tam Pham, Zen J. Lau, Jan C. Brammer, François Lépinas, Hung Pham, Christopher Schözel, and S. H. Annabel Chen. 2021. NeuroKit2: A Python toolbox for neurophysiological signal processing. *Behavior Research Methods* 53, 4 (feb 2021), 1689–1696. <https://doi.org/10.3758/s13428-020-01516-y>
- [18] Sharon Parmet, Cassio Lynn, and Richard M Glass. 2003. Electrocardiograms. *JAMA* 289, 16 (2003), 2166–2166.
- [19] Edi Prifti, Ahmad Fall, Giovanni Davogustto, Alfredo Pulini, Isabelle Denjoy, Christian Funck-Brentano, Yasmin Khan, Alexandre Durand-Salmon, Fabio Badilini, Quinn S Wells, et al. 2021. Deep learning analysis of electrocardiogram for risk prediction of drug-induced arrhythmias and diagnosis of long QT syndrome. *European Heart Journal* 42, 38 (2021), 3948–3961.
- [20] Md Moklesur Rahman, Massimo Walter Rivolta, Fabio Badilini, and Roberto Sassi. 2023. A Systematic Survey of Data Augmentation of ECG Signals for AI Applications. *Sensors* 23, 11 (2023), 5237.
- [21] Pentti M Rautaharju, James Warren, David Seale, and John Sherwood. 1981. Exploitation of the redundancy of the conventional limb lead electrocardiograms for prolongation of the record length. *Journal of Electrocardiology* 14, 1 (1981), 39–41.
- [22] Olaf Ronneberger, Philipp Fischer, and Thomas Brox. 2015. U-net: Convolutional networks for biomedical image segmentation. In *Medical Image Computing and Computer-Assisted Intervention–MICCAI 2015: 18th International Conference, Munich, Germany, October 5–9, 2015, Proceedings, Part III* 18. Springer, 234–241.
- [23] Joe-Elie Salem, Marine Germain, Jean-Sébastien Hulot, Pascal Voiriot, Bruno Lebourgeois, Jean Waldura, David-Alexandre Tregouet, Beny Charbit, and Christian Funck-Brentano. 2017. GENoME wide analysis of sotalol-induced IKr inhibition during ventricular REPOLarization, “GENEREPOL study”: Lack of common variants with large effect sizes. *PLoS One* 12, 8 (2017), e0181875.
- [24] Hyo-Chang Seo, Gi-Won Yoon, Segyeong Joo, and Gi-Byoung Nam. 2022. Multiple electrocardiogram generator with single-lead electrocardiogram. *Computer Methods and Programs in Biomedicine* 221 (2022), 106858.
- [25] Reza Soleimani and Edgar Lobaton. 2022. Enhancing Inference on Physiological and Kinematic Periodic Signals via Phase-Based Interpretability and Multi-Task Learning. *Information* 13, 7 (2022), 326.
- [26] Joske van der Zande, Marc Strik, Rémi Dubois, Sylvain Ploux, Saer Abu Alrub, Théo Caillol, Mathieu Nasarre, Dirk W Donker, Eline Oppersma, and Pierre Bordachar. 2023. Using a smartwatch to record precordial electrocardiograms: a validation study. *Sensors* 23, 5 (2023), 2555.
- [27] Patrick Wagner, Nils Strodtthoff, Ralf-Dieter Bousseljot, Dieter Kreiseler, Fatima I Lunze, Wojciech Samek, and Tobias Schaeffter. 2020. PTB-XL, a large publicly available electrocardiography dataset. *Scientific data* 7, 1 (2020), 154.
- [28] Brian A Walker, Ahsan H Khandoker, and Jim Black. 2009. Low cost ECG monitor for developing countries. In *2009 International Conference on Intelligent Sensors, Sensor Networks and Information Processing (ISSNIP)*. IEEE, 195–199.
- [29] Lu-di Wang, Wei Zhou, Ying Xing, Na Liu, Mahmood Movahedipour, and Xiaoguang Zhou. 2019. A novel method based on convolutional neural networks for deriving standard 12-lead ECG from serial 3-lead ECG. *Frontiers of Information Technology & Electronic Engineering* 20, 3 (2019), 405–413.
- [30] Fei Ye, Fei Zhu, Yuchen Fu, and Bairong Shen. 2019. ECG generation with sequence generative adversarial nets optimized by policy gradient. *IEEE Access* 7 (2019), 159369–159378.
- [31] Chuanzhe Zhang, Jiahao Li, Shaopeng Pang, Fangzhou Xu, and Shuwang Zhou. 2022. A 12-lead ECG correlation network model exploring the inter-lead relationships. *Europhysics Letters* 140, 3 (2022), 31001.
- [32] Jianwei Zheng, Jianming Zhang, Sidy Danioko, Hai Yao, Hangyuan Guo, and Cyril Rakovski. 2020. A 12-lead electrocardiogram database for arrhythmia research covering more than 10,000 patients. *Scientific data* 7, 1 (2020), 48.
- [33] Xue Zhou, Xin Zhu, Keijiro Nakamura, and Mahito Noro. 2021. Electrocardiogram quality assessment with a generalized deep learning model assisted by conditional generative adversarial networks. *Life* 11, 10 (2021), 1013.

A ADDITIONAL RESULTS

In this section, we discuss additional simulations and results that, due to space constraints, were not included in the main paper. For better readability, we have collected the comprehensive set of results in 19 tables, which can be found in Appendix B.

A.1 On the α parameter

In Section 2.2, we introduced the objective function in Equation (1) used to train our U-Net model

$$\mathcal{L} = \mathcal{L}_{\text{MSE}} + \alpha \cdot \mathcal{L}_{\text{Pearson}}.$$

In the following section, we investigate the role of the hyper-parameter α to train the model. In particular, we consider $\alpha \in \{0, 0.1, 0.5, 1, \infty\}$, where for $\alpha = 0$, $\mathcal{L} \equiv \mathcal{L}_{\text{MSE}}$ and for $\alpha = \infty$, $\mathcal{L} \equiv \mathcal{L}_{\text{Pearson}}$. We provide in Table 3 the results over the validation set of the five models trained with the different values of α . As we can see, when the model is trained on the mean squared error alone, it focuses solely on minimizing the magnitude differences between the predicted and original ECG signals. Notably, while the results for RMSE and MAE remain consistent for the models with $\alpha \leq 1$, the values for the PCC and DTW present higher variability, with an improvement of 4.65% in terms of PCC for the model with $\alpha = 0.5$ w.r.t. the model with $\alpha = 0$ and of 10.44% in terms of DTW. Interestingly, setting $\alpha = \infty$, resulted in the model performing well in terms of PCC but significantly worse across other metrics. This observation underscores the importance of employing a hybrid loss that considers the ECG signal's spatial and temporal aspects.

For our testing phase, we chose $\alpha = 0.1$ based on its performance during validation, showing promising results compared to $\alpha = 0$ and $\alpha = 1$, without extensive exploration of other values. However, a more detailed examination revealed $\alpha = 0.5$ to potentially offer better outcomes. This finding suggests that while $\alpha = 0.1$ provided satisfactory results, a further optimization of α could enhance model performance. In future work, we plan to investigate this aspect more thoroughly to identify the most effective α parameter value.

Table 3: ECGrecover performances for different values of α in Equation (1). Note that by ∞ , we denote the case when the Pearson loss is considered only.

α	PCC	RMSE	MAE	DTW
0	0.86	0.19	0.15	18.10
0.1	0.88	0.18	0.14	16.87
0.5	0.90	0.18	0.14	16.21
1	0.90	0.18	0.15	16.52
∞	0.91	0.43	0.39	95.37

A.2 Random masking

To assess the performance of the proposed ECGrecover, we evaluated its capability to reconstruct ECG signals when subjected to random masking. This entailed applying primers of random duration to randomly chosen parts of each lead, a scenario less likely to occur in real-life settings. This evaluation aimed to verify if the model had learned the inter-lead relationships rather than memorizing specific reconstruction patterns.

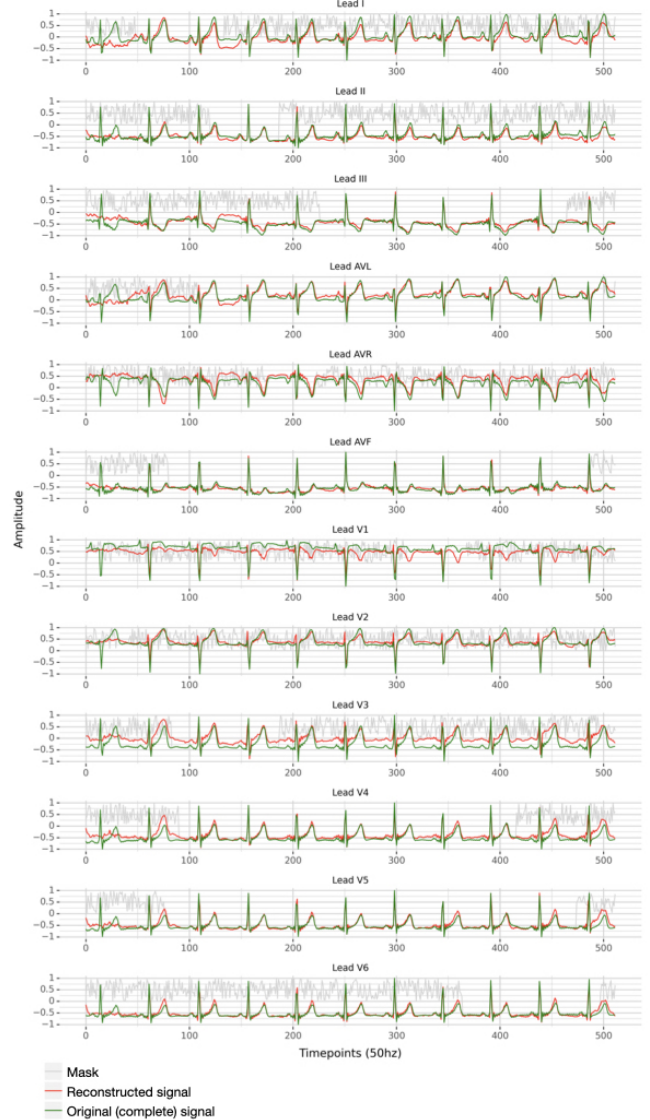


Figure 7: Example of ECG to which we apply a random mask. In green, we indicate the original signals, in red we denote reconstructed ones and in gray we provide the mask. The primer in the figure corresponds to the portion of the gray signals overlapping with the green one.

An illustration of an ECG subjected to such random masking, referred to as C_{Rdm} , is depicted in Figure 7. For this process, a random start and end point between 0 and the total length of the signal were selected for each ECG lead. The segments outside the range between these two points were masked.

The results, detailed in Table 4, indicate that ECGrecover consistently outperforms its competitors across various metrics, even in this challenging scenario. For instance, in the most difficult case concerning lead III, ECGrecover not only improves upon the best competitor, Pix2Pix, by 510% in terms of PCC but also surpasses it by approximately 77.78% in terms of DTW. Furthermore, ECGrecover

Table 4: Our method (ECGRecover) and the competitors for evaluating the PCC and DTW (mean \pm standard deviation) in case of the C_{Rdm} mask.

Lead	PCC (\uparrow)			DTW (\downarrow)		
	ECGrecover	EKGAN [12]	Pix2Pix [10]	ECGrecover	EKGAN [12]	Pix2Pix [10]
C_{Rdm}	0.79\pm0.11	0.23 \pm 0.15	0.09 \pm 0.11	0.05\pm0.05	0.37 \pm 0.24	0.19 \pm 0.25
	0.84\pm0.11	0.26 \pm 0.16	0.34 \pm 0.17	0.03\pm0.05	0.13 \pm 0.06	0.10 \pm 0.09
	0.61\pm0.22	-0.02 \pm 0.21	0.10 \pm 0.19	0.08\pm0.07	0.46 \pm 0.5	0.36 \pm 0.24
	0.82\pm0.17	0.22 \pm 0.13	0.18 \pm 0.14	0.03\pm0.06	0.09 \pm 0.08	0.08 \pm 0.07
	0.88\pm0.09	0.24 \pm 0.14	0.29 \pm 0.14	0.02\pm0.04	0.12 \pm 0.06	0.10 \pm 0.07

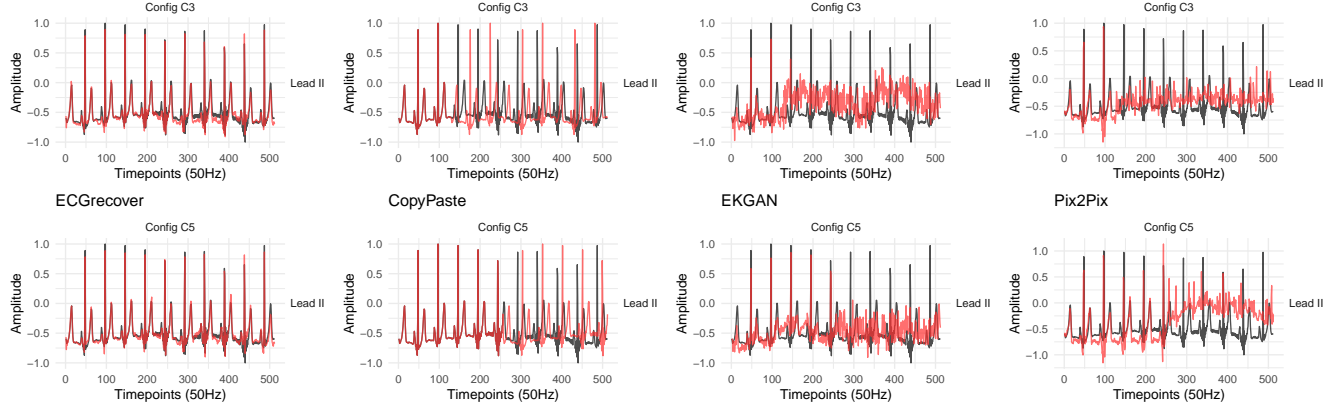


Figure 8: Lead II signals obtained with different approaches for C3 and C5. Reconstructed leads are in red, the original ones are in black.

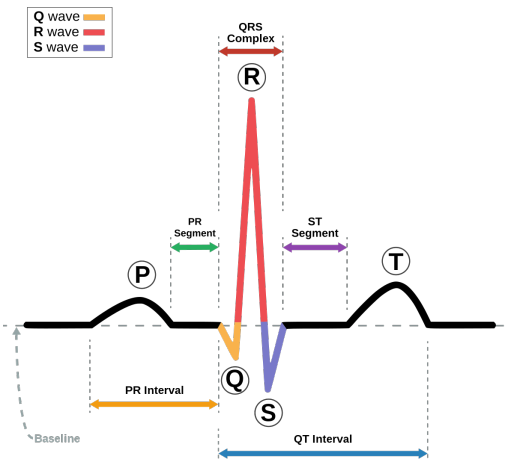


Figure 9: ECG waveforms with areas of interest: P waves, T waves and the QRS complex. From https://fr.wikipedia.org/wiki/Syndrome_du_QT_court.

demonstrates stable performance across different leads, contrasting

with the variability seen in competitors like EKGAN and Pix2Pix, which show wide fluctuations in PCC and DTW scores.

A.3 ECGrecover on PTB-XL

We present the evaluation of the proposed ECGrecover on a publicly available dataset, PTB-XL [27]. Specifically, the dataset contains 21799 recordings from 18869 patients of 10-second 12- lead ECGs sampled at 500Hz labeled as *normal*, *myocardial infarction*, *ST/T change*, *conduction disturbance* and *hypertrophy*. In Figure 10, we show the summary of the results. In particular, we followed the same experimental setting as the one already described for the Generepol dataset in Section 3.1.

To get an overall view, we also include the same representation of the results for the Generepol dataset in the figure.

A.4 Additional plots

We include additional plots in Figure 8 and Figure 9, which could not be accommodated in the main paper due to space limitations. Specifically, in Figure 8, we illustrate a lead II signal reconstruction from input masks C3 and C5 across all methodologies evaluated in our study. Meanwhile, Figure 9 presents the ECG waveforms alongside their labeled wave coordinates (peaks) to enhance comprehension of the findings discussed in Section 3.2.2.

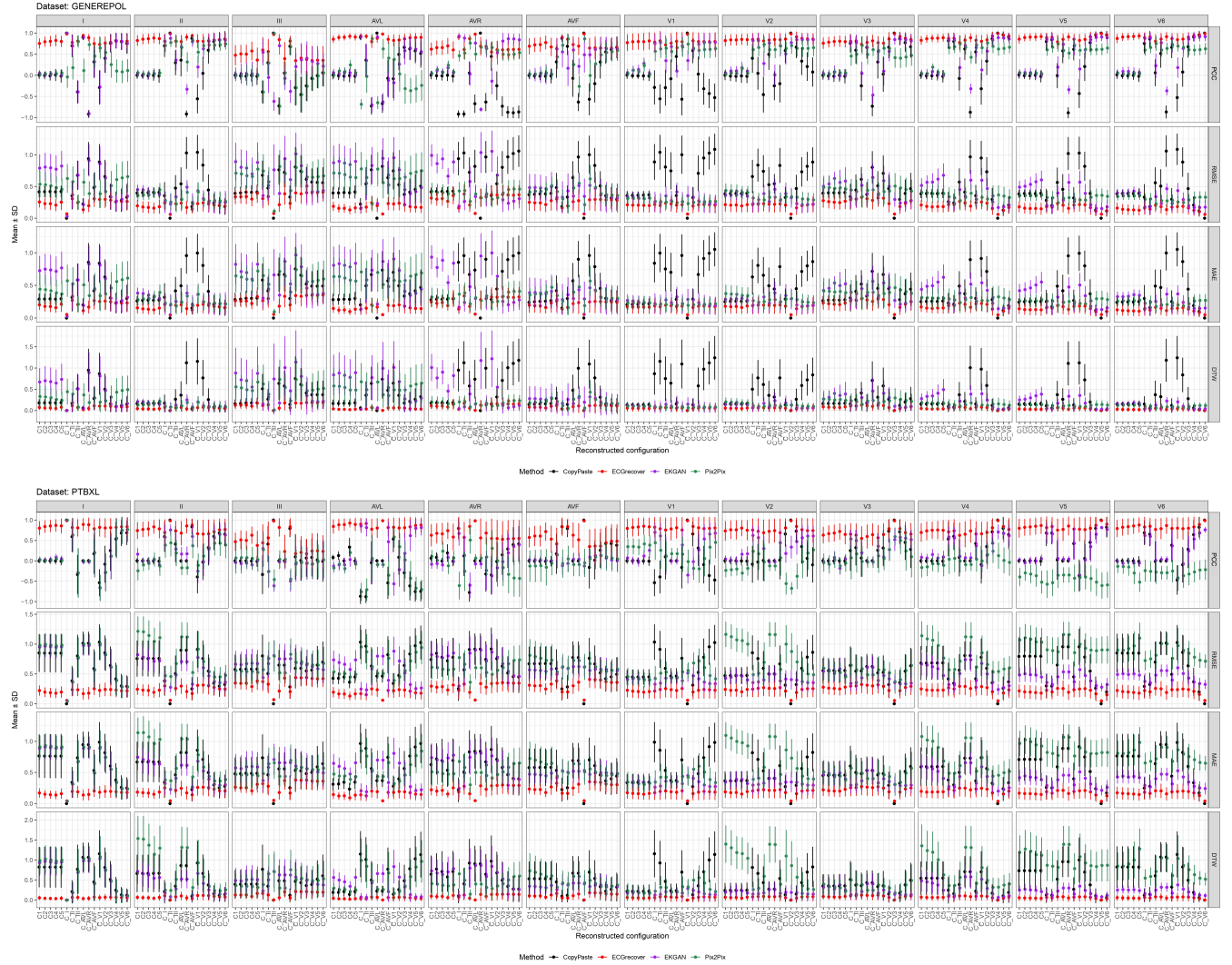


Figure 10: Comprehensive set of results on Generepol [23] and PTB-XL [27] datasets.

A.5 Experimental environment

The calculations were run on a Nvidia A100 80GB GPU, with the total training duration approximating 1 hour and 30 minutes.

B TABLES

This section includes the comprehensive numerical results of the evaluation. Specifically, Tables 5 to 7 present the results for the PCC metric; Tables 8 to 10 the results for RMSE metric; Tables 11 to 13 the results for MAE metric; Tables 14 to 16 the results for DTW metric.

Finally, in Tables 17 to 19 we include the results on the QT-segment preservation w.r.t. all the possible input masks. Additionally, we expanded the analysis on the QRS complex (see Figure 9) in Tables 20 to 22. Moreover, in Tables 23 to 25, we show the percentage of R peaks detected (%-R) in the reconstructed signals.

Table 5: ECG segment-recovery: PCC results for all the leads.

Lead	PCC (\uparrow)			
	ECGrecover	EKGAN [12]	Pix2Pix [10]	CopyPaste
C1	I 0.78 \pm 0.12	0.05 \pm 0.07	0.02 \pm 0.05	-0.01 \pm 0.09
	II 0.87 \pm 0.13	0.03 \pm 0.09	0.06 \pm 0.07	-0.02 \pm 0.08
	III 0.53 \pm 0.24	0.02 \pm 0.16	-0.0 \pm 0.1	-0.01 \pm 0.08
	AVL 0.64 \pm 0.16	0.04 \pm 0.07	0.04 \pm 0.06	-0.02 \pm 0.1
	AVR 0.87 \pm 0.09	0.05 \pm 0.1	0.01 \pm 0.07	-0.02 \pm 0.1
	AVF 0.74 \pm 0.19	0.02 \pm 0.12	0.02 \pm 0.08	-0.02 \pm 0.08
	V1 0.84 \pm 0.2	0.06 \pm 0.09	0.04 \pm 0.06	-0.02 \pm 0.09
	V2 0.87 \pm 0.14	0.06 \pm 0.08	0.02 \pm 0.05	-0.03 \pm 0.12
	V3 0.79 \pm 0.13	0.03 \pm 0.1	0.01 \pm 0.06	-0.03 \pm 0.1
	V4 0.86 \pm 0.1	0.03 \pm 0.1	0.04 \pm 0.06	-0.02 \pm 0.09
C2	V5 0.89 \pm 0.1	0.05 \pm 0.1	0.06 \pm 0.05	-0.01 \pm 0.08
	V6 0.9 \pm 0.1	0.06 \pm 0.09	0.05 \pm 0.06	-0.01 \pm 0.1
	I 0.82 \pm 0.12	0.01 \pm 0.05	0.03 \pm 0.06	-0.02 \pm 0.09
	II 0.9 \pm 0.12	0.02 \pm 0.1	0.03 \pm 0.08	-0.02 \pm 0.07
	III 0.54 \pm 0.21	0.04 \pm 0.24	-0.01 \pm 0.17	-0.02 \pm 0.09
	AVL 0.68 \pm 0.17	0.11 \pm 0.11	0.14 \pm 0.07	-0.03 \pm 0.09
	AVR 0.92 \pm 0.07	0.03 \pm 0.11	0.10 \pm 0.08	-0.03 \pm 0.1
	AVF 0.77 \pm 0.17	0.02 \pm 0.16	0.03 \pm 0.09	-0.02 \pm 0.07
	V1 0.86 \pm 0.2	0.12 \pm 0.11	0.13 \pm 0.08	-0.02 \pm 0.07
	V2 0.88 \pm 0.13	0.10 \pm 0.1	0.06 \pm 0.07	-0.04 \pm 0.11
C3	V3 0.82 \pm 0.12	0.01 \pm 0.11	0.03 \pm 0.06	-0.03 \pm 0.1
	V4 0.89 \pm 0.09	0.02 \pm 0.12	0.04 \pm 0.06	-0.03 \pm 0.08
	V5 0.92 \pm 0.09	0.06 \pm 0.1	0.04 \pm 0.05	-0.02 \pm 0.08
	V6 0.94 \pm 0.09	0.09 \pm 0.1	0.03 \pm 0.06	-0.02 \pm 0.07
	I 0.84 \pm 0.13	0.01 \pm 0.06	0.04 \pm 0.06	-0.03 \pm 0.11
	II 0.91 \pm 0.12	0.01 \pm 0.1	0.04 \pm 0.08	-0.03 \pm 0.09
	III 0.54 \pm 0.22	0.03 \pm 0.27	0.01 \pm 0.24	-0.03 \pm 0.11
	AVL 0.69 \pm 0.17	0.08 \pm 0.09	0.07 \pm 0.08	-0.03 \pm 0.11
	AVR 0.92 \pm 0.07	0.05 \pm 0.12	0.09 \pm 0.1	-0.04 \pm 0.12
	AVF 0.78 \pm 0.17	0.03 \pm 0.19	0.06 \pm 0.1	-0.03 \pm 0.09
C4	V1 0.87 \pm 0.19	0.14 \pm 0.11	0.09 \pm 0.08	-0.03 \pm 0.07
	V2 0.88 \pm 0.13	0.11 \pm 0.11	0.05 \pm 0.06	-0.04 \pm 0.13
	V3 0.84 \pm 0.12	0.07 \pm 0.15	0.08 \pm 0.09	-0.04 \pm 0.13
	V4 0.9 \pm 0.09	0.10 \pm 0.11	0.20 \pm 0.09	-0.03 \pm 0.1
	V5 0.93 \pm 0.09	0.06 \pm 0.11	0.05 \pm 0.06	-0.02 \pm 0.09
	V6 0.95 \pm 0.09	0.10 \pm 0.11	0.03 \pm 0.06	-0.02 \pm 0.08
	I 0.87 \pm 0.14	0.04 \pm 0.07	0.04 \pm 0.08	-0.02 \pm 0.14
	II 0.93 \pm 0.12	0.04 \pm 0.12	0.04 \pm 0.11	-0.02 \pm 0.13
	III 0.6 \pm 0.22	0.04 \pm 0.29	-0.0 \pm 0.26	-0.02 \pm 0.15
	AVL 0.74 \pm 0.19	0.17 \pm 0.14	0.25 \pm 0.1	-0.03 \pm 0.13
C5	AVR 0.94 \pm 0.07	0.04 \pm 0.13	0.25 \pm 0.11	-0.02 \pm 0.16
	AVF 0.82 \pm 0.16	0.04 \pm 0.23	0.07 \pm 0.16	-0.02 \pm 0.14
	V1 0.87 \pm 0.2	0.31 \pm 0.13	0.24 \pm 0.13	-0.03 \pm 0.11
	V2 0.89 \pm 0.13	0.18 \pm 0.14	0.17 \pm 0.09	-0.05 \pm 0.17
	V3 0.85 \pm 0.13	-0.01 \pm 0.1	0.06 \pm 0.07	-0.03 \pm 0.15
	V4 0.91 \pm 0.1	0.03 \pm 0.1	0.07 \pm 0.08	-0.02 \pm 0.12
	V5 0.93 \pm 0.09	0.04 \pm 0.12	0.05 \pm 0.07	-0.02 \pm 0.11
	V6 0.95 \pm 0.09	0.07 \pm 0.12	0.04 \pm 0.07	-0.02 \pm 0.11
	I 0.84 \pm 0.13	0.0 \pm 0.07	0.06 \pm 0.08	-0.03 \pm 0.15
	II 0.92 \pm 0.13	0.05 \pm 0.09	0.06 \pm 0.1	-0.02 \pm 0.16
C6	III 0.41 \pm 0.3	0.01 \pm 0.13	-0.0 \pm 0.07	-0.03 \pm 0.2
	AVL 0.64 \pm 0.2	0.06 \pm 0.08	0.08 \pm 0.08	-0.02 \pm 0.15
	AVR 0.93 \pm 0.08	0.01 \pm 0.08	0.06 \pm 0.09	-0.04 \pm 0.16
	AVF 0.73 \pm 0.22	0.03 \pm 0.1	0.02 \pm 0.12	-0.02 \pm 0.17
	V1 0.89 \pm 0.2	0.05 \pm 0.1	0.02 \pm 0.08	-0.03 \pm 0.12
	V2 0.89 \pm 0.14	0.09 \pm 0.09	0.05 \pm 0.07	-0.05 \pm 0.16
	V3 0.83 \pm 0.13	0.01 \pm 0.09	0.05 \pm 0.09	-0.04 \pm 0.17
	V4 0.92 \pm 0.09	0.0 \pm 0.09	0.03 \pm 0.08	-0.03 \pm 0.15
	V5 0.95 \pm 0.08	0.01 \pm 0.1	0.04 \pm 0.08	-0.03 \pm 0.14
	V6 0.96 \pm 0.08	0.07 \pm 0.1	0.03 \pm 0.07	-0.03 \pm 0.13

Table 6: ECG (limb) lead-reconstruction: PCC results for all the leads.

Lead	PCC (\uparrow)			
	ECGrecover	EKGAN [12]	Pix2Pix [10]	CopyPaste
C1	II 0.86 \pm 0.16	0.86 \pm 0.18	0.74 \pm 0.16	0.79 \pm 0.26
	III 0.69 \pm 0.3	0.66 \pm 0.31	-0.46 \pm 0.28	-0.44 \pm 0.27
	AVL 0.93 \pm 0.07	0.95 \pm 0.08	0.47 \pm 0.13	-0.95 \pm 0.09
	AVR 0.95 \pm 0.06	0.94 \pm 0.08	-0.70 \pm 0.12	0.91 \pm 0.06
	AVF 0.70 \pm 0.24	0.72 \pm 0.26	0.47 \pm 0.28	0.38 \pm 0.38
	V1 0.87 \pm 0.22	0.84 \pm 0.22	0.63 \pm 0.23	-0.37 \pm 0.4
	V2 0.90 \pm 0.15	0.88 \pm 0.15	0.65 \pm 0.2	0.45 \pm 0.34
	V3 0.85 \pm 0.15	0.83 \pm 0.16	0.49 \pm 0.22	0.84 \pm 0.22
	V4 0.90 \pm 0.11	0.87 \pm 0.14	0.68 \pm 0.15	0.88 \pm 0.18
	V5 0.93 \pm 0.11	0.89 \pm 0.13	0.62 \pm 0.14	0.87 \pm 0.2
C2	V6 0.94 \pm 0.12	0.92 \pm 0.13	0.62 \pm 0.13	0.84 \pm 0.24
	I 0.83 \pm 0.15	0.79 \pm 0.26	0.18 \pm 0.28	0.79 \pm 0.26
	III 0.64 \pm 0.29	0.01 \pm 0.36	0.33 \pm 0.3	0.34 \pm 0.3
	AVL 0.66 \pm 0.23	0.91 \pm 0.09	0.54 \pm 0.15	-0.95 \pm 0.08
	AVR 0.94 \pm 0.06	0.43 \pm 0.39	-0.06 \pm 0.38	0.44 \pm 0.38
	AVF 0.92 \pm 0.07	0.70 \pm 0.37	0.73 \pm 0.14	0.89 \pm 0.08
	V1 0.89 \pm 0.23	0.86 \pm 0.23	0.68 \pm 0.21	-0.65 \pm 0.34
	V2 0.91 \pm 0.15	0.88 \pm 0.17	0.71 \pm 0.21	0.07 \pm 0.39
	V3 0.85 \pm 0.14	0.83 \pm 0.18	0.51 \pm 0.24	0.69 \pm 0.32
	V4 0.91 \pm 0.11	0.87 \pm 0.14	0.71 \pm 0.15	0.87 \pm 0.2
C3	V5 0.94 \pm 0.12	0.90 \pm 0.13	0.69 \pm 0.13	0.90 \pm 0.18
	V6 0.95 \pm 0.11	0.92 \pm 0.13	0.68 \pm 0.13	0.92 \pm 0.19
	I 0.84 \pm 0.12	-0.44 \pm 0.27	0.84 \pm 0.14	-0.44 \pm 0.27
	II 0.85 \pm 0.15	0.37 \pm 0.25	0.85 \pm 0.15	0.34 \pm 0.3
	AVL 0.89 \pm 0.1	0.02 \pm 0.27	0.81 \pm 0.16	0.06 \pm 0.28
	AVR 0.85 \pm 0.15	-0.75 \pm 0.19	0.90 \pm 0.12	-0.78 \pm 0.2
	AVF 0.89 \pm 0.13	0.24 \pm 0.42	0.90 \pm 0.11	0.74 \pm 0.21
	V1 0.79 \pm 0.22	0.34 \pm 0.29	0.71 \pm 0.24	-0.36 \pm 0.42
	V2 0.87 \pm 0.16	0.27 \pm 0.3	0.79 \pm 0.19	-0.59 \pm 0.42
	V3 0.79 \pm 0.18	0.03 \pm 0.27	0.78 \pm 0.21	-0.31 \pm 0.35
C4	V4 0.83 \pm 0.17	0.19 \pm 0.25	0.80 \pm 0.2	-0.09 \pm 0.29
	V5 0.85 \pm 0.17	0.21 \pm 0.26	0.80 \pm 0.18	0.01 \pm 0.3
	V6 0.86 \pm 0.17	0.26 \pm 0.29	0.80 \pm 0.17	0.08 \pm 0.32
	I 0.95 \pm 0.04	0.91 \pm 0.06	0.14 \pm 0.28	0.91 \pm 0.06
	II 0.85 \pm 0.16	0.74 \pm 0.24	0.71 \pm 0.2	0.44 \pm 0.38
	III 0.88 \pm 0.13	0.77 \pm 0.2	-0.79 \pm 0.2	-0.78 \pm 0.2
	AVR 0.91 \pm 0.1	0.91 \pm 0.05	-0.65 \pm 0.15	1.00 \pm 0.0
	AVF 0.79 \pm 0.19	0.68 \pm 0.26	0.28 \pm 0.34	-0.07 \pm 0.44
	V1 0.84 \pm 0.24	0.75 \pm 0.24	0.64 \pm 0.25	-0.13 \pm 0.46
	V2 0.89 \pm 0.16	0.81 \pm 0.18	0.65 \pm 0.2	0.59 \pm 0.37
C5	V3 0.83 \pm 0.16	0.71 \pm 0.22	0.55 \pm 0.23	0.75 \pm 0.26
	V4 0.87 \pm 0.14	0.76 \pm 0.19	0.70 \pm 0.17	0.69 \pm 0.26
	V5 0.89 \pm 0.14	0.78 \pm 0.19	0.61 \pm 0.16	0.65 \pm 0.29
	V6 0.90 \pm 0.14	0.82 \pm 0.19	0.62 \pm 0.16	0.61 \pm 0.34
	I 0.92 $\pm</math$			

Table 7: ECG (thoracic) lead-reconstruction: PCC results for all the leads.

		PCC (\uparrow)			
Lead		ECGrecover	EKGAN [12]	Pix2Pix [10]	CopyPaste
CV ₁	I	0.79 \pm 0.18	-0.36 \pm 0.4	0.75 \pm 0.25	-0.37 \pm 0.4
	II	0.87 \pm 0.17	0.18 \pm 0.26	0.61 \pm 0.25	-0.65 \pm 0.34
	III	0.41 \pm 0.31	0.21 \pm 0.31	-0.36 \pm 0.41	-0.36 \pm 0.42
	AVL	0.60 \pm 0.23	-0.17 \pm 0.31	0.69 \pm 0.15	0.50 \pm 0.34
	AVR	0.87 \pm 0.14	-0.24 \pm 0.42	0.51 \pm 0.4	-0.13 \pm 0.46
	AVF	0.71 \pm 0.24	0.52 \pm 0.2	-0.04 \pm 0.38	-0.71 \pm 0.38
	V2	0.90 \pm 0.13	0.56 \pm 0.25	0.68 \pm 0.16	0.66 \pm 0.3
	V3	0.81 \pm 0.15	0.11 \pm 0.33	0.66 \pm 0.16	0.04 \pm 0.42
	V4	0.85 \pm 0.15	0.13 \pm 0.25	0.67 \pm 0.15	-0.38 \pm 0.38
	V5	0.88 \pm 0.15	0.14 \pm 0.23	0.62 \pm 0.13	-0.49 \pm 0.34
CV ₂	V6	0.90 \pm 0.15	0.17 \pm 0.24	0.72 \pm 0.13	-0.59 \pm 0.33
	I	0.80 \pm 0.16	0.45 \pm 0.34	0.63 \pm 0.28	0.45 \pm 0.34
	II	0.87 \pm 0.17	0.68 \pm 0.23	0.77 \pm 0.21	0.07 \pm 0.39
	III	0.50 \pm 0.35	0.46 \pm 0.37	-0.59 \pm 0.42	-0.59 \pm 0.42
	AVL	0.65 \pm 0.21	0.60 \pm 0.28	0.61 \pm 0.14	-0.27 \pm 0.34
	AVR	0.87 \pm 0.13	0.31 \pm 0.4	0.06 \pm 0.42	0.59 \pm 0.37
	AVF	0.74 \pm 0.27	0.68 \pm 0.24	0.31 \pm 0.35	-0.24 \pm 0.44
	V1	0.88 \pm 0.2	0.66 \pm 0.22	0.71 \pm 0.23	0.66 \pm 0.3
	V3	0.91 \pm 0.16	0.61 \pm 0.23	0.67 \pm 0.19	0.72 \pm 0.26
	V4	0.88 \pm 0.13	0.61 \pm 0.22	0.80 \pm 0.14	0.38 \pm 0.33
CV ₃	V5	0.90 \pm 0.13	0.63 \pm 0.21	0.64 \pm 0.12	0.21 \pm 0.34
	V6	0.90 \pm 0.13	0.67 \pm 0.2	0.69 \pm 0.13	0.07 \pm 0.35
	I	0.83 \pm 0.16	0.84 \pm 0.22	0.28 \pm 0.31	0.84 \pm 0.22
	II	0.88 \pm 0.17	0.86 \pm 0.18	0.76 \pm 0.18	0.69 \pm 0.32
	III	0.46 \pm 0.34	0.51 \pm 0.4	-0.32 \pm 0.36	-0.31 \pm 0.35
	AVL	0.66 \pm 0.23	0.86 \pm 0.19	0.51 \pm 0.15	-0.81 \pm 0.24
	AVR	0.90 \pm 0.12	0.68 \pm 0.32	-0.38 \pm 0.35	0.75 \pm 0.26
	AVF	0.73 \pm 0.26	0.74 \pm 0.27	0.53 \pm 0.27	0.39 \pm 0.39
	V1	0.87 \pm 0.21	0.81 \pm 0.22	0.64 \pm 0.21	0.04 \pm 0.42
	V2	0.95 \pm 0.13	0.89 \pm 0.14	0.69 \pm 0.2	0.72 \pm 0.26
CV ₄	V4	0.96 \pm 0.1	0.89 \pm 0.15	0.72 \pm 0.16	0.91 \pm 0.15
	V5	0.95 \pm 0.12	0.89 \pm 0.14	0.62 \pm 0.13	0.83 \pm 0.21
	V6	0.94 \pm 0.11	0.91 \pm 0.14	0.63 \pm 0.13	0.75 \pm 0.26
	I	0.85 \pm 0.15	0.88 \pm 0.18	0.11 \pm 0.27	0.88 \pm 0.18
	II	0.89 \pm 0.16	0.90 \pm 0.17	0.75 \pm 0.15	0.87 \pm 0.2
	III	0.43 \pm 0.34	0.41 \pm 0.36	-0.10 \pm 0.29	-0.09 \pm 0.29
	AVL	0.67 \pm 0.22	0.91 \pm 0.13	0.50 \pm 0.15	-0.92 \pm 0.14
	AVR	0.92 \pm 0.1	0.72 \pm 0.27	-0.42 \pm 0.3	0.69 \pm 0.26
	AVF	0.72 \pm 0.25	0.73 \pm 0.28	0.58 \pm 0.24	0.61 \pm 0.28
	V1	0.87 \pm 0.21	0.85 \pm 0.22	0.66 \pm 0.2	-0.38 \pm 0.38
CV ₅	V2	0.92 \pm 0.13	0.89 \pm 0.14	0.68 \pm 0.2	0.38 \pm 0.33
	V3	0.94 \pm 0.11	0.90 \pm 0.12	0.43 \pm 0.23	0.91 \pm 0.15
	V5	0.98 \pm 0.07	0.94 \pm 0.11	0.63 \pm 0.13	0.98 \pm 0.08
	V6	0.97 \pm 0.07	0.95 \pm 0.11	0.62 \pm 0.13	0.94 \pm 0.1
	I	0.86 \pm 0.14	0.86 \pm 0.2	0.08 \pm 0.27	0.87 \pm 0.2
	II	0.90 \pm 0.15	0.90 \pm 0.16	0.75 \pm 0.14	0.90 \pm 0.18
	III	0.43 \pm 0.33	0.34 \pm 0.33	0.0 \pm 0.3	0.01 \pm 0.3
	AVL	0.66 \pm 0.21	0.90 \pm 0.12	0.51 \pm 0.14	-0.93 \pm 0.13
	AVR	0.93 \pm 0.11	0.70 \pm 0.28	-0.37 \pm 0.32	0.65 \pm 0.29
	AVF	0.72 \pm 0.23	0.73 \pm 0.27	0.60 \pm 0.23	0.67 \pm 0.26
CV ₆	V1	0.87 \pm 0.21	0.86 \pm 0.22	0.67 \pm 0.2	-0.49 \pm 0.34
	V2	0.91 \pm 0.14	0.89 \pm 0.14	0.69 \pm 0.21	0.21 \pm 0.34
	V3	0.91 \pm 0.14	0.88 \pm 0.15	0.46 \pm 0.23	0.83 \pm 0.21
	V4	0.97 \pm 0.08	0.92 \pm 0.11	0.66 \pm 0.14	0.98 \pm 0.08
	V6	0.98 \pm 0.09	0.95 \pm 0.11	0.63 \pm 0.13	0.98 \pm 0.1
	I	0.87 \pm 0.16	0.84 \pm 0.24	0.10 \pm 0.27	0.84 \pm 0.24
	II	0.91 \pm 0.15	0.90 \pm 0.17	0.78 \pm 0.13	0.92 \pm 0.19
	III	0.43 \pm 0.33	0.25 \pm 0.3	0.08 \pm 0.32	0.08 \pm 0.32
	AVL	0.68 \pm 0.23	0.89 \pm 0.14	0.55 \pm 0.13	-0.92 \pm 0.15
	AVR	0.94 \pm 0.11	0.65 \pm 0.32	-0.30 \pm 0.36	0.61 \pm 0.34

Table 8: ECG segment-recovery: RMSE results for all the leads.

		RMSE (\downarrow)			
Lead		ECGrecover	EKGAN [12]	Pix2Pix [10]	CopyPaste
C1	I	0.24 \pm 0.09	0.82 \pm 0.22	0.47 \pm 0.21	0.40 \pm 0.09
	II	0.16 \pm 0.09	0.45 \pm 0.08	0.34 \pm 0.09	0.39 \pm 0.07
	III	0.32 \pm 0.11	0.83 \pm 0.3	0.74 \pm 0.23	0.38 \pm 0.1
	AVL	0.30 \pm 0.1	1.03 \pm 0.17	0.38 \pm 0.14	0.41 \pm 0.07
	AVR	0.17 \pm 0.07	0.88 \pm 0.27	0.69 \pm 0.27	0.38 \pm 0.1
	AVF	0.21 \pm 0.13	0.39 \pm 0.22	0.40 \pm 0.1	0.36 \pm 0.09
	V1	0.18 \pm 0.11	0.32 \pm 0.08	0.29 \pm 0.09	0.35 \pm 0.07
	V2	0.18 \pm 0.11	0.34 \pm 0.1	0.41 \pm 0.11	0.38 \pm 0.06
	V3	0.25 \pm 0.11	0.47 \pm 0.14	0.43 \pm 0.18	0.39 \pm 0.08
	V4	0.19 \pm 0.08	0.51 \pm 0.11	0.35 \pm 0.14	0.38 \pm 0.07
C2	V5	0.15 \pm 0.08	0.49 \pm 0.1	0.33 \pm 0.09	0.38 \pm 0.06
	V6	0.14 \pm 0.08	0.39 \pm 0.07	0.33 \pm 0.06	0.39 \pm 0.06
	I	0.21 \pm 0.09	0.84 \pm 0.22	0.47 \pm 0.2	0.40 \pm 0.09
	II	0.15 \pm 0.09	0.44 \pm 0.08	0.35 \pm 0.08	0.39 \pm 0.07
	III	0.32 \pm 0.11	0.72 \pm 0.28	0.72 \pm 0.21	0.38 \pm 0.1
	AVL	0.28 \pm 0.1	0.90 \pm 0.15	0.36 \pm 0.13	0.41 \pm 0.07
	AVR	0.14 \pm 0.07	0.90 \pm 0.27	0.69 \pm 0.26	0.39 \pm 0.09
	AVF	0.21 \pm 0.13	0.39 \pm 0.21	0.42 \pm 0.1	0.36 \pm 0.09
	V1	0.18 \pm 0.11	0.32 \pm 0.08	0.28 \pm 0.09	0.35 \pm 0.06
	V2	0.17 \pm 0.11	0.34 \pm 0.09	0.41 \pm 0.11	0.38 \pm 0.06
C3	V3	0.24 \pm 0.11	0.51 \pm 0.14	0.43 \pm 0.18	0.40 \pm 0.08
	V4	0.17 \pm 0.08	0.56 \pm 0.11	0.35 \pm 0.14	0.39 \pm 0.07
	V5	0.13 \pm 0.08	0.50 \pm 0.11	0.33 \pm 0.09	0.39 \pm 0.06
	V6	0.12 \pm 0.08	0.39 \pm 0.07	0.34 \pm 0.06	0.39 \pm 0.06
	I	0.20 \pm 0.1	0.83 \pm 0.22	0.45 \pm 0.2	0.41 \pm 0.09
	II	0.14 \pm 0.09	0.42 \pm 0.07	0.36 \pm 0.08	0.40 \pm 0.08
	III	0.32 \pm 0.12	0.71 \pm 0.27	0.67 \pm 0.2	0.38 \pm 0.11
	AVL	0.29 \pm 0.11	0.97 \pm 0.16	0.36 \pm 0.13	0.41 \pm 0.07
	AVR	0.14 \pm 0.07	0.87 \pm 0.27	0.66 \pm 0.26	0.39 \pm 0.09
	AVF	0.20 \pm 0.13	0.39 \pm 0.21	0.42 \pm 0.1	0.36 \pm 0.09
C4	V1	0.18 \pm 0.11	0.30 \pm 0.09	0.29 \pm 0.09	0.35 \pm 0.06
	V2	0.17 \pm 0.11	0.35 \pm 0.09	0.40 \pm 0.11	0.38 \pm 0.06
	V3	0.23 \pm 0.11	0.62 \pm 0.1	0.42 \pm 0.17	0.40 \pm 0.08
	V4	0.15 \pm 0.08	0.57 \pm 0.14	0.33 \pm 0.14	0.39 \pm 0.07
	V5	0.12 \pm 0.09	0.54 \pm 0.12	0.33 \pm 0.09	0.39 \pm 0.06
	V6	0.11 \pm 0.08	0.40 \pm 0.07	0.34 \pm 0.06	0.39 \pm 0.06
	I	0.18 \pm 0.09	0.81 \pm 0.22	0.42 \pm 0.18	0.40 \pm 0.09
	II	0.13 \pm 0.09	0.39 \pm 0.06	0.39 \pm 0.08	0.40 \pm 0.08
	III	0.28 \pm 0.11	0.62 \pm 0.26	0.64 \pm 0.19	0.38 \pm 0.11
	AVL	0.24 \pm 0.11	0.68 \pm 0.13	0.35 \pm 0.12	0.42 \pm 0.07
C5</td					

Table 9: ECG (limb) lead-reconstruction: RMSE results for all the leads.

		RMSE (\downarrow)			
Lead	ECGrecover	EKGAN [12]	Pix2Pix [10]	CopyPaste	
C _I	II	0.20 \pm 0.13	0.19 \pm 0.17	0.23 \pm 0.14	0.29 \pm 0.21
	III	0.28 \pm 0.15	0.33 \pm 0.17	0.70 \pm 0.26	0.64 \pm 0.23
	AVR	0.15 \pm 0.06	0.16 \pm 0.1	0.41 \pm 0.14	0.93 \pm 0.26
	AVL	0.13 \pm 0.08	0.14 \pm 0.07	0.76 \pm 0.27	0.20 \pm 0.1
	AVF	0.25 \pm 0.16	0.24 \pm 0.22	0.38 \pm 0.19	0.43 \pm 0.23
	V1	0.19 \pm 0.12	0.21 \pm 0.16	0.24 \pm 0.11	0.91 \pm 0.28
	V2	0.18 \pm 0.13	0.19 \pm 0.13	0.29 \pm 0.11	0.66 \pm 0.26
	V3	0.26 \pm 0.14	0.29 \pm 0.15	0.41 \pm 0.17	0.29 \pm 0.2
	V4	0.19 \pm 0.11	0.23 \pm 0.11	0.30 \pm 0.15	0.22 \pm 0.16
	V5	0.16 \pm 0.1	0.17 \pm 0.1	0.30 \pm 0.11	0.24 \pm 0.18
C _{II}	V6	0.13 \pm 0.1	0.15 \pm 0.11	0.27 \pm 0.09	0.28 \pm 0.21
	I	0.29 \pm 0.14	0.31 \pm 0.22	0.55 \pm 0.24	0.29 \pm 0.21
	III	0.32 \pm 0.14	0.46 \pm 0.23	0.53 \pm 0.23	0.41 \pm 0.2
	AVL	0.37 \pm 0.15	0.23 \pm 0.14	0.41 \pm 0.15	1.07 \pm 0.25
	AVR	0.15 \pm 0.09	0.52 \pm 0.26	0.60 \pm 0.28	0.49 \pm 0.26
	AVF	0.14 \pm 0.08	0.22 \pm 0.25	0.26 \pm 0.15	0.16 \pm 0.08
	V1	0.17 \pm 0.12	0.19 \pm 0.16	0.24 \pm 0.11	1.08 \pm 0.27
	V2	0.18 \pm 0.13	0.19 \pm 0.12	0.26 \pm 0.11	0.86 \pm 0.26
	V3	0.27 \pm 0.14	0.28 \pm 0.13	0.37 \pm 0.18	0.41 \pm 0.24
	V4	0.19 \pm 0.11	0.21 \pm 0.1	0.29 \pm 0.14	0.20 \pm 0.14
C _{III}	V5	0.14 \pm 0.11	0.16 \pm 0.12	0.31 \pm 0.11	0.16 \pm 0.13
	V6	0.12 \pm 0.09	0.14 \pm 0.12	0.29 \pm 0.09	0.14 \pm 0.13
	I	0.21 \pm 0.11	0.64 \pm 0.23	0.22 \pm 0.12	0.64 \pm 0.23
	II	0.20 \pm 0.11	0.31 \pm 0.12	0.18 \pm 0.13	0.41 \pm 0.2
	AVL	0.18 \pm 0.11	0.52 \pm 0.23	0.23 \pm 0.12	0.72 \pm 0.23
	AVR	0.22 \pm 0.11	0.80 \pm 0.29	0.19 \pm 0.12	0.72 \pm 0.24
	AVF	0.16 \pm 0.11	0.33 \pm 0.27	0.16 \pm 0.11	0.30 \pm 0.18
	V1	0.22 \pm 0.12	0.32 \pm 0.15	0.23 \pm 0.11	0.82 \pm 0.31
	V2	0.20 \pm 0.12	0.36 \pm 0.14	0.26 \pm 0.11	0.72 \pm 0.25
	V3	0.29 \pm 0.15	0.48 \pm 0.19	0.29 \pm 0.17	0.59 \pm 0.19
C _{AVL}	V4	0.24 \pm 0.12	0.42 \pm 0.14	0.24 \pm 0.16	0.53 \pm 0.21
	V5	0.20 \pm 0.11	0.37 \pm 0.12	0.22 \pm 0.11	0.51 \pm 0.23
	V6	0.18 \pm 0.11	0.32 \pm 0.1	0.21 \pm 0.09	0.49 \pm 0.24
	I	0.12 \pm 0.06	0.20 \pm 0.09	0.54 \pm 0.21	0.20 \pm 0.1
	II	0.20 \pm 0.13	0.24 \pm 0.16	0.25 \pm 0.15	0.49 \pm 0.26
	III	0.19 \pm 0.11	0.37 \pm 0.16	0.78 \pm 0.26	0.72 \pm 0.24
	AVR	0.17 \pm 0.1	0.25 \pm 0.09	0.74 \pm 0.27	0.0 \pm 0.0
	AVF	0.21 \pm 0.15	0.29 \pm 0.2	0.43 \pm 0.2	0.61 \pm 0.26
	V1	0.20 \pm 0.12	0.24 \pm 0.15	0.24 \pm 0.11	0.73 \pm 0.29
	V2	0.19 \pm 0.13	0.22 \pm 0.14	0.30 \pm 0.11	0.48 \pm 0.28
C _{AVR}	V3	0.28 \pm 0.14	0.34 \pm 0.18	0.40 \pm 0.18	0.33 \pm 0.19
	V4	0.21 \pm 0.12	0.32 \pm 0.14	0.29 \pm 0.15	0.38 \pm 0.21
	V5	0.18 \pm 0.11	0.27 \pm 0.12	0.29 \pm 0.11	0.42 \pm 0.24
	V6	0.16 \pm 0.11	0.21 \pm 0.11	0.25 \pm 0.09	0.47 \pm 0.26
	I	0.17 \pm 0.1	0.90 \pm 0.25	0.31 \pm 0.19	0.93 \pm 0.26
	II	0.14 \pm 0.1	0.46 \pm 0.11	0.37 \pm 0.15	1.07 \pm 0.25
	III	0.35 \pm 0.17	0.89 \pm 0.36	0.70 \pm 0.22	0.72 \pm 0.23
	AVL	0.29 \pm 0.14	1.05 \pm 0.32	0.27 \pm 0.14	0.0 \pm 0.0
	AVF	0.21 \pm 0.18	0.45 \pm 0.2	0.53 \pm 0.17	0.99 \pm 0.25
	V1	0.18 \pm 0.12	0.37 \pm 0.14	0.22 \pm 0.11	0.32 \pm 0.16
C _{AVR}	V2	0.18 \pm 0.13	0.42 \pm 0.16	0.30 \pm 0.1	0.52 \pm 0.15
	V3	0.25 \pm 0.14	0.60 \pm 0.21	0.39 \pm 0.19	0.78 \pm 0.26
	V4	0.17 \pm 0.09	0.58 \pm 0.16	0.34 \pm 0.15	1.0 \pm 0.27
	V5	0.13 \pm 0.09	0.55 \pm 0.13	0.28 \pm 0.13	1.07 \pm 0.26
	V6	0.11 \pm 0.09	0.45 \pm 0.08	0.24 \pm 0.1	1.11 \pm 0.25
	I	0.28 \pm 0.13	0.44 \pm 0.23	0.45 \pm 0.23	0.43 \pm 0.23
	II	0.13 \pm 0.07	0.20 \pm 0.14	0.18 \pm 0.13	0.16 \pm 0.08
	III	0.21 \pm 0.1	0.52 \pm 0.3	0.39 \pm 0.2	0.30 \pm 0.18
	AVL	0.31 \pm 0.14	0.32 \pm 0.18	0.36 \pm 0.14	0.99 \pm 0.25
	AVR	0.21 \pm 0.1	0.63 \pm 0.28	0.48 \pm 0.27	0.61 \pm 0.26
C _{AVF}	V1	0.18 \pm 0.12	0.21 \pm 0.15	0.24 \pm 0.11	1.03 \pm 0.3
	V2	0.19 \pm 0.13	0.24 \pm 0.13	0.26 \pm 0.1	0.85 \pm 0.27
	V3	0.30 \pm 0.14	0.35 \pm 0.14	0.34 \pm 0.17	0.47 \pm 0.23
	V4	0.22 \pm 0.11	0.28 \pm 0.13	0.26 \pm 0.14	0.31 \pm 0.17
	V5	0.18 \pm 0.11	0.23 \pm 0.12	0.27 \pm 0.11	0.27 \pm 0.17
	V6	0.15 \pm 0.1	0.20 \pm 0.12	0.27 \pm 0.09	0.24 \pm 0.18

Table 10: ECG (thoracic) lead-reconstruction: RMSE results for all the leads.

		RMSE (\downarrow)			
Lead	ECGrecover	EKGAN [12]	Pix2Pix [10]	CopyPaste	
C _{V1}	I	0.26 \pm 0.13	0.88 \pm 0.27	0.30 \pm 0.22	0.91 \pm 0.28
	II	0.19 \pm 0.12	0.41 \pm 0.13	0.39 \pm 0.15	1.08 \pm 0.27
	III	0.39 \pm 0.13	0.96 \pm 0.33	0.81 \pm 0.3	0.82 \pm 0.31
	AVL	0.35 \pm 0.14	1.09 \pm 0.32	0.26 \pm 0.13	0.32 \pm 0.16
	AVR	0.20 \pm 0.1	0.96 \pm 0.32	0.57 \pm 0.31	0.73 \pm 0.29
	V2	0.18 \pm 0.11	0.36 \pm 0.17	0.31 \pm 0.1	0.30 \pm 0.16
	V3	0.29 \pm 0.13	0.56 \pm 0.24	0.36 \pm 0.2	0.69 \pm 0.28
	V4	0.23 \pm 0.11	0.60 \pm 0.19	0.28 \pm 0.15	1.0 \pm 0.27
	V5	0.19 \pm 0.11	0.57 \pm 0.18	0.26 \pm 0.1	1.07 \pm 0.26
	V6	0.15 \pm 0.1	0.43 \pm 0.12	0.23 \pm 0.09	1.1 \pm 0.25
C _{V2}	I	0.26 \pm 0.13	0.64 \pm 0.26	0.35 \pm 0.23	0.66 \pm 0.26
	II	0.20 \pm 0.14	0.27 \pm 0.13	0.26 \pm 0.12	0.86 \pm 0.26
	III	0.35 \pm 0.16	0.79 \pm 0.34	0.72 \pm 0.24	0.72 \pm 0.25
	AVL	0.36 \pm 0.15	0.66 \pm 0.29	0.28 \pm 0.13	0.52 \pm 0.15
	AVR	0.21 \pm 0.11	0.74 \pm 0.31	0.58 \pm 0.29	0.48 \pm 0.28
	V1	0.24 \pm 0.18	0.41 \pm 0.26	0.47 \pm 0.16	0.85 \pm 0.27
	V3	0.19 \pm 0.13	0.50 \pm 0.22	0.39 \pm 0.21	0.43 \pm 0.22
	V4	0.20 \pm 0.12	0.46 \pm 0.16	0.26 \pm 0.17	0.74 \pm 0.23
	V5	0.18 \pm 0.12	0.37 \pm 0.15	0.25 \pm 0.1	0.84 \pm 0.23
	V6	0.16 \pm 0.11	0.27 \pm 0.11	0.22 \pm 0.09	0.90 \pm 0.23
C _{V3}	I	0.25 \pm 0.14	0.28 \pm 0.2	0.46 \pm 0.23	0.29 \pm 0.2
	II	0.18 \pm 0.14	0.20 \pm 0.17	0.23 \pm 0.13	0.41 \pm 0.24
	III	0.37 \pm 0.16	0.43 \pm 0.3	0.63 \pm 0.21	0.59 \pm 0.19
	AVL	0.35 \pm 0.15	0.23 \pm 0.19	0.35 \pm 0.14	0.78 \pm 0.26
	AVR	0.18 \pm 0.11	0.39 \pm 0.26	0.62 \pm 0.25	0.33 \pm 0.19
	V1	0.23 \pm 0.18	0.28 \pm 0.26	0.36 \pm 0.15	0.47 \pm 0.23
	V2	0.18 \pm 0.11	0.23 \pm 0.16	0.23 \pm 0.1	0.69 \pm 0.28
	V4	0.13 \pm 0.1	0.23 \pm 0.11	0.32 \pm 0.16	0.27 \pm 0.18
	V5	0.12 \pm 0.11	0.18 \pm 0.12	0.30 \pm 0.11	0.38 \pm 0.22
	V6	0.13 \pm 0.1	0.17 \pm 0.1	0.27 \pm 0.09	0.45 \pm 0.25
C _{V4}	I	0.24 \pm 0.13	0.23 \pm 0.16	0.59 \pm 0.25	0.22 \pm 0.16
	II	0.17 \pm 0.12	0.18 \pm 0.17	0.23 \pm 0.13	0.20 \pm 0.14
	III	0.37 \pm 0.15	0.35 \pm 0.22	0.56 \pm 0.25	0.53 \pm 0.21
	AVL	0.35 \pm 0.14	0.21 \pm 0.11	0.44 \pm 0.15	1.0 \pm 0.27</

Table 11: ECG segment-recovery: MAE results for all the leads.

		MAE (↓)			
Lead		ECGrecover	EKGAN [12]	Pix2Pix [10]	CopyPaste
C1	I	0.18±0.08	0.76±0.22	0.37±0.23	0.27±0.09
	II	0.13±0.08	0.38±0.08	0.26±0.09	0.25±0.07
	III	0.25±0.1	0.76±0.31	0.67±0.25	0.27±0.1
	AVL	0.23±0.08	0.97±0.18	0.26±0.15	0.28±0.06
	AVR	0.13±0.06	0.81±0.28	0.62±0.29	0.27±0.09
	AVF	0.16±0.12	0.29±0.23	0.34±0.11	0.22±0.09
	V1	0.14±0.1	0.24±0.09	0.20±0.1	0.19±0.07
	V2	0.15±0.1	0.25±0.11	0.35±0.13	0.24±0.06
	V3	0.21±0.11	0.38±0.14	0.35±0.2	0.26±0.07
	V4	0.15±0.07	0.43±0.12	0.26±0.16	0.24±0.06
	V5	0.12±0.08	0.42±0.1	0.23±0.1	0.24±0.06
	V6	0.10±0.08	0.32±0.07	0.24±0.07	0.23±0.06
C2	I	0.16±0.08	0.79±0.23	0.36±0.23	0.28±0.08
	II	0.12±0.07	0.38±0.08	0.27±0.09	0.25±0.08
	III	0.24±0.09	0.62±0.28	0.64±0.23	0.27±0.1
	AVL	0.21±0.08	0.80±0.15	0.26±0.14	0.28±0.06
	AVR	0.11±0.06	0.84±0.29	0.62±0.29	0.28±0.08
	AVF	0.16±0.11	0.30±0.22	0.37±0.11	0.22±0.1
	V1	0.14±0.1	0.23±0.09	0.20±0.1	0.19±0.07
	V2	0.14±0.1	0.26±0.1	0.34±0.13	0.25±0.06
	V3	0.19±0.1	0.42±0.14	0.35±0.2	0.27±0.07
	V4	0.14±0.07	0.48±0.11	0.25±0.16	0.25±0.06
	V5	0.10±0.08	0.43±0.11	0.24±0.1	0.24±0.06
	V6	0.09±0.08	0.32±0.07	0.25±0.07	0.24±0.06
C3	I	0.15±0.08	0.77±0.23	0.34±0.22	0.28±0.09
	II	0.11±0.08	0.35±0.07	0.28±0.09	0.26±0.08
	III	0.24±0.1	0.62±0.28	0.59±0.21	0.28±0.12
	AVL	0.22±0.09	0.92±0.17	0.25±0.14	0.28±0.07
	AVR	0.11±0.06	0.81±0.28	0.60±0.29	0.28±0.08
	AVF	0.15±0.11	0.29±0.22	0.37±0.11	0.22±0.1
	V1	0.14±0.1	0.22±0.09	0.20±0.1	0.19±0.07
	V2	0.14±0.11	0.27±0.09	0.34±0.13	0.26±0.07
	V3	0.19±0.1	0.42±0.14	0.35±0.2	0.27±0.07
	V4	0.13±0.07	0.49±0.14	0.25±0.16	0.25±0.07
	V5	0.10±0.08	0.47±0.12	0.24±0.1	0.24±0.06
	V6	0.09±0.08	0.33±0.07	0.25±0.07	0.24±0.07
C4	I	0.14±0.08	0.75±0.23	0.31±0.2	0.28±0.09
	II	0.11±0.07	0.31±0.07	0.32±0.09	0.25±0.09
	III	0.21±0.09	0.52±0.26	0.55±0.2	0.28±0.12
	AVL	0.17±0.08	0.56±0.11	0.26±0.13	0.28±0.07
	AVR	0.09±0.05	0.79±0.27	0.56±0.27	0.28±0.09
	AVF	0.13±0.09	0.30±0.21	0.39±0.12	0.23±0.11
	V1	0.14±0.1	0.21±0.1	0.21±0.1	0.20±0.08
	V2	0.13±0.1	0.28±0.08	0.32±0.13	0.25±0.07
	V3	0.18±0.1	0.45±0.21	0.34±0.19	0.27±0.08
	V4	0.13±0.08	0.55±0.17	0.25±0.15	0.25±0.07
	V5	0.10±0.09	0.52±0.14	0.24±0.09	0.24±0.06
	V6	0.09±0.08	0.36±0.08	0.25±0.07	0.23±0.07
C5	I	0.18±0.12	0.81±0.25	0.29±0.2	0.28±0.09
	II	0.12±0.1	0.28±0.08	0.39±0.12	0.26±0.09
	III	0.29±0.14	0.76±0.33	0.76±0.29	0.28±0.12
	AVL	0.27±0.13	0.87±0.19	0.27±0.11	0.28±0.08
	AVR	0.11±0.08	0.85±0.31	0.51±0.29	0.29±0.1
	AVF	0.19±0.15	0.31±0.25	0.48±0.15	0.23±0.12
	V1	0.14±0.1	0.21±0.1	0.21±0.1	0.20±0.08
	V2	0.15±0.12	0.24±0.11	0.31±0.13	0.26±0.07
	V3	0.20±0.12	0.49±0.23	0.34±0.19	0.27±0.09
	V4	0.13±0.09	0.64±0.2	0.26±0.15	0.25±0.08
	V5	0.09±0.09	0.56±0.15	0.26±0.1	0.25±0.07
	V6	0.08±0.08	0.35±0.08	0.26±0.08	0.24±0.08

Table 12: ECG (limb) lead-reconstruction: MAE results for all the leads.

		MAE (↓)			
Lead		ECGrecover	EKGAN [12]	Pix2Pix [10]	CopyPaste
C1	II	0.17±0.13	0.15±0.17	0.17±0.14	0.25±0.22
	III	0.24±0.15	0.28±0.16	0.61±0.29	0.54±0.25
	AVL	0.12±0.06	0.13±0.1	0.33±0.16	0.86±0.29
	AVR	0.11±0.08	0.11±0.07	0.69±0.29	0.18±0.1
	AVF	0.21±0.16	0.19±0.21	0.28±0.19	0.36±0.23
	V1	0.15±0.12	0.17±0.15	0.19±0.11	0.87±0.29
	V2	0.16±0.13	0.16±0.13	0.22±0.12	0.63±0.27
	V3	0.23±0.15	0.25±0.15	0.37±0.19	0.25±0.21
	V4	0.16±0.11	0.20±0.1	0.26±0.16	0.18±0.15
	V5	0.13±0.1	0.14±0.1	0.23±0.12	0.21±0.18
	V6	0.10±0.1	0.12±0.1	0.20±0.1	0.24±0.21
C2	I	0.25±0.14	0.27±0.22	0.50±0.25	0.25±0.22
	III	0.27±0.14	0.39±0.22	0.47±0.24	0.36±0.21
	AVL	0.32±0.15	0.2±0.14	0.36±0.16	0.99±0.28
	AVR	0.12±0.09	0.46±0.26	0.55±0.3	0.44±0.27
	AVF	0.11±0.08	0.18±0.24	0.21±0.15	0.13±0.08
	V1	0.14±0.12	0.16±0.15	0.19±0.11	1.04±0.29
	V2	0.16±0.13	0.17±0.12	0.20±0.11	0.83±0.27
	V3	0.25±0.14	0.24±0.13	0.33±0.2	0.37±0.25
	V4	0.16±0.11	0.17±0.1	0.24±0.15	0.18±0.14
	V5	0.12±0.1	0.12±0.12	0.24±0.12	0.13±0.12
	V6	0.10±0.09	0.12±0.12	0.23±0.1	0.12±0.12
C3	I	0.16±0.12	0.54±0.25	0.17±0.12	0.54±0.25
	II	0.16±0.11	0.22±0.12	0.14±0.13	0.36±0.21
	AVL	0.14±0.11	0.41±0.25	0.18±0.12	0.67±0.26
	AVR	0.17±0.11	0.70±0.31	0.15±0.12	0.62±0.26
	AVF	0.12±0.11	0.25±0.27	0.12±0.11	0.26±0.18
	V1	0.16±0.12	0.24±0.15	0.18±0.11	0.75±0.34
	V2	0.17±0.12	0.29±0.15	0.22±0.12	0.63±0.28
	V3	0.26±0.15	0.41±0.2	0.25±0.18	0.48±0.21
	V4	0.21±0.12	0.35±0.15	0.19±0.16	0.44±0.23
	V5	0.16±0.11	0.30±0.12	0.16±0.11	0.42±0.25
	V6	0.14±0.1	0.23±0.1	0.15±0.09	0.42±0.25
C4	I	0.09±0.06	0.17±0.1	0.49±0.23	0.18±0.1
	II	0.16±0.13	0.19±0.16	0.18±0.15	0.44±0.27
	III	0.15±0.11	0.33±0.16	0.68±0.28	0.62±0.26
	AVR	0.14±0.1	0.23±0.09	0.68±0.29	0.00±0.0
	AVF	0.17±0.15	0.23±0.2	0.34±0.21	0.52±0.27
	V1	0.16±0.12	0.20±0.15	0.18±0.11	0.69±0.3
	V2	0.16±0.13	0.18±0.14	0.24±0.13	0.44±0.28
	V3	0.25±0.15	0.30±0.19	0.36±0.19	0.29±0.2
	V4	0.18±0.12	0.28±0.14	0.24±0.16	0.34±0.22
	V5	0.14±0.11	0.23±0.12	0.21±0.12	0.38±0.25
	V6	0.12±0.11	0.16±0.1	0.18±0.1	0.43±0.27
C5	I	0.14±0.1	0.83±0.28	0.28±0.21	0.86±0.29
	II	0.11±0.1	0.35±0.13	0.30±0.17	0.99±0.28
	III	0.30±0.17	0.83±0.38	0.64±0.24	0.67±0.26
	AVL	0.25±0.14	0.98±0.35	0.22±0.15	0.0±0.0
	AVF	0.17±0.17	0.37±0.22	0.46±0.19	0.93±0.28
	V1	0.15±0.11	0.28±0.15	0.17±0.11	0.24±0.16
	V2	0.16±0.13	0.35±0.17	0.25±0.12	0.41±0.17
	V3	0.22±0.14	0.53±0.23	0.34±0.21	0.71±0.28
	V4	0.14±0.09	0.50±0.18	0.25±0.19	0.94±0.29
	V5	0.11±0.08	0.46±0.15	0.20±0.15	1.0±0.28
	V6	0.09±0.08	0.35±0.1	0.17±0.11	1.06±0.27
C_AVF	I	0.24±0.13	0.37±0.24	0.40±0.24	0.36±0.23
	II	0.1±0.07	0.15±0.14	0.14±0.13	0.13±0.08
	III	0.18±0.1	0.44±0.29	0.36±0.2	0.26±0.18
	AVL	0.26±0.14	0.26±0.18	0.32±0.15	0.93±0.28
	AVR	0.17±0.1	0.54±0.29	0.42±0.28	0.52±0.27
	V1	0.15±0.12	0.17±0.15	0.19±0.11	1.0±0.32
	V2	0.16±0.13	0.20±0.13	0.21±0.11	0.81±0.29
	V3	0.27±0.14	0.30±0.15	0.31±0.18	0.40±0.24
	V4	0.19±0.12	0.23±0.12	0.22±0.15	0.25±0.17
	V5	0.15±0.11	0.18±0.12	0.21±0.11	0.22±0.17
	V6	0.12±0.09	0.15±0.11	0.21±0.1	0.20±0.17

Table 13: ECG (thoracic) lead-reconstruction: MAE results for all the leads.

		MAE (↓)			
Lead		ECGrecover	EKGAN [12]	Pix2Pix [10]	CopyPaste
C_{V1}	I	0.21±0.13	0.84±0.29	0.25±0.23	0.87±0.29
	II	0.16±0.12	0.33±0.14	0.34±0.16	1.04±0.29
	III	0.33±0.13	0.92±0.34	0.74±0.33	0.75±0.34
	AVL	0.29±0.15	1.04±0.34	0.21±0.13	0.24±0.16
	AVR	0.16±0.1	0.91±0.33	0.53±0.32	0.69±0.3
	AVF	0.20±0.16	0.40±0.24	0.54±0.23	1.0±0.32
	V2	0.16±0.11	0.32±0.17	0.26±0.12	0.26±0.16
	V3	0.26±0.14	0.50±0.24	0.32±0.21	0.66±0.29
	V4	0.19±0.11	0.54±0.2	0.21±0.16	0.97±0.28
C_{V2}	V5	0.15±0.11	0.51±0.18	0.18±0.12	1.04±0.27
	V6	0.12±0.1	0.36±0.13	0.17±0.1	1.08±0.26
	I	0.22±0.14	0.61±0.26	0.29±0.24	0.63±0.27
	II	0.16±0.14	0.21±0.13	0.21±0.12	0.83±0.27
	III	0.30±0.15	0.76±0.34	0.62±0.27	0.63±0.28
	AVL	0.30±0.15	0.63±0.3	0.20±0.14	0.41±0.17
	AVR	0.17±0.11	0.70±0.32	0.51±0.31	0.44±0.28
	AVF	0.20±0.18	0.37±0.26	0.39±0.17	0.81±0.29
	V1	0.13±0.11	0.24±0.16	0.18±0.11	0.26±0.16
C_{V3}	V3	0.17±0.14	0.46±0.23	0.35±0.22	0.42±0.22
	V4	0.17±0.12	0.42±0.17	0.21±0.17	0.73±0.23
	V5	0.15±0.12	0.32±0.15	0.18±0.12	0.82±0.23
	V6	0.13±0.1	0.21±0.11	0.15±0.1	0.88±0.24
	I	0.21±0.14	0.25±0.2	0.41±0.24	0.25±0.21
	II	0.15±0.13	0.16±0.16	0.17±0.13	0.37±0.25
	III	0.32±0.15	0.37±0.3	0.53±0.22	0.48±0.21
	AVL	0.30±0.15	0.19±0.19	0.29±0.16	0.71±0.28
	AVR	0.15±0.11	0.35±0.27	0.55±0.28	0.29±0.2
C_{V4}	AVF	0.19±0.17	0.23±0.25	0.27±0.15	0.40±0.24
	V1	0.15±0.11	0.19±0.15	0.18±0.11	0.66±0.29
	V2	0.11±0.11	0.16±0.13	0.24±0.13	0.42±0.22
	V4	0.11±0.1	0.20±0.11	0.28±0.17	0.26±0.18
	V5	0.10±0.11	0.14±0.11	0.23±0.12	0.36±0.22
	V6	0.10±0.1	0.14±0.1	0.19±0.1	0.41±0.25
	I	0.20±0.13	0.19±0.16	0.55±0.27	0.18±0.15
	II	0.14±0.12	0.15±0.17	0.18±0.14	0.18±0.14
	III	0.32±0.15	0.29±0.21	0.48±0.27	0.44±0.23
C_{V5}	AVL	0.30±0.14	0.18±0.11	0.38±0.16	0.94±0.29
	AVR	0.13±0.09	0.30±0.21	0.60±0.3	0.34±0.22
	AVF	0.19±0.17	0.19±0.23	0.25±0.17	0.25±0.17
	V1	0.15±0.12	0.16±0.15	0.18±0.11	0.97±0.28
	V2	0.14±0.12	0.15±0.12	0.20±0.12	0.73±0.23
	V3	0.14±0.11	0.18±0.11	0.39±0.21	0.26±0.18
	V5	0.07±0.07	0.10±0.09	0.27±0.12	0.09±0.09
	V6	0.08±0.08	0.12±0.1	0.24±0.1	0.16±0.13
	I	0.20±0.12	0.22±0.18	0.57±0.27	0.21±0.18
C_{V6}	II	0.14±0.11	0.15±0.17	0.17±0.14	0.13±0.12
	III	0.32±0.14	0.31±0.18	0.52±0.28	0.42±0.25
	AVL	0.29±0.14	0.21±0.13	0.40±0.16	1.0±0.28
	AVR	0.12±0.08	0.34±0.22	0.64±0.31	0.38±0.25
	AVF	0.20±0.15	0.18±0.22	0.25±0.18	0.22±0.17
	V1	0.15±0.12	0.15±0.14	0.19±0.11	1.04±0.27
	V2	0.15±0.12	0.16±0.12	0.20±0.12	0.82±0.23
	V3	0.19±0.13	0.20±0.12	0.37±0.2	0.36±0.22
	V4	0.09±0.06	0.14±0.07	0.27±0.16	0.09±0.09
	V6	0.07±0.06	0.11±0.1	0.25±0.1	0.08±0.08

Table 14: ECG segment-recovery: DTW results for all the leads.

		DTW (↓)			
Lead		ECGrecover	EKGAN [12]	Pix2Pix [10]	CopyPaste
C_{V1}	I	0.06±0.06	0.67±0.33	0.22±0.26	0.16±0.09
	II	0.03±0.05	0.20±0.07	0.11±0.08	0.15±0.07
	III	0.10±0.09	0.68±0.59	0.54±0.32	0.14±0.1
	AVL	0.09±0.07	1.06±0.32	0.14±0.15	0.17±0.06
	AVR	0.03±0.04	0.77±0.47	0.47±0.41	0.15±0.09
	AVF	0.04±0.11	0.15±0.29	0.16±0.1	0.13±0.08
	V1	0.03±0.08	0.10±0.07	0.08±0.07	0.12±0.06
	V2	0.03±0.07	0.11±0.1	0.17±0.1	0.15±0.05
	V3	0.06±0.08	0.22±0.15	0.19±0.2	0.15±0.07
C_{V2}	V4	0.04±0.04	0.26±0.12	0.12±0.15	0.15±0.06
	V5	0.02±0.05	0.24±0.1	0.11±0.09	0.15±0.05
	V6	0.02±0.05	0.15±0.06	0.11±0.06	0.15±0.05
	I	0.04±0.06	0.71±0.34	0.22±0.26	0.16±0.08
	II	0.02±0.05	0.20±0.07	0.12±0.07	0.16±0.08
	III	0.10±0.08	0.52±0.51	0.51±0.3	0.14±0.1
	AVL	0.08±0.07	0.80±0.25	0.13±0.14	0.17±0.06
	AVR	0.02±0.03	0.80±0.49	0.47±0.4	0.15±0.08
	AVF	0.04±0.1	0.16±0.29	0.18±0.1	0.13±0.08
C_{V3}	V1	0.03±0.08	0.10±0.07	0.08±0.07	0.12±0.06
	V2	0.03±0.07	0.12±0.09	0.17±0.1	0.15±0.05
	V3	0.06±0.07	0.26±0.16	0.18±0.2	0.16±0.07
	V4	0.03±0.04	0.31±0.13	0.12±0.14	0.15±0.06
	V5	0.02±0.05	0.25±0.11	0.11±0.08	0.15±0.05
	V6	0.01±0.05	0.15±0.06	0.11±0.06	0.15±0.05
	I	0.04±0.06	0.69±0.33	0.20±0.25	0.16±0.09
	II	0.02±0.05	0.18±0.06	0.13±0.07	0.16±0.08
	III	0.10±0.09	0.51±0.5	0.45±0.28	0.15±0.11
C_{V4}	AVL	0.08±0.08	0.94±0.29	0.13±0.14	0.17±0.06
	AVR	0.02±0.03	0.76±0.47	0.44±0.4	0.15±0.08
	AVF	0.04±0.1	0.15±0.28	0.18±0.1	0.13±0.09
	V1	0.03±0.07	0.09±0.07	0.08±0.07	0.12±0.05
	V2	0.03±0.08	0.12±0.08	0.16±0.1	0.15±0.05
	V3	0.05±0.07	0.38±0.13	0.17±0.19	0.16±0.07
	V4	0.02±0.04	0.32±0.16	0.11±0.15	0.15±0.06
	V5	0.02±0.05	0.30±0.13	0.11±0.08	0.15±0.05
	V6	0.01±0.05	0.16±0.06	0.12±0.06	0.15±0.06
C_{V5}	I	0.03±0.06	0.65±0.32	0.18±0.21	0.16±0.09
	II	0.02±0.04	0.15±0.06	0.16±0.07	0.16±0.08
	III	0.08±0.08	0.38±0.42	0.42±0.27	0.14±0.11
	AVL	0.06±0.07	0.46±0.16	0.12±0.13	0.17±0.07
	AVR	0.01±0.03	0.72±0.43	0.38±0.36	0.15±0.08
	AVF	0.03±0.08	0.15±0.26	0.21±0.11	0.13±0.1
	V1	0.03±0.07	0.08±0.09	0.08±0.07	0.12±0.06
	V2	0.03±0.07	0.13±0.08	0.14±0.09	0.15±0.05
	V3	0.05±0.07	0.27±0.25	0.18±0.19	0.16±0.07
C_{V6}	V4	0.03±0.04	0.39±0.21	0.12±0.14	0.15±0.06
	V5	0.02±0.05	0.35±0.15	0.11±0.08	0.15±0.05
	V6	0.01±0.05	0.18±0.07	0.11±0.06	0.15±0.06
	I	0.05±0.09	0.74±0.37	0.15±0.21	0.16±0.09
	II	0.02±0.07	0.13±0.07	0.20±0.1	0.16±0.09
	III	0.13±0.14	0.65±0.63	0.65±0.4	0.15±0.11
	AVL	0.11±0.12	0.85±0.3	0.13±0.11	0.17±0.07
	AVR	0.02±0.04	0.82±0.53	0.35±0.39	0.16±0.1
	AVF	0.05±0.14	0.17±0.33	0.27±0.14	0.13±0.12
C_{V7}	V1	0.03±0.07	0.09±0.08	0.09±0.07	0.13±0.06
	V2	0.03±0.09	0.10±0.1	0.14±0.09	0.15±0.05
	V3	0.06±0.09	0.30±0.28	0.17±0.18	0.16±0.08
	V4	0.02±0.05	0.47±0.25	0.12±0.13	0.15±0.07
	V5	0.01±0.05	0.37±0.17	0.12±0.08	0.15±0.06
	V6	0.01±0.05	0.16±0.06	0.12±0.06	0.15±0.07

Table 15: ECG (limb) lead-reconstruction: DTW results for all the leads.

		DTW (\downarrow)			
Lead		ECGrecover	EKGAN [12]	Pix2Pix [10]	CopyPaste
C _I	II	0.04 \pm 0.09	0.04 \pm 0.14	0.06 \pm 0.12	0.09 \pm 0.2
	III	0.08 \pm 0.12	0.11 \pm 0.15	0.49 \pm 0.45	0.41 \pm 0.35
	AVR	0.02 \pm 0.03	0.02 \pm 0.06	0.17 \pm 0.14	0.87 \pm 0.5
	AVL	0.02 \pm 0.04	0.02 \pm 0.03	0.57 \pm 0.44	0.04 \pm 0.05
	AVF	0.06 \pm 0.15	0.06 \pm 0.23	0.14 \pm 0.24	0.18 \pm 0.27
	V1	0.04 \pm 0.09	0.04 \pm 0.14	0.06 \pm 0.09	0.82 \pm 0.49
	V2	0.03 \pm 0.09	0.04 \pm 0.1	0.08 \pm 0.09	0.43 \pm 0.37
	V3	0.07 \pm 0.11	0.08 \pm 0.13	0.17 \pm 0.17	0.08 \pm 0.19
	V4	0.04 \pm 0.06	0.05 \pm 0.07	0.09 \pm 0.13	0.05 \pm 0.12
	V5	0.02 \pm 0.06	0.03 \pm 0.06	0.09 \pm 0.1	0.06 \pm 0.14
C _{II}	V6	0.02 \pm 0.06	0.02 \pm 0.07	0.08 \pm 0.08	0.08 \pm 0.18
	I	0.08 \pm 0.11	0.09 \pm 0.22	0.31 \pm 0.29	0.09 \pm 0.2
	III	0.10 \pm 0.12	0.21 \pm 0.33	0.28 \pm 0.31	0.17 \pm 0.24
	AVR	0.13 \pm 0.13	0.05 \pm 0.1	0.17 \pm 0.14	1.13 \pm 0.51
	AVL	0.02 \pm 0.05	0.27 \pm 0.32	0.36 \pm 0.4	0.24 \pm 0.32
	AVF	0.02 \pm 0.04	0.05 \pm 0.29	0.07 \pm 0.14	0.03 \pm 0.04
	V1	0.03 \pm 0.09	0.04 \pm 0.13	0.06 \pm 0.08	1.16 \pm 0.54
	V2	0.03 \pm 0.09	0.04 \pm 0.08	0.07 \pm 0.08	0.74 \pm 0.42
	V3	0.07 \pm 0.1	0.08 \pm 0.09	0.14 \pm 0.18	0.17 \pm 0.26
	V4	0.04 \pm 0.07	0.04 \pm 0.06	0.09 \pm 0.13	0.04 \pm 0.1
C _{III}	V5	0.02 \pm 0.07	0.02 \pm 0.08	0.09 \pm 0.09	0.03 \pm 0.09
	V6	0.01 \pm 0.06	0.02 \pm 0.08	0.08 \pm 0.07	0.02 \pm 0.09
	I	0.04 \pm 0.07	0.41 \pm 0.34	0.05 \pm 0.09	0.41 \pm 0.35
	II	0.04 \pm 0.07	0.10 \pm 0.11	0.03 \pm 0.09	0.17 \pm 0.24
	AVR	0.03 \pm 0.07	0.27 \pm 0.34	0.05 \pm 0.08	0.52 \pm 0.36
	AVL	0.05 \pm 0.08	0.64 \pm 0.53	0.04 \pm 0.08	0.52 \pm 0.39
	AVF	0.02 \pm 0.06	0.11 \pm 0.38	0.03 \pm 0.07	0.09 \pm 0.16
	V1	0.05 \pm 0.08	0.10 \pm 0.14	0.06 \pm 0.08	0.67 \pm 0.52
	V2	0.04 \pm 0.09	0.13 \pm 0.14	0.07 \pm 0.08	0.52 \pm 0.39
	V3	0.08 \pm 0.12	0.23 \pm 0.23	0.08 \pm 0.16	0.35 \pm 0.26
C _{AVL}	V4	0.06 \pm 0.08	0.18 \pm 0.13	0.06 \pm 0.12	0.28 \pm 0.3
	V5	0.04 \pm 0.08	0.14 \pm 0.11	0.05 \pm 0.08	0.26 \pm 0.32
	V6	0.03 \pm 0.07	0.11 \pm 0.09	0.04 \pm 0.07	0.24 \pm 0.33
	I	0.01 \pm 0.02	0.04 \pm 0.05	0.30 \pm 0.27	0.04 \pm 0.05
	II	0.04 \pm 0.09	0.06 \pm 0.14	0.06 \pm 0.13	0.24 \pm 0.32
	III	0.04 \pm 0.07	0.14 \pm 0.14	0.61 \pm 0.47	0.52 \pm 0.39
	AVR	0.03 \pm 0.06	0.06 \pm 0.04	0.56 \pm 0.45	0.0 \pm 0.0
	AVF	0.05 \pm 0.12	0.08 \pm 0.21	0.19 \pm 0.26	0.37 \pm 0.37
	V1	0.04 \pm 0.09	0.06 \pm 0.14	0.06 \pm 0.09	0.54 \pm 0.46
	V2	0.04 \pm 0.09	0.05 \pm 0.12	0.09 \pm 0.09	0.23 \pm 0.34
C _{AVR}	V3	0.08 \pm 0.11	0.12 \pm 0.17	0.16 \pm 0.18	0.11 \pm 0.2
	V4	0.05 \pm 0.08	0.10 \pm 0.11	0.08 \pm 0.14	0.15 \pm 0.22
	V5	0.03 \pm 0.08	0.07 \pm 0.08	0.08 \pm 0.1	0.18 \pm 0.26
	V6	0.02 \pm 0.07	0.04 \pm 0.07	0.06 \pm 0.08	0.22 \pm 0.31
	I	0.03 \pm 0.06	0.81 \pm 0.47	0.10 \pm 0.2	0.87 \pm 0.5
	II	0.02 \pm 0.05	0.22 \pm 0.13	0.14 \pm 0.15	1.13 \pm 0.51
	III	b \pm 0.17	0.80 \pm 0.74	0.49 \pm 0.33	0.52 \pm 0.36
	AVL	0.08 \pm 0.12	1.11 \pm 0.67	0.08 \pm 0.12	0.0 \pm 0.0
	AVF	0.04 \pm 0.16	0.20 \pm 0.27	0.28 \pm 0.21	0.99 \pm 0.48
	V1	0.03 \pm 0.09	0.14 \pm 0.15	0.05 \pm 0.08	0.10 \pm 0.15
C _{AVF}	V2	0.03 \pm 0.09	0.18 \pm 0.18	0.09 \pm 0.08	0.27 \pm 0.19
	V3	0.06 \pm 0.1	0.36 \pm 0.31	0.15 \pm 0.2	0.60 \pm 0.45
	V4	0.03 \pm 0.05	0.34 \pm 0.21	0.12 \pm 0.16	1.0 \pm 0.52
	V5	0.02 \pm 0.05	0.30 \pm 0.16	0.08 \pm 0.12	1.14 \pm 0.52
	V6	0.01 \pm 0.05	0.20 \pm 0.09	0.06 \pm 0.09	1.24 \pm 0.5
	I	0.08 \pm 0.1	0.19 \pm 0.28	0.20 \pm 0.26	0.18 \pm 0.27
	II	0.02 \pm 0.03	0.04 \pm 0.11	0.03 \pm 0.09	0.03 \pm 0.04
	III	0.05 \pm 0.07	0.27 \pm 0.56	0.15 \pm 0.22	0.09 \pm 0.16
	AVL	0.10 \pm 0.11	0.10 \pm 0.18	0.13 \pm 0.12	0.99 \pm 0.48
	AVR	0.04 \pm 0.07	0.40 \pm 0.42	0.23 \pm 0.34	0.37 \pm 0.37
CV ₁	V1	0.03 \pm 0.09	0.04 \pm 0.13	0.06 \pm 0.08	1.07 \pm 0.57
	V2	0.04 \pm 0.09	0.06 \pm 0.1	0.07 \pm 0.08	0.73 \pm 0.44
	V3	0.09 \pm 0.11	0.12 \pm 0.12	0.12 \pm 0.16	0.22 \pm 0.27
	V4	0.05 \pm 0.07	0.08 \pm 0.09	0.07 \pm 0.12	0.10 \pm 0.16
	V5	0.03 \pm 0.08	0.06 \pm 0.09	0.07 \pm 0.08	0.07 \pm 0.16
	V6	0.02 \pm 0.07	0.04 \pm 0.09	0.07 \pm 0.07	0.06 \pm 0.17
	I	0.07 \pm 0.1	0.78 \pm 0.46	0.09 \pm 0.23	0.82 \pm 0.49
	II	0.04 \pm 0.09	0.17 \pm 0.13	0.15 \pm 0.14	1.16 \pm 0.54
	III	0.15 \pm 0.12	0.92 \pm 0.74	0.65 \pm 0.49	0.67 \pm 0.52
	AVL	0.12 \pm 0.13	1.19 \pm 0.66	0.33 \pm 0.45	0.54 \pm 0.46
CV ₂	AVR	0.04 \pm 0.07	0.92 \pm 0.62	0.36 \pm 0.28	1.07 \pm 0.57
	V1	0.06 \pm 0.16	0.20 \pm 0.35	0.13 \pm 0.21	0.09 \pm 0.15
	V2	0.03 \pm 0.08	0.13 \pm 0.17	0.10 \pm 0.08	0.09 \pm 0.15
	V3	0.08 \pm 0.1	0.31 \pm 0.31	0.13 \pm 0.2	0.48 \pm 0.43
	V4	0.05 \pm 0.07	0.36 \pm 0.24	0.08 \pm 0.13	1.0 \pm 0.5
	V5	0.04 \pm 0.07	0.33 \pm 0.21	0.07 \pm 0.09	1.15 \pm 0.51
	V6	0.02 \pm 0.07	0.18 \pm 0.11	0.05 \pm 0.07	1.21 \pm 0.51
	I	0.07 \pm 0.1	0.41 \pm 0.35	0.12 \pm 0.24	0.43 \pm 0.37
	II	0.04 \pm 0.1	0.07 \pm 0.11	0.07 \pm 0.09	0.74 \pm 0.42
	III	0.12 \pm 0.15	0.63 \pm 0.65	0.52 \pm 0.37	0.52 \pm 0.39
CV ₃	AVL	0.13 \pm 0.13	0.44 \pm 0.45	0.08 \pm 0.11	0.27 \pm 0.19
	AVR	0.04 \pm 0.08	0.55 \pm 0.5	0.34 \pm 0.42	0.23 \pm 0.34
	V1	0.06 \pm 0.18	0.17 \pm 0.35	0.22 \pm 0.17	0.73 \pm 0.44
	V2	0.03 \pm 0.07	0.08 \pm 0.16	0.05 \pm 0.09	0.09 \pm 0.15
	V3	0.04 \pm 0.11	0.25 \pm 0.25	0.15 \pm 0.21	0.19 \pm 0.25
	V4	0.04 \pm 0.07	0.21 \pm 0.17	0.07 \pm 0.14	0.55 \pm 0.35
	V5	0.03 \pm 0.08	0.14 \pm 0.13	0.06 \pm 0.08	0.70 \pm 0.37
	V6	0.03 \pm 0.07	0.07 \pm 0.08	0.05 \pm 0.07	0.81 \pm 0.4
	I	0.06 \pm 0.11	0.08 \pm 0.18	0.21 \pm 0.27	0.08 \pm 0.19
	II	0.03 \pm 0.1	0.04 \pm 0.14	0.05 \pm 0.1	0.17 \pm 0.26
CV ₄	III	0.14 \pm 0.15	0.19 \pm 0.44	0.39 \pm 0.3	0.35 \pm 0.26
	AVL	0.12 \pm 0.14	0.05 \pm 0.19	0.13 \pm 0.13	0.60 \pm 0.45
	AVR	0.03 \pm 0.07	0.15 \pm 0.31	0.38 \pm 0.37	0.11 \pm 0.2
	V1	0.05 \pm 0.17	0.08 \pm 0.31	0.13 \pm 0.15	0.22 \pm 0.27
	V2	0.03 \pm 0.08	0.05 \pm 0.14	0.05 \pm 0.08	0.48 \pm 0.43
	V3	0.02 \pm 0.07	0.04 \pm 0.09	0.09 \pm 0.1	0.19 \pm 0.25
	V4	0.02 \pm 0.05	0.05 \pm 0.08	0.10 \pm 0.15	0.07 \pm 0.15
	V5	0.02 \pm 0.06	0.03 \pm 0.07	0.09 \pm 0.1	0.14 \pm 0.22
	V6	0.01 \pm 0.05	0.02 \pm 0.07	0.10 \pm 0.08	0.03 \pm 0.08
	I	0.06 \pm 0.09	0.05 \pm 0.13	0.35 \pm 0.32	0.05 \pm 0.12
CV ₅	II	0.03 \pm 0.08	0.03 \pm 0.14	0.05 \pm 0.11	0.04 \pm 0.1
	III	0.12 \pm 0.15	0.12 \pm 0.26	0.32 \pm 0.4	0.28 \pm 0.3
	AVL	0.12 \pm 0.13	0.04 \pm 0.07	0.19 \pm 0.15	1.0 \pm 0.52
	AVR	0.02 \pm 0.05	0.11 \pm 0.22	0.44 \pm 0.44	0.15 \pm 0.22
	V1	0.05 \pm 0.16</td			

Table 17: ECG segment-recovery: difference of QT-distance between real and reconstructed lead overall Sot+ and Sot- ECGs.

Lead	Δ-QT (Sot-) ↓				Δ-QT (Sot+) ↓				
	ECGrecover	EKGAN [12]	Pix2Pix [10]	CopyPaste	ECGrecover	EKGAN [12]	Pix2Pix [10]	CopyPaste	
C1	I	0.01±0.02	0.11±0.06	0.09±0.04	0.05±0.05	0.02±0.03	0.12±0.07	0.11±0.05	0.07±0.05
	II	0.01±0.01	0.12±0.06	0.08±0.04	0.04±0.04	0.01±0.03	0.15±0.07	0.10±0.05	0.06±0.07
	III	0.07±0.07	0.11±0.09	0.11±0.09	0.05±0.08	0.06±0.06	0.11±0.09	0.13±0.09	0.06±0.07
	AVL	0.03±0.06	0.04±0.06	0.03±0.04	0.03±0.07	0.03±0.03	0.04±0.06	0.03±0.04	0.03±0.06
	AVR	0.03±0.03	0.11±0.06	0.10±0.06	0.04±0.05	0.04±0.05	0.11±0.06	0.10±0.06	0.05±0.06
	AVF	0.02±0.04	0.15±0.07	0.09±0.05	0.05±0.05	0.04±0.05	0.14±0.07	0.10±0.06	0.06±0.06
	V1	0.03±0.04	0.05±0.05	0.04±0.04	0.02±0.04	0.03±0.04	0.05±0.05	0.04±0.04	0.02±0.04
	V2	0.01±0.02	0.14±0.05	0.12±0.04	0.04±0.04	0.02±0.03	0.16±0.06	0.14±0.05	0.06±0.05
	V3	0.01±0.02	0.10±0.06	0.10±0.04	0.03±0.04	0.02±0.03	0.13±0.07	0.12±0.05	0.06±0.06
	V4	0.01±0.01	0.12±0.06	0.09±0.04	0.04±0.04	0.01±0.03	0.14±0.07	0.10±0.06	0.06±0.06
C2	V5	0.01±0.01	0.13±0.06	0.07±0.05	0.04±0.05	0.01±0.03	0.14±0.07	0.09±0.06	0.06±0.06
	V6	0.01±0.01	0.13±0.06	0.06±0.04	0.02±0.05	0.01±0.03	0.16±0.06	0.08±0.06	0.03±0.06
	I	0.01±0.02	0.08±0.05	0.08±0.04	0.03±0.04	0.01±0.03	0.09±0.06	0.10±0.05	0.04±0.05
	II	0.01±0.01	0.09±0.06	0.07±0.04	0.03±0.04	0.01±0.02	0.11±0.06	0.09±0.05	0.05±0.05
	III	0.06±0.06	0.10±0.08	0.10±0.08	0.05±0.05	0.05±0.06	0.12±0.09	0.12±0.09	0.05±0.07
	AVL	0.03±0.06	0.03±0.04	0.03±0.04	0.02±0.05	0.02±0.03	0.04±0.05	0.03±0.03	0.02±0.05
	AVR	0.03±0.03	0.10±0.06	0.09±0.05	0.03±0.04	0.04±0.05	0.10±0.07	0.10±0.06	0.04±0.05
	AVF	0.02±0.03	0.13±0.06	0.07±0.05	0.03±0.04	0.03±0.04	0.16±0.07	0.08±0.06	0.05±0.05
	V1	0.03±0.04	0.04±0.05	0.04±0.04	0.02±0.03	0.03±0.04	0.04±0.05	0.04±0.04	0.02±0.03
	V2	0.01±0.02	0.12±0.05	0.12±0.04	0.02±0.03	0.01±0.03	0.14±0.06	0.14±0.05	0.03±0.05
C3	V3	0.01±0.01	0.07±0.05	0.09±0.04	0.02±0.03	0.01±0.03	0.09±0.06	0.11±0.05	0.05±0.05
	V4	0.01±0.01	0.10±0.05	0.06±0.04	0.03±0.03	0.01±0.03	0.11±0.06	0.08±0.05	0.05±0.05
	V5	0.01±0.01	0.10±0.06	0.07±0.05	0.02±0.03	0.01±0.03	0.12±0.06	0.09±0.06	0.04±0.04
	V6	0.01±0.01	0.10±0.05	0.06±0.05	0.02±0.03	0.01±0.02	0.13±0.06	0.08±0.05	0.04±0.04
	I	0.01±0.01	0.05±0.04	0.08±0.04	0.02±0.03	0.01±0.03	0.07±0.05	0.09±0.05	0.03±0.04
	II	0.01±0.01	0.07±0.05	0.05±0.04	0.02±0.02	0.01±0.02	0.10±0.06	0.07±0.04	0.03±0.04
	III	0.06±0.07	0.11±0.09	0.10±0.08	0.04±0.06	0.05±0.05	0.11±0.09	0.13±0.09	0.05±0.06
	AVL	0.03±0.06	0.03±0.05	0.03±0.04	0.01±0.05	0.02±0.03	0.04±0.06	0.04±0.03	0.01±0.04
	AVR	0.03±0.03	0.07±0.06	0.09±0.05	0.02±0.03	0.04±0.05	0.09±0.06	0.09±0.06	0.03±0.04
	AVF	0.02±0.03	0.13±0.06	0.06±0.04	0.03±0.03	0.03±0.04	0.16±0.07	0.08±0.05	0.03±0.04
C4	V1	0.03±0.03	0.04±0.04	0.04±0.04	0.02±0.03	0.02±0.04	0.04±0.05	0.03±0.04	0.02±0.02
	V2	0.01±0.02	0.11±0.04	0.13±0.04	0.02±0.02	0.01±0.03	0.13±0.06	0.14±0.05	0.02±0.03
	V3	0.01±0.02	0.09±0.05	0.10±0.04	0.02±0.02	0.01±0.03	0.11±0.06	0.12±0.05	0.03±0.03
	V4	0.01±0.01	0.11±0.05	0.07±0.04	0.02±0.03	0.01±0.03	0.12±0.06	0.09±0.05	0.03±0.04
	V5	0.01±0.01	0.09±0.05	0.05±0.04	0.02±0.03	0.01±0.03	0.11±0.06	0.08±0.05	0.03±0.03
	V6	0.01±0.01	0.10±0.05	0.05±0.04	0.02±0.03	0.01±0.02	0.13±0.06	0.07±0.05	0.03±0.04
	I	0.01±0.02	0.05±0.03	0.06±0.04	0.02±0.03	0.01±0.03	0.06±0.05	0.08±0.05	0.02±0.03
	II	0.01±0.01	0.06±0.05	0.05±0.03	0.02±0.02	0.01±0.02	0.10±0.06	0.06±0.04	0.02±0.03
	III	0.05±0.06	0.10±0.08	0.10±0.07	0.03±0.05	0.04±0.06	0.13±0.09	0.11±0.08	0.03±0.04
	AVL	0.03±0.06	0.03±0.04	0.03±0.04	0.01±0.05	0.02±0.03	0.04±0.04	0.03±0.04	0.01±0.04
C5	AVR	0.03±0.03	0.06±0.06	0.08±0.05	0.02±0.02	0.04±0.05	0.08±0.06	0.08±0.05	0.02±0.03
	AVF	0.02±0.03	0.12±0.06	0.05±0.04	0.02±0.03	0.02±0.04	0.15±0.06	0.06±0.05	0.02±0.03
	V1	0.03±0.03	0.04±0.04	0.04±0.03	0.01±0.02	0.02±0.04	0.04±0.04	0.04±0.04	0.01±0.02
	V2	0.01±0.02	0.11±0.04	0.11±0.04	0.01±0.02	0.01±0.03	0.13±0.05	0.13±0.05	0.01±0.02
	V3	0.01±0.02	0.05±0.04	0.06±0.04	0.01±0.02	0.01±0.03	0.08±0.06	0.08±0.05	0.02±0.03
	V4	0.01±0.01	0.08±0.05	0.04±0.03	0.02±0.02	0.01±0.03	0.12±0.06	0.06±0.04	0.02±0.03
	V5	0.01±0.01	0.08±0.05	0.04±0.03	0.02±0.02	0.01±0.03	0.11±0.06	0.05±0.04	0.02±0.03
	V6	0.01±0.01	0.08±0.05	0.04±0.03	0.02±0.02	0.01±0.02	0.11±0.06	0.05±0.04	0.02±0.03

Table 18: ECG (limb) lead-reconstruction: difference of QT-distance between real and reconstructed lead overall Sot- and Sot+ ECGs.

Lead	Δ-QT (Sot-) ↓				Δ-QT (Sot+) ↓				
	ECGrecover	EKGAN [12]	Pix2Pix [10]	CopyPaste	ECGrecover	EKGAN [12]	Pix2Pix [10]	CopyPaste	
C _I	II	0.01±0.01	0.01±0.01	0.01±0.03	0.01±0.02	0.01±0.03	0.01±0.03	0.02±0.04	0.01±0.03
	III	0.06±0.07	0.08±0.08	0.09±0.08	0.08±0.07	0.06±0.07	0.07±0.07	0.09±0.07	0.09±0.07
	AVL	0.03±0.07	0.02±0.05	0.04±0.04	0.14±0.04	0.02±0.03	0.02±0.05	0.04±0.04	0.16±0.05
	AVR	0.03±0.03	0.01±0.03	0.08±0.05	0.01±0.02	0.04±0.06	0.01±0.05	0.08±0.05	0.01±0.03
	AVF	0.02±0.04	0.04±0.04	0.02±0.05	0.02±0.04	0.03±0.05	0.06±0.06	0.03±0.05	0.03±0.05
	V1	0.03±0.04	0.04±0.04	0.10±0.05	0.09±0.06	0.03±0.04	0.03±0.04	0.12±0.06	0.12±0.06
	V2	0.01±0.02	0.01±0.02	0.02±0.03	0.01±0.02	0.02±0.03	0.02±0.03	0.03±0.03	0.02±0.03
	V3	0.01±0.02	0.01±0.02	0.02±0.02	0.01±0.02	0.01±0.03	0.01±0.04	0.03±0.03	0.02±0.04
	V4	0.01±0.01	0.01±0.01	0.01±0.02	0.01±0.01	0.01±0.03	0.01±0.03	0.02±0.04	0.01±0.04
	V5	0.01±0.01	0.01±0.01	0.02±0.02	0.01±0.01	0.01±0.03	0.01±0.03	0.03±0.03	0.01±0.04
	V6	0.01±0.01	0.01±0.01	0.02±0.02	0.01±0.02	0.01±0.03	0.01±0.03	0.03±0.03	0.01±0.03
C _{II}	I	0.01±0.02	0.01±0.02	0.02±0.02	0.01±0.02	0.01±0.04	0.01±0.04	0.03±0.04	0.01±0.04
	III	0.09±0.1	0.09±0.08	0.08±0.07	0.08±0.06	0.08±0.09	0.11±0.08	0.08±0.07	0.09±0.07
	AVL	0.03±0.06	0.02±0.03	0.04±0.04	0.14±0.03	0.02±0.03	0.02±0.03	0.03±0.04	0.16±0.05
	AVR	0.03±0.03	0.02±0.03	0.06±0.05	0.02±0.03	0.03±0.05	0.03±0.06	0.06±0.05	0.02±0.05
	AVF	0.02±0.04	0.04±0.04	0.02±0.04	0.01±0.04	0.02±0.05	0.06±0.05	0.02±0.05	0.02±0.05
	V1	0.03±0.04	0.04±0.04	0.09±0.05	0.09±0.05	0.03±0.04	0.03±0.04	0.09±0.06	0.12±0.06
	V2	0.01±0.02	0.01±0.02	0.02±0.03	0.01±0.02	0.02±0.03	0.02±0.03	0.02±0.03	0.02±0.03
	V3	0.01±0.02	0.01±0.02	0.02±0.02	0.01±0.02	0.01±0.03	0.01±0.03	0.02±0.03	0.01±0.03
	V4	0.01±0.01	0.01±0.01	0.01±0.01	0.01±0.01	0.01±0.03	0.01±0.04	0.02±0.03	0.01±0.04
	V5	0.01±0.01	0.01±0.01	0.02±0.02	0.01±0.01	0.01±0.03	0.01±0.04	0.03±0.03	0.01±0.04
	V6	0.01±0.01	0.01±0.01	0.02±0.02	0.01±0.01	0.01±0.02	0.01±0.03	0.02±0.03	0.01±0.03
C _{III}	I	0.01±0.02	0.07±0.06	0.02±0.03	0.08±0.06	0.02±0.04	0.08±0.06	0.03±0.04	0.08±0.07
	II	0.01±0.01	0.08±0.05	0.01±0.02	0.08±0.06	0.02±0.03	0.10±0.06	0.02±0.04	0.09±0.07
	AVL	0.03±0.06	0.11±0.06	0.02±0.03	0.10±0.09	0.02±0.03	0.10±0.06	0.03±0.03	0.12±0.09
	AVR	0.03±0.03	0.08±0.06	0.02±0.03	0.08±0.07	0.04±0.06	0.08±0.06	0.03±0.05	0.08±0.07
	AVF	0.02±0.04	0.04±0.04	0.02±0.04	0.01±0.04	0.03±0.05	0.10±0.05	0.03±0.05	0.07±0.08
	V1	0.04±0.04	0.04±0.04	0.04±0.05	0.07±0.07	0.03±0.04	0.03±0.04	0.04±0.05	0.08±0.08
	V2	0.01±0.02	0.10±0.05	0.02±0.03	0.08±0.07	0.02±0.03	0.12±0.06	0.03±0.05	0.09±0.07
	V3	0.01±0.02	0.10±0.05	0.02±0.03	0.08±0.06	0.02±0.03	0.11±0.06	0.02±0.04	0.08±0.07
	V4	0.01±0.02	0.09±0.05	0.02±0.03	0.08±0.06	0.02±0.03	0.11±0.06	0.03±0.04	0.09±0.06
	V5	0.01±0.01	0.06±0.05	0.02±0.03	0.08±0.06	0.02±0.04	0.08±0.06	0.03±0.04	0.09±0.07
	V6	0.01±0.02	0.07±0.05	0.02±0.02	0.08±0.06	0.02±0.03	0.10±0.06	0.03±0.03	0.09±0.07
C _{AVL}	I	0.01±0.02	0.13±0.04	0.02±0.02	0.14±0.04	0.01±0.03	0.14±0.05	0.02±0.04	0.15±0.05
	II	0.01±0.01	0.12±0.04	0.03±0.02	0.14±0.03	0.01±0.02	0.14±0.05	0.03±0.04	0.16±0.05
	III	0.10±0.09	0.08±0.06	0.09±0.08	0.10±0.09	0.08±0.09	0.09±0.06	0.10±0.09	0.13±0.1
	AVR	0.03±0.03	0.11±0.05	0.02±0.03	0.14±0.05	0.04±0.05	0.11±0.05	0.02±0.04	0.14±0.06
	AVF	0.02±0.04	0.03±0.04	0.07±0.07	0.14±0.05	0.03±0.05	0.05±0.05	0.11±0.08	0.16±0.06
	V1	0.03±0.04	0.04±0.03	0.04±0.04	0.04±0.05	0.03±0.05	0.04±0.03	0.03±0.04	0.04±0.05
	V2	0.01±0.02	0.08±0.03	0.03±0.04	0.15±0.04	0.02±0.03	0.10±0.04	0.06±0.06	0.16±0.05
	V3	0.01±0.02	0.10±0.03	0.02±0.03	0.14±0.04	0.01±0.03	0.11±0.04	0.02±0.04	0.16±0.05
	V4	0.01±0.01	0.10±0.04	0.03±0.03	0.14±0.04	0.01±0.03	0.11±0.05	0.04±0.05	0.15±0.05
	V5	0.01±0.01	0.10±0.04	0.02±0.02	0.14±0.04	0.01±0.03	0.11±0.05	0.03±0.04	0.15±0.05
	V6	0.01±0.01	0.12±0.04	0.02±0.01	0.14±0.03	0.01±0.02	0.13±0.05	0.02±0.04	0.15±0.05
C _{AVR}	I	0.01±0.02	0.01±0.03	0.02±0.03	0.01±0.03	0.01±0.03	0.01±0.04	0.03±0.04	0.01±0.04
	II	0.01±0.01	0.01±0.02	0.02±0.03	0.02±0.03	0.01±0.03	0.02±0.04	0.02±0.04	0.02±0.04
	III	0.05±0.08	0.07±0.07	0.08±0.08	0.08±0.08	0.04±0.07	0.08±0.06	0.09±0.06	0.09±0.06
	AVL	0.03±0.06	0.03±0.05	0.03±0.04	0.14±0.05	0.02±0.03	0.03±0.06	0.03±0.03	0.15±0.06
	AVF	0.02±0.04	0.04±0.04	0.02±0.05	0.02±0.05	0.03±0.05	0.06±0.05	0.03±0.05	0.03±0.05
	V1	0.03±0.04	0.04±0.04	0.09±0.06	0.10±0.06	0.03±0.04	0.03±0.04	0.11±0.06	0.11±0.06
	V2	0.01±0.02	0.01±0.03	0.02±0.03	0.02±0.03	0.02±0.03	0.02±0.04	0.03±0.04	0.02±0.04
	V3	0.01±0.02	0.02±0.02	0.02±0.03	0.01±0.03	0.02±0.03	0.02±0.04	0.03±0.04	0.02±0.05
	V4	0.01±0.01	0.01±0.02	0.02±0.03	0.01±0.03	0.01±0.03	0.02±0.04	0.03±0.05	0.02±0.05
	V5	0.01±0.01	0.01±0.02	0.02±0.02	0.01±0.03	0.01±0.03	0.02±0.04	0.03±0.04	0.02±0.05
	V6	0.01±0.01	0.01±0.02	0.02±0.02	0.01±0.03	0.01±0.03	0.02±0.04	0.03±0.03	0.02±0.05
C _{AVF}	I	0.01±0.02	0.02±0.04	0.02±0.02	0.02±0.04	0.02±0.04	0.03±0.05	0.03±0.04	0.03±0.05
	II	0.01±0.01	0.02±0.04	0.01±0.02	0.01±0.04	0.01±0.03	0.04±0.06	0.02±0.03	0.02±0.05
	III	0.06±0.08	0.10±0.07	0.07±0.07	0.06±0.07	0.05±0.08	0.12±0.07	0.06±0.07	0.06±0.08
	AVL	0.02±0.06	0.04±0.05	0.02±0.03	0.14±0.05	0.02±0.03	0.05±0.04	0.03±0.03	0.16±0.06
	AVR	0.03±0.03	0.03±0.05	0.03±0.04	0.02±0.04	0.04±0.05	0.05±0.06	0.04±0.05	0.04±0.06
	V1	0.03±0.04	0.04±0.04	0.05±0.05	0.09±0.06	0.03±0.04	0.03±0.04	0.05±0.05	0.11±0.06
	V2	0.01±0.02	0.02±0.04	0.02±0.03	0.02±0.04	0.02±0.03	0.04±0.05	0.02±0.04	0.02±0.05
	V3	0.01±0.02	0.02±0.05	0.02±0.03	0.02±0.04	0.02±0.03	0.04±0.06	0.03±0.03	0.02±0.06
	V4	0.01±0.01	0.02±0.04	0.01±0.02	0.02±0.04	0.02±0.03	0.04±0.06	0.03±0.04	0.02±0.06
	V5	0.01±0.01	0.02±0.04	0.02±0.02	0.02±0.04	0.02±0.04	0.03±0.05	0.02±0.03	0.03±0.06
	V6	0.01±0.01	0.02±0.04	0.02±0.02	0				

Table 19: ECG (thoracic) lead-reconstruction: difference of QT-distance between real and reconstructed lead overall Sot+ and Sot- ECGs.

Lead	Δ-QT(Sot-) ↓				Δ-QT (Sot+) ↓			
	ECGrecover	EKGAN [12]	Pix2Pix [10]	CopyPaste	ECGrecover	EKGAN [12]	Pix2Pix [10]	CopyPaste
CV ₁	I 0.02 ±0.02	0.10±0.05	0.02 ±0.02	0.09±0.05	0.02 ±0.04	0.11±0.05	0.02 ±0.04	0.11±0.05
	II 0.01 ±0.01	0.10±0.05	0.02±0.02	0.09±0.05	0.02 ±0.03	0.10±0.04	0.03±0.04	0.12±0.06
	III 0.10±0.08	0.08±0.06	0.07 ±0.07	0.07 ±0.07	0.10±0.08	0.08 ±0.06	0.10±0.09	0.09±0.08
	AVL 0.02 ±0.06	0.10±0.05	0.03±0.03	0.04±0.05	0.02 ±0.03	0.10±0.06	0.03±0.03	0.04±0.05
	AVR 0.03±0.03	0.10±0.04	0.02 ±0.03	0.10±0.06	0.03±0.04	0.10±0.05	0.02 ±0.05	0.11±0.06
	AVF 0.02 ±0.04	0.07±0.04	0.03±0.04	0.09±0.06	0.03 ±0.05	0.09±0.05	0.04±0.05	0.11±0.07
	V2 0.01 ±0.02	0.05±0.03	0.08±0.05	0.10±0.06	0.02 ±0.03	0.06±0.04	0.09±0.06	0.12±0.06
	V3 0.01 ±0.02	0.07±0.03	0.02±0.04	0.10±0.05	0.02 ±0.03	0.08±0.04	0.04±0.05	0.12±0.06
	V4 0.01 ±0.01	0.07±0.03	0.10±0.06	0.09±0.05	0.02 ±0.03	0.08±0.04	0.11±0.07	0.12±0.06
	V5 0.01 ±0.01	0.07±0.04	0.04±0.03	0.09±0.05	0.02 ±0.04	0.09±0.04	0.04±0.04	0.11±0.06
CV ₂	V6 0.01 ±0.01	0.07±0.04	0.04±0.02	0.09±0.05	0.02 ±0.03	0.09±0.04	0.03±0.04	0.11±0.05
	I 0.01 ±0.01	0.01 ±0.02	0.01 ±0.02	0.01 ±0.02	0.02 ±0.04	0.02 ±0.05	0.02 ±0.04	0.02 ±0.05
	II 0.01 ±0.01	0.01 ±0.02	0.01 ±0.02	0.01 ±0.02	0.01 ±0.03	0.02±0.04	0.02±0.03	0.02±0.03
	III 0.10±0.09	0.07 ±0.06	0.08±0.07	0.08±0.07	0.09 ±0.09	0.09 ±0.06	0.09 ±0.07	0.09 ±0.07
	AVL 0.03 ±0.06	0.11±0.08	0.03 ±0.03	0.15±0.04	0.02 ±0.03	0.12±0.08	0.04±0.02	0.16±0.05
	AVR 0.03±0.03	0.03±0.04	0.06±0.05	0.02 ±0.03	0.03±0.05	0.04±0.05	0.06±0.05	0.02 ±0.06
	AVF 0.02 ±0.04	0.03±0.04	0.02 ±0.04	0.02 ±0.04	0.03 ±0.05	0.05±0.05	0.03 ±0.05	0.03 ±0.06
	V1 0.03 ±0.04	0.04±0.04	0.09±0.05	0.10±0.05	0.03 ±0.04	0.03 ±0.04	0.08±0.06	0.12±0.06
	V3 0.01 ±0.01	0.01 ±0.02	0.02±0.03	0.01 ±0.01	0.01 ±0.03	0.02±0.04	0.04±0.05	0.01 ±0.03
	V4 0.01 ±0.01	0.02±0.02	0.01 ±0.04	0.01 ±0.02	0.01 ±0.03	0.03±0.04	0.04±0.07	0.02±0.04
CV ₃	V5 0.01 ±0.01	0.01 ±0.02	0.04±0.03	0.01 ±0.02	0.01 ±0.03	0.02±0.04	0.03±0.04	0.02±0.04
	V6 0.01 ±0.01	0.01 ±0.01	0.03±0.02	0.02±0.02	0.01 ±0.03	0.02±0.04	0.03±0.04	0.02±0.04
	I 0.01 ±0.01	0.01 ±0.02	0.02±0.03	0.01 ±0.02	0.01 ±0.03	0.02±0.05	0.03±0.04	0.02±0.05
	II 0.01 ±0.01	0.01 ±0.01	0.01 ±0.02	0.01 ±0.01	0.01 ±0.03	0.02±0.04	0.02±0.03	0.01 ±0.03
	III 0.10±0.08	0.09±0.07	0.08 ±0.07	0.08 ±0.06	0.08 ±0.09	0.08 ±0.07	0.08 ±0.07	0.08 ±0.07
	AVL 0.02 ±0.06	0.04±0.07	0.04±0.04	0.15±0.04	0.02 ±0.03	0.03±0.06	0.04±0.03	0.16±0.05
	AVR 0.03±0.03	0.02±0.03	0.07±0.05	0.01 ±0.03	0.04±0.05	0.03±0.06	0.07±0.05	0.02 ±0.05
	AVF 0.02 ±0.04	0.03±0.04	0.02 ±0.04	0.02 ±0.04	0.03±0.05	0.06±0.05	0.03±0.05	0.02 ±0.06
	V1 0.04 ±0.04	0.04 ±0.04	0.11±0.05	0.10±0.05	0.03 ±0.04	0.03 ±0.04	0.11±0.06	0.12±0.06
	V2 0.01 ±0.02	0.01 ±0.02	0.02±0.03	0.01 ±0.02	0.01 ±0.02	0.01 ±0.03	0.03±0.03	0.01 ±0.02
CV ₄	V4 0.01 ±0.01	0.01 ±0.02	0.02±0.02	0.01 ±0.01	0.01 ±0.03	0.02±0.04	0.03±0.05	0.01 ±0.03
	V5 0.01 ±0.01	0.01 ±0.02	0.03±0.02	0.01 ±0.01	0.01 ±0.03	0.01 ±0.05	0.03±0.03	0.01 ±0.04
	V6 0.01 ±0.01	0.01 ±0.01	0.02±0.02	0.01 ±0.01	0.01 ±0.03	0.02±0.04	0.03±0.03	0.02±0.04
	I 0.01 ±0.02	0.01 ±0.01	0.02±0.02	0.01 ±0.01	0.01 ±0.03	0.01 ±0.05	0.03±0.04	0.01 ±0.04
	II 0.01 ±0.01	0.01 ±0.01	0.01 ±0.01	0.01 ±0.01	0.01 ±0.03	0.01 ±0.04	0.02±0.03	0.01 ±0.03
	III 0.09±0.08	0.08 ±0.08	0.08 ±0.06	0.08 ±0.06	0.09±0.08	0.09±0.08	0.08 ±0.07	0.09±0.07
	AVL 0.02 ±0.06	0.02 ±0.05	0.04±0.04	0.14±0.04	0.02 ±0.03	0.02 ±0.04	0.04±0.04	0.16±0.05
	AVR 0.03±0.03	0.01 ±0.03	0.08±0.05	0.01 ±0.03	0.04±0.05	0.02 ±0.06	0.07±0.05	0.02 ±0.05
	AVF 0.02 ±0.04	0.04±0.04	0.02 ±0.04	0.02 ±0.04	0.03±0.05	0.07±0.05	0.03±0.05	0.02 ±0.06
	V1 0.03 ±0.04	0.04±0.04	0.10±0.05	0.09±0.05	0.03 ±0.04	0.03 ±0.04	0.11±0.06	0.12±0.06
CV ₅	V2 0.01 ±0.02	0.01 ±0.02	0.02±0.02	0.01 ±0.02	0.01 ±0.03	0.01 ±0.03	0.02±0.03	0.02±0.03
	V3 0.01 ±0.01	0.01 ±0.02	0.02±0.02	0.01 ±0.01	0.01 ±0.03	0.01 ±0.03	0.02±0.03	0.01 ±0.02
	V5 0.01 ±0.01	0.01 ±0.01	0.02±0.02	0.01 ±0.01	0.01 ±0.03	0.01 ±0.05	0.03±0.03	0.01 ±0.03
	V6 0.01 ±0.01	0.01 ±0.01	0.02±0.02	0.01 ±0.01	0.01 ±0.03	0.01 ±0.04	0.03±0.03	0.01 ±0.03
	I 0.01 ±0.02	0.01 ±0.02	0.02±0.02	0.01 ±0.02	0.01 ±0.04	0.01 ±0.04	0.03±0.04	0.01 ±0.04
	II 0.01 ±0.01	0.01 ±0.01	0.01 ±0.01	0.01 ±0.01	0.01 ±0.02	0.01 ±0.04	0.01 ±0.03	0.01 ±0.02
	III 0.09±0.08	0.08 ±0.08	0.08 ±0.06	0.08 ±0.06	0.08 ±0.08	0.09±0.08	0.08 ±0.07	0.09±0.07
	AVL 0.03 ±0.06	0.02 ±0.04	0.04±0.04	0.14±0.03	0.02 ±0.03	0.02 ±0.03	0.04±0.04	0.16±0.05
	AVR 0.03±0.03	0.01 ±0.03	0.07±0.05	0.01 ±0.03	0.04±0.05	0.02 ±0.05	0.07±0.05	0.02 ±0.05
	AVF 0.02 ±0.04	0.04±0.04	0.02 ±0.04	0.02 ±0.04	0.03±0.05	0.06±0.05	0.03±0.05	0.02 ±0.05
CV ₆	V1 0.04 ±0.04	0.04 ±0.04	0.08±0.05	0.09±0.05	0.03 ±0.04	0.03 ±0.04	0.10±0.06	0.12±0.06
	V2 0.01 ±0.02	0.01 ±0.02	0.02±0.03	0.02±0.02	0.01 ±0.03	0.01 ±0.03	0.02±0.03	0.02±0.03
	V3 0.01 ±0.02	0.01 ±0.02	0.02±0.02	0.01 ±0.02	0.01 ±0.03	0.01 ±0.04	0.02±0.03	0.01 ±0.03
	V4 0.01 ±0.01	0.01±0.01	0.01±0.01	0.01 ±0.01	0.01 ±0.03	0.01 ±0.04	0.02±0.04	0.01 ±0.03
	V5 0.01 ±0.01	0.01±0.01	0.02±0.02	0.01 ±0.01	0.01±0.03	0.01±0.04	0.02±0.03	0.01 ±0.03
	I 0.01 ±0.02	0.01 ±0.02	0.02±0.02	0.01 ±0.02	0.01 ±0.03	0.01 ±0.04	0.03±0.03	0.01 ±0.03
	II 0.01 ±0.01	0.01 ±0.01	0.01 ±0.01	0.01 ±0.01	0.01 ±0.02	0.01 ±0.04	0.01 ±0.03	0.01 ±0.02
	III 0.10±0.09	0.08 ±0.08	0.08 ±0.06	0.08 ±0.06	0.08 ±0.08	0.09±0.08	0.08 ±0.07	0.09±0.07
	AVL 0.03 ±0.06	0.02 ±0.04	0.04±0.04	0.14±0.03	0.02 ±0.04	0.02 ±0.03	0.04±0.05	0.16±0.05
	AVR 0.03±0.03	0.01 ±0.03	0.06±0.05	0.01 ±0.03	0.04±0.05	0.02 ±0.05	0.07±0.05	0.02 ±0.05
	AVF 0.02 ±0.04	0.04±0.04	0.02 ±0.04	0.02 ±0.04	0.03±0.05	0.06±0.05	0.02 ±0.05	0.02 ±0.05

Table 20: ECG segment-recovery: difference of QRS-complex between real and reconstructed lead overall Sot+ and Sot- ECGs.

Lead	Δ-QRS (Sot-) ↓				Δ-QRS (Sot+) ↓			
	ECGrecover	EKGAN [12]	Pix2Pix [10]	CopyPaste	ECGrecover	EKGAN [12]	Pix2Pix [10]	CopyPaste
C1	I 0.01±0.02	0.02±0.02	0.03±0.02	0.03±0.07	0.01±0.02	0.02±0.03	0.02±0.02	0.03±0.09
	II 0.01±0.01	0.02±0.02	0.03±0.02	0.02±0.06	0.01±0.02	0.02±0.02	0.03±0.02	0.03±0.1
	III 0.05±0.04	0.04±0.05	0.04±0.06	0.03±0.06	0.05±0.05	0.04±0.06	0.05±0.06	0.04±0.05
	AVL 0.03±0.03	0.04±0.04	0.03±0.04	0.02±0.04	0.03±0.03	0.04±0.05	0.03±0.05	0.03±0.04
	AVR 0.02±0.04	0.03±0.03	0.03±0.03	0.02±0.05	0.02±0.04	0.02±0.03	0.03±0.03	0.02±0.06
	AVF 0.02±0.03	0.03±0.04	0.03±0.03	0.03±0.06	0.02±0.04	0.03±0.04	0.02±0.04	0.03±0.08
	V1 0.01±0.01	0.02±0.02	0.03±0.02	0.01±0.03	0.01±0.01	0.02±0.02	0.03±0.02	0.01±0.04
	V2 0.01±0.01	0.02±0.02	0.03±0.02	0.02±0.07	0.01±0.01	0.02±0.02	0.03±0.02	0.01±0.06
	V3 0.01±0.01	0.02±0.02	0.02±0.02	0.02±0.09	0.01±0.01	0.02±0.02	0.03±0.02	0.02±0.11
	V4 0.01±0.01	0.01±0.02	0.03±0.02	0.02±0.08	0.01±0.01	0.02±0.02	0.03±0.03	0.02±0.09
C2	V5 0.01±0.01	0.02±0.02	0.03±0.02	0.02±0.07	0.01±0.01	0.02±0.02	0.03±0.02	0.03±0.09
	V6 0.01±0.01	0.02±0.02	0.05±0.03	0.02±0.03	0.01±0.02	0.02±0.02	0.05±0.03	0.02±0.04
	I 0.01±0.02	0.02±0.03	0.03±0.02	0.02±0.03	0.01±0.02	0.02±0.03	0.03±0.02	0.02±0.04
	II 0.01±0.01	0.02±0.02	0.03±0.02	0.02±0.04	0.01±0.02	0.01±0.02	0.03±0.02	0.02±0.04
	III 0.04±0.03	0.04±0.05	0.04±0.05	0.02±0.03	0.04±0.04	0.04±0.06	0.04±0.06	0.03±0.04
	AVL 0.03±0.03	0.03±0.03	0.03±0.04	0.02±0.04	0.03±0.04	0.03±0.05	0.03±0.05	0.02±0.04
	AVR 0.02±0.04	0.03±0.03	0.03±0.04	0.02±0.04	0.02±0.03	0.02±0.03	0.02±0.03	0.02±0.04
	AVF 0.02±0.03	0.03±0.03	0.03±0.03	0.02±0.03	0.02±0.04	0.02±0.04	0.03±0.04	0.02±0.04
	V1 0.01±0.01	0.02±0.02	0.03±0.02	0.01±0.02	0.01±0.01	0.02±0.02	0.03±0.02	0.01±0.02
	V2 0.01±0.01	0.01±0.02	0.03±0.01	0.01±0.03	0.01±0.01	0.02±0.02	0.03±0.02	0.01±0.04
C3	V3 0.01±0.01	0.02±0.02	0.02±0.02	0.02±0.04	0.01±0.01	0.02±0.02	0.02±0.02	0.01±0.04
	V4 0.0±0.01	0.01±0.02	0.03±0.02	0.02±0.04	0.01±0.01	0.01±0.02	0.03±0.02	0.02±0.04
	V5 0.01±0.01	0.02±0.02	0.03±0.02	0.02±0.04	0.01±0.01	0.02±0.02	0.03±0.03	0.02±0.04
	V6 0.01±0.01	0.02±0.02	0.04±0.03	0.02±0.04	0.01±0.02	0.02±0.02	0.04±0.03	0.02±0.04
	I 0.01±0.02	0.02±0.02	0.02±0.02	0.02±0.03	0.01±0.02	0.02±0.02	0.02±0.02	0.01±0.02
	II 0.01±0.01	0.01±0.02	0.03±0.02	0.02±0.02	0.01±0.01	0.01±0.02	0.03±0.02	0.01±0.03
	III 0.04±0.03	0.04±0.06	0.04±0.06	0.02±0.03	0.04±0.04	0.04±0.06	0.04±0.06	0.03±0.03
	AVL 0.03±0.04	0.03±0.04	0.03±0.04	0.01±0.03	0.03±0.04	0.03±0.05	0.03±0.05	0.02±0.04
	AVR 0.02±0.04	0.03±0.04	0.02±0.03	0.02±0.03	0.02±0.03	0.02±0.03	0.02±0.03	0.02±0.03
	AVF 0.01±0.03	0.02±0.03	0.03±0.03	0.01±0.02	0.02±0.04	0.03±0.04	0.03±0.04	0.02±0.03
C4	V1 0.01±0.01	0.01±0.02	0.03±0.02	0.01±0.01	0.01±0.01	0.02±0.02	0.03±0.02	0.01±0.02
	V2 0.01±0.01	0.02±0.01	0.02±0.01	0.01±0.02	0.01±0.01	0.01±0.01	0.02±0.01	0.01±0.02
	V3 0.01±0.01	0.01±0.01	0.03±0.02	0.01±0.02	0.01±0.01	0.01±0.01	0.03±0.02	0.01±0.02
	V4 0.0±0.01	0.01±0.01	0.03±0.02	0.02±0.02	0.01±0.01	0.02±0.01	0.03±0.02	0.01±0.02
	V5 0.0±0.01	0.02±0.02	0.02±0.02	0.01±0.02	0.01±0.01	0.02±0.02	0.02±0.02	0.01±0.02
	V6 0.01±0.01	0.02±0.01	0.03±0.02	0.01±0.02	0.01±0.01	0.02±0.02	0.04±0.02	0.01±0.02
	I 0.01±0.02	0.02±0.02	0.02±0.02	0.01±0.03	0.01±0.02	0.01±0.02	0.02±0.02	0.01±0.03
	II 0.01±0.01	0.01±0.02	0.02±0.02	0.01±0.02	0.01±0.02	0.02±0.02	0.02±0.02	0.01±0.02
	III 0.03±0.03	0.04±0.06	0.04±0.05	0.02±0.02	0.03±0.04	0.04±0.06	0.04±0.06	0.02±0.03
	AVL 0.02±0.04	0.03±0.04	0.03±0.04	0.01±0.03	0.03±0.03	0.03±0.04	0.03±0.04	0.01±0.03
C5	AVR 0.02±0.04	0.02±0.04	0.03±0.03	0.01±0.03	0.02±0.04	0.02±0.03	0.03±0.03	0.01±0.02
	AVF 0.01±0.02	0.02±0.03	0.02±0.03	0.01±0.02	0.02±0.03	0.03±0.04	0.03±0.04	0.01±0.02
	V1 0.01±0.01	0.01±0.02	0.03±0.02	0.01±0.01	0.01±0.01	0.02±0.02	0.03±0.02	0.01±0.01
	V2 0.01±0.01	0.01±0.01	0.02±0.01	0.01±0.02	0.01±0.01	0.01±0.01	0.02±0.01	0.01±0.02
	V3 0.01±0.01	0.01±0.01	0.03±0.02	0.01±0.02	0.01±0.01	0.01±0.01	0.03±0.02	0.01±0.02
	V4 0.0±0.01	0.01±0.01	0.02±0.01	0.01±0.02	0.01±0.01	0.02±0.01	0.03±0.02	0.01±0.01
	V5 0.0±0.01	0.01±0.01	0.02±0.02	0.01±0.02	0.01±0.02	0.01±0.01	0.02±0.02	0.01±0.02
	V6 0.01±0.01	0.01±0.01	0.02±0.02	0.01±0.02	0.01±0.02	0.02±0.02	0.03±0.02	0.01±0.02

Table 21: ECG (limb) lead-reconstruction: difference of QRS-complex between real and reconstructed lead overall Sot- and Sot+ ECGs.

Lead	Δ-QRS (Sot-) ↓				Δ-QRS (Sot+) ↓			
	ECGrecover	EKGAN [12]	Pix2Pix [10]	CopyPaste	ECGrecover	EKGAN [12]	Pix2Pix [10]	CopyPaste
C _I	II	0.01±0.01	0.01±0.01	0.02±0.03	0.01±0.03	0.01±0.02	0.01±0.02	0.02±0.02
	III	0.04±0.05	0.04±0.04	0.05±0.06	0.05±0.06	0.04±0.06	0.03±0.04	0.05±0.06
	AVL	0.03±0.04	0.02±0.03	0.03±0.03	0.04±0.05	0.03±0.04	0.02±0.04	0.03±0.04
	AVR	0.02±0.05	0.01±0.03	0.02±0.03	0.01±0.03	0.02±0.04	0.01±0.03	0.02±0.03
	AVF	0.02±0.03	0.02±0.03	0.02±0.04	0.02±0.04	0.02±0.05	0.02±0.04	0.02±0.05
	V1	0.01±0.01	0.01±0.01	0.02±0.02	0.02±0.03	0.01±0.01	0.01±0.01	0.02±0.02
	V2	0.01±0.01	0.01±0.01	0.02±0.02	0.01±0.03	0.01±0.01	0.01±0.01	0.02±0.01
	V3	0.01±0.01	0.01±0.01	0.02±0.04	0.01±0.02	0.01±0.01	0.01±0.02	0.01±0.03
	V4	0.01±0.01	0.01±0.01	0.02±0.04	0.01±0.02	0.01±0.01	0.01±0.01	0.02±0.02
	V5	0.01±0.01	0.01±0.01	0.02±0.04	0.01±0.02	0.01±0.01	0.01±0.01	0.02±0.04
C _{II}	V6	0.01±0.01	0.01±0.01	0.02±0.03	0.01±0.03	0.01±0.02	0.01±0.02	0.03±0.03
	I	0.01±0.02	0.01±0.02	0.02±0.02	0.01±0.02	0.01±0.02	0.01±0.03	0.02±0.02
	III	0.05±0.05	0.05±0.05	0.04±0.06	0.04±0.06	0.05±0.06	0.04±0.06	0.05±0.06
	AVL	0.03±0.03	0.02±0.03	0.04±0.04	0.04±0.05	0.03±0.04	0.02±0.04	0.04±0.04
	AVR	0.02±0.04	0.02±0.04	0.03±0.03	0.01±0.04	0.02±0.03	0.02±0.03	0.01±0.04
	AVF	0.02±0.03	0.02±0.03	0.01±0.03	0.01±0.03	0.02±0.04	0.02±0.04	0.02±0.04
	V1	0.01±0.01	0.01±0.01	0.01±0.01	0.01±0.02	0.01±0.01	0.01±0.01	0.02±0.02
	V2	0.01±0.01	0.01±0.01	0.02±0.02	0.01±0.01	0.01±0.01	0.01±0.01	0.02±0.02
	V3	0.01±0.01	0.01±0.01	0.01±0.03	0.01±0.02	0.01±0.01	0.01±0.02	0.01±0.03
	V4	0.01±0.01	0.01±0.01	0.01±0.02	0.01±0.01	0.01±0.01	0.01±0.01	0.01±0.03
C _{III}	V5	0.01±0.01	0.01±0.01	0.01±0.02	0.01±0.01	0.01±0.01	0.01±0.01	0.01±0.02
	V6	0.01±0.01	0.01±0.01	0.01±0.02	0.01±0.01	0.01±0.02	0.01±0.01	0.01±0.02
C _{IV}	I	0.01±0.04	0.05±0.06	0.02±0.06	0.05±0.06	0.01±0.04	0.05±0.06	0.02±0.06
	II	0.01±0.02	0.02±0.03	0.01±0.03	0.04±0.06	0.01±0.02	0.02±0.03	0.01±0.03
	AVL	0.03±0.03	0.03±0.04	0.03±0.03	0.04±0.05	0.04±0.04	0.03±0.05	0.03±0.04
	AVR	0.02±0.07	0.04±0.05	0.02±0.06	0.05±0.06	0.02±0.09	0.04±0.05	0.02±0.08
	AVF	0.02±0.04	0.02±0.03	0.02±0.03	0.03±0.05	0.02±0.04	0.02±0.04	0.03±0.06
	V1	0.01±0.01	0.01±0.01	0.02±0.02	0.03±0.06	0.01±0.01	0.01±0.01	0.02±0.02
	V2	0.01±0.01	0.01±0.01	0.01±0.02	0.01±0.01	0.01±0.01	0.01±0.01	0.02±0.02
	V3	0.01±0.01	0.01±0.01	0.01±0.03	0.01±0.02	0.01±0.01	0.01±0.02	0.01±0.03
	V4	0.01±0.01	0.01±0.01	0.01±0.02	0.01±0.01	0.01±0.01	0.01±0.01	0.01±0.03
	V5	0.01±0.01	0.01±0.01	0.01±0.02	0.01±0.01	0.01±0.01	0.01±0.01	0.01±0.02
C _{AVL}	V6	0.01±0.02	0.02±0.03	0.02±0.04	0.05±0.06	0.01±0.02	0.02±0.03	0.02±0.05
	I	0.01±0.03	0.01±0.04	0.03±0.02	0.01±0.04	0.01±0.02	0.01±0.03	0.02±0.02
	II	0.01±0.02	0.01±0.02	0.02±0.04	0.01±0.05	0.01±0.02	0.01±0.02	0.01±0.06
	III	0.04±0.05	0.03±0.04	0.05±0.06	0.05±0.07	0.03±0.05	0.03±0.04	0.05±0.07
	AVR	0.02±0.05	0.01±0.02	0.03±0.03	0.0±0.0	0.02±0.04	0.01±0.02	0.02±0.03
	AVF	0.02±0.03	0.02±0.03	0.02±0.05	0.03±0.05	0.02±0.04	0.02±0.04	0.03±0.05
	V1	0.01±0.01	0.01±0.01	0.02±0.02	0.02±0.05	0.01±0.01	0.01±0.01	0.02±0.06
	V2	0.01±0.01	0.01±0.02	0.01±0.02	0.01±0.05	0.01±0.03	0.02±0.02	0.01±0.05
	V3	0.01±0.01	0.01±0.02	0.02±0.04	0.01±0.05	0.01±0.01	0.01±0.02	0.01±0.06
	V4	0.01±0.01	0.01±0.02	0.02±0.04	0.01±0.05	0.01±0.02	0.01±0.02	0.01±0.05
C _{AVR}	V5	0.01±0.01	0.01±0.02	0.03±0.04	0.01±0.05	0.01±0.01	0.01±0.02	0.02±0.04
	V6	0.01±0.01	0.01±0.02	0.04±0.03	0.01±0.05	0.01±0.02	0.01±0.02	0.01±0.05
C _{AVF}	I	0.01±0.02	0.03±0.03	0.02±0.02	0.02±0.04	0.01±0.02	0.04±0.04	0.02±0.03
	II	0.01±0.01	0.01±0.01	0.01±0.02	0.01±0.03	0.01±0.02	0.01±0.02	0.02±0.04
	III	0.03±0.04	0.05±0.05	0.03±0.05	0.03±0.05	0.04±0.05	0.04±0.06	0.03±0.06
	AVL	0.03±0.04	0.02±0.04	0.03±0.03	0.04±0.05	0.03±0.04	0.03±0.05	0.03±0.06
	AVR	0.02±0.05	0.03±0.04	0.02±0.03	0.02±0.05	0.02±0.04	0.03±0.04	0.02±0.05
	V1	0.01±0.01	0.01±0.01	0.02±0.01	0.02±0.03	0.01±0.01	0.01±0.01	0.02±0.02
	V2	0.01±0.01	0.01±0.01	0.02±0.01	0.02±0.04	0.01±0.01	0.01±0.01	0.02±0.02
	V3	0.01±0.01	0.01±0.01	0.01±0.03	0.02±0.04	0.01±0.01	0.01±0.02	0.01±0.03
	V4	0.01±0.01	0.01±0.02	0.01±0.02	0.02±0.04	0.01±0.02	0.01±0.02	0.02±0.05
	V5	0.01±0.01	0.01±0.02	0.01±0.03	0.02±0.04	0.01±0.01	0.02±0.03	0.01±0.04
	V6	0.01±0.02	0.01±0.02	0.02±0.03	0.02±0.04	0.01±0.02	0.02±0.02	0.03±0.04

Table 22: ECG (thorachic) lead-reconstruction: difference of QRS-complex between real and reconstructed lead overall Sot+ and Sot- ECGs.

Lead	Δ-QRS (Sot-) ↓				Δ-QRS (Sot+) ↓			
	ECGrecover	EKGAN [12]	Pix2Pix [10]	CopyPaste	ECGrecover	EKGAN [12]	Pix2Pix [10]	CopyPaste
CV ₁	I 0.01 ±0.02	0.02±0.02	0.02±0.02	0.02±0.02	0.01 ±0.02	0.02±0.02	0.02±0.03	0.01 ±0.02
	II 0.01 ±0.01	0.01 ±0.01	0.01 ±0.02	0.01 ±0.02	0.01 ±0.02	0.01 ±0.01	0.01 ±0.02	0.01 ±0.02
	III 0.06±0.05	0.04±0.05	0.03 ±0.05	0.03 ±0.06	0.07±0.05	0.03 ±0.05	0.03 ±0.05	0.04±0.06
	AVL 0.03 ±0.03	0.03 ±0.03	0.03 ±0.03	0.03 ±0.04	0.03 ±0.04	0.03 ±0.04	0.03 ±0.04	0.03 ±0.05
	AVR 0.02 ±0.04	0.02±0.03	0.04±0.03	0.02 ±0.04	0.02 ±0.03	0.02±0.03	0.04±0.04	0.02 ±0.03
	AVF 0.02 ±0.03	0.02 ±0.03	0.02 ±0.03	0.02 ±0.03	0.02 ±0.04	0.02 ±0.04	0.02 ±0.04	0.02±0.04
	V2 0.01 ±0.01	0.01 ±0.01	0.01 ±0.01	0.01 ±0.01	0.01 ±0.01	0.02±0.01	0.01 ±0.01	0.01 ±0.02
	V3 0.01 ±0.01	0.01 ±0.01	0.01 ±0.02	0.01 ±0.01	0.01 ±0.01	0.01 ±0.01	0.01 ±0.02	0.01 ±0.02
	V4 0.01 ±0.01	0.01 ±0.01	0.01 ±0.02	0.01 ±0.01	0.01 ±0.01	0.02±0.01	0.02±0.02	0.01 ±0.02
	V5 0.01 ±0.01	0.01 ±0.01	0.08±0.04	0.01 ±0.01	0.01 ±0.01	0.01 ±0.01	0.07±0.05	0.01 ±0.02
CV ₂	V6 0.01 ±0.01	0.01 ±0.01	0.05±0.02	0.01 ±0.01	0.01 ±0.02	0.01 ±0.02	0.05±0.03	0.02±0.02
	I 0.01 ±0.02	0.01 ±0.02	0.03±0.02	0.01 ±0.02	0.01 ±0.02	0.01 ±0.02	0.03±0.02	0.01 ±0.02
	II 0.01 ±0.01	0.01 ±0.01	0.01 ±0.02	0.01 ±0.01	0.01 ±0.02	0.01 ±0.02	0.01 ±0.02	0.01 ±0.02
	III 0.06±0.05	0.05±0.04	0.04 ±0.06	0.04 ±0.06	0.06±0.06	0.04 ±0.05	0.04 ±0.06	0.04 ±0.06
	AVL 0.03 ±0.03	0.05±0.04	0.03 ±0.03	0.04±0.04	0.03 ±0.04	0.05±0.04	0.03 ±0.04	0.04±0.05
	AVR 0.01 ±0.04	0.02±0.03	0.04±0.03	0.01 ±0.04	0.02±0.03	0.02±0.03	0.04±0.03	0.01 ±0.03
	AVF 0.02 ±0.03	0.02 ±0.03	0.02 ±0.03	0.02 ±0.03	0.02 ±0.04	0.02 ±0.04	0.02 ±0.04	0.02 ±0.04
	V1 0.01 ±0.01	0.01 ±0.01	0.02±0.02	0.01 ±0.01	0.01 ±0.01	0.01 ±0.01	0.02±0.02	0.01 ±0.01
	V3 0.01 ±0.01	0.01 ±0.01	0.01 ±0.02	0.01 ±0.01	0.01 ±0.01	0.01 ±0.01	0.01±0.01	0.01 ±0.01
	V4 0.01 ±0.01	0.01 ±0.01	0.01 ±0.01	0.01 ±0.01	0.01 ±0.02	0.01 ±0.02	0.02±0.01	0.01 ±0.01
CV ₃	V5 0.01 ±0.01	0.01 ±0.01	0.08±0.05	0.01 ±0.01	0.01 ±0.01	0.01 ±0.01	0.07±0.06	0.01 ±0.01
	V6 0.01 ±0.01	0.01 ±0.01	0.07±0.03	0.01 ±0.01	0.01 ±0.02	0.01 ±0.02	0.07±0.03	0.01 ±0.02
	I 0.01 ±0.02	0.01 ±0.02	0.03±0.02	0.01 ±0.02	0.01±0.02	0.01 ±0.02	0.03±0.02	0.01 ±0.02
	II 0.01 ±0.01	0.01 ±0.01	0.02±0.02	0.01 ±0.02	0.01 ±0.02	0.01 ±0.02	0.02±0.02	0.01 ±0.02
	III 0.06±0.05	0.05±0.04	0.04 ±0.06	0.04 ±0.06	0.05±0.06	0.04 ±0.05	0.05±0.06	0.05±0.06
	AVL 0.03 ±0.03	0.03 ±0.03	0.03 ±0.03	0.04±0.04	0.03 ±0.04	0.03 ±0.04	0.03 ±0.03	0.04±0.05
	AVR 0.01 ±0.04	0.02±0.03	0.03±0.03	0.01 ±0.04	0.01 ±0.03	0.02±0.03	0.03±0.03	0.01 ±0.03
	AVF 0.02 ±0.03	0.02 ±0.03	0.02 ±0.04	0.02 ±0.03	0.02 ±0.04	0.02 ±0.04	0.02 ±0.05	0.02 ±0.05
	V1 0.01 ±0.01	0.01 ±0.01	0.02±0.02	0.01 ±0.02	0.01 ±0.01	0.01 ±0.01	0.02±0.02	0.01 ±0.02
	V2 0.01 ±0.01	0.01 ±0.01	0.01 ±0.01	0.01 ±0.01	0.01 ±0.01	0.01 ±0.01	0.02±0.01	0.01 ±0.02
CV ₄	V4 0.01 ±0.01	0.01±0.01	0.02±0.02	0.01 ±0.01	0.01 ±0.01	0.01 ±0.01	0.02±0.02	0.01 ±0.01
	V5 0.01 ±0.01	0.01 ±0.01	0.03±0.05	0.01 ±0.01	0.01 ±0.01	0.01 ±0.01	0.03±0.05	0.01 ±0.02
	V6 0.01 ±0.01	0.01 ±0.01	0.04±0.03	0.01 ±0.01	0.01 ±0.02	0.01 ±0.02	0.04±0.03	0.01 ±0.02
	I 0.01 ±0.02	0.01 ±0.02	0.03±0.03	0.01 ±0.02	0.01 ±0.02	0.01 ±0.02	0.03±0.02	0.01 ±0.03
	II 0.01 ±0.01	0.01 ±0.01	0.02±0.02	0.01 ±0.01	0.01 ±0.02	0.01 ±0.02	0.02±0.02	0.01 ±0.02
	III 0.06±0.04	0.05±0.05	0.04 ±0.06	0.04 ±0.06	0.06±0.05	0.04 ±0.05	0.05±0.06	0.05±0.06
	AVL 0.03 ±0.03	0.03 ±0.03	0.03 ±0.03	0.05±0.04	0.03 ±0.04	0.02 ±0.03	0.03±0.04	0.05±0.05
	AVR 0.02 ±0.04	0.03±0.04	0.03±0.03	0.01 ±0.04	0.01 ±0.03	0.01 ±0.03	0.03±0.03	0.01 ±0.03
	AVF 0.02 ±0.03	0.02 ±0.03	0.02 ±0.04	0.02 ±0.03	0.02 ±0.05	0.02 ±0.04	0.02 ±0.04	0.02±0.05
	V1 0.01 ±0.01	0.01 ±0.01	0.01±0.02	0.01 ±0.02	0.01 ±0.01	0.01 ±0.01	0.01±0.01	0.01 ±0.03
CV ₅	V2 0.01 ±0.01	0.01 ±0.01	0.02±0.01	0.01 ±0.01	0.01 ±0.01	0.01 ±0.01	0.02±0.01	0.01 ±0.02
	V3 0.01 ±0.01	0.01 ±0.01	0.01 ±0.03	0.01 ±0.01	0.01 ±0.01	0.01 ±0.01	0.01 ±0.02	0.01 ±0.01
	V4 0.01 ±0.01	0.01 ±0.01	0.01±0.02	0.01 ±0.01				
	V5 0.01 ±0.01	0.01 ±0.01	0.01±0.02	0.01 ±0.01	0.01 ±0.01	0.01 ±0.01	0.01 ±0.02	0.01 ±0.01
	V6 0.01 ±0.01	0.01 ±0.01	0.02±0.02	0.01 ±0.01	0.01 ±0.02	0.01 ±0.02	0.02±0.02	0.01 ±0.02
	I 0.01 ±0.02	0.01 ±0.02	0.03±0.02	0.01 ±0.02	0.01 ±0.02	0.01 ±0.02	0.02±0.02	0.01 ±0.02
	II 0.01 ±0.01	0.01 ±0.01	0.01 ±0.02	0.01 ±0.01	0.01 ±0.02	0.01 ±0.02	0.01 ±0.02	0.01 ±0.01
	III 0.06±0.05	0.04±0.06	0.04 ±0.06	0.04 ±0.06	0.06±0.05	0.04 ±0.06	0.05±0.06	0.05±0.06
	AVL 0.02 ±0.04	0.02 ±0.04	0.04±0.04	0.04 ±0.05	0.03±0.04	0.02 ±0.04	0.03±0.04	0.05±0.05
	AVR 0.01 ±0.04	0.01 ±0.04	0.02±0.03	0.01 ±0.04	0.01 ±0.03	0.01 ±0.03	0.02±0.03	0.01 ±0.03
CV ₆	AVF 0.02 ±0.03	0.02 ±0.03	0.02 ±0.03	0.02 ±0.03	0.02 ±0.04	0.02 ±0.04	0.02 ±0.04	0.03±0.04
	V1 0.01 ±0.01	0.01 ±0.01	0.02±0.01	0.01 ±0.01	0.01 ±0.01	0.01 ±0.01	0.01 ±0.01	0.02±0.02
	V2 0.01 ±0.01	0.01 ±0.01	0.02±0.01	0.01 ±0.01	0.01 ±0.01	0.01 ±0.01	0.01 ±0.01	0.01 ±0.02
	V3 0.01 ±0.01	0.01 ±0.01	0.01 ±0.02	0.01 ±0.01	0.01 ±0.01	0.01 ±0.01	0.01 ±0.02	0.01 ±0.02
	V4 0.01 ±0.01	0.01 ±0.01	0.01±0.01	0.01 ±0.01	0.01 ±0.01	0.01 ±0.01	0.01 ±0.01	0.01 ±0.02
	V5 0.01 ±0.01	0.01 ±0.01	0.01±0.01	0.01 ±0.01	0.01 ±0.01	0.01 ±0.01	0.01 ±0.01	0.01 ±0.02
	I 0.01 ±0.02	0.01 ±0.02	0.02±0.02	0.01 ±0.02				
	II 0.01 ±0.01	0.01 ±0.01	0.01 ±0.02	0.01 ±0.01	0.01 ±0.02	0.01 ±0.02	0.01 ±0.02	0.01 ±0.01
	III 0.06±0.05	0.04±0.06	0.04 ±0.06	0.04 ±0.06	0.06±0.05	0.04 ±0.06	0.05±0.06	0.05±0.06
	AVL 0.02 ±0.04	0.02 ±0.04	0.04±0.04	0.04 ±0.05	0.03±0.04	0.02 ±0.04	0.04±0.04	0.04±0.05
CV ₇	AVR 0.01 ±0.04	0.01 ±0.04	0.02±0.03	0.01 ±0.04	0.01 ±0.04	0.01 ±0.04	0.01 ±0.04	0.01 ±0.03
	AVF 0.02 ±0.03	0.02 ±0.03	0.02 ±0.03	0.02 ±0.03	0.02 ±0.04	0.02 ±0.04	0.02 ±0.04	0.03±0.04
	V1 0.01 ±0.01	0.01 ±0.01	0.02±0.01	0.01 ±0.01	0.01 ±0.01	0.01 ±0.01	0.01 ±0.01	0.02±0.02
	V2 0.01 ±0.01	0.01 ±0.01	0.02±0.01	0.01 ±0.01	0.01 ±0.01	0.01 ±0.01	0.01 ±0.01	0.01 ±0.02
	V3 0.01 ±0.01	0.01 ±0.01	0.01 ±0.02	0.01 ±0.01	0.01 ±0.01	0.01 ±0.01	0.01 ±0.02	0.01 ±0.02
	V4 0.01 ±0.01	0.01 ±0.01	0.01±0.01	0.01 ±0.01	0.01 ±0.01	0.01 ±0.01	0.01 ±0.01	0.01 ±0.02
	V5 0.01 ±0.01	0.01 ±0.01	0.01±0.01	0.01 ±0.01	0.01 ±0.01	0.01 ±0.01	0.01 ±0.01	0.01 ±0.02
	I 0.01 ±0.02	0.01 ±0.						

Table 23: ECG segment-recovery: percentage of detected R peaks in all the reconstructed leads.

Lead	%R (Sot-) ↑				%R (Sot+) ↑				
	ECGrecover	EKGAN [12]	Pix2Pix [10]	CopyPaste	ECGrecover	EKGAN [12]	Pix2Pix [10]	CopyPaste	
C1	I	100 ±5.54	18.18±11.35	41.18±14.65	80.0±17.35	100 ±9.56	16.67±11.48	42.86±15.87	75.0±17.36
	II	100 ±3.15	16.67±10.89	55.56±15.09	77.78±15.86	100 ±9.5	16.67±11.39	55.56±15.82	77.78±15.16
	III	100 ±10.35	16.67±11.47	22.22±14.43	75.0±24.25	100 ±14.15	14.29±11.95	20.0±14.55	71.43±26.69
	AVL	100 ±5.92	11.11±11.27	40.0±16.57	70.0±23.64	100 ±6.66	12.5±12.43	37.98±16.78	70.0±25.13
	AVR	100 ±8.16	18.18±11.62	33.33±14.57	80.0±14.66	100 ±13.55	18.18±11.77	33.33±15.15	77.78±16.03
	AVF	100 ±6.52	18.18±11.41	50.0±14.51	77.78±13.77	100 ±9.9	12.5±12.73	50.0±16.38	77.78±17.05
	V1	100 ±2.24	20.0±12.11	45.45±15.73	75.0±14.69	100 ±2.79	19.09±13.75	44.44±16.64	75.0±19.22
	V2	100 ±6.22	22.22±13.26	50.0±15.42	77.78±15.35	100 ±4.83	22.22±14.35	50.0±16.97	75.0±15.74
	V3	100 ±4.5	20.0±11.35	45.45±13.8	80.0±16.96	100 ±8.32	22.22±13.03	50.0±15.21	77.78±17.7
	V4	100 ±4.34	20.0±11.81	44.44±15.18	77.78±16.15	100 ±9.15	22.22±12.69	44.44±15.54	77.78±14.38
C2	V5	100 ±3.27	16.67±11.35	40.0±13.58	78.57±16.57	100 ±8.8	16.67±12.38	37.5±15.34	78.89±14.21
	V6	100 ±2.79	16.67±12.1	45.45±13.7	70.0±22.67	100 ±8.09	17.42±12.1	44.44±16.76	75.0±21.94
	I	100 ±4.26	25.0±11.46	50.0±14.64	80.0±16.85	100 ±6.97	22.22±10.63	50.0±13.98	77.78±15.85
	II	100 ±2.3	25.0±10.83	57.14±14.6	77.78±16.22	100 ±8.26	22.22±11.16	57.14±15.3	77.78±14.77
	III	100 ±14.65	22.22±13.86	33.33±14.77	75.0±19.82	100 ±14.86	22.22±15.58	33.33±15.94	70.0±22.06
	AVL	100 ±4.64	22.22±13.34	50.0±15.01	70.0±19.87	100 ±4.54	22.22±13.45	50.0±15.35	66.67±19.76
	AVR	100 ±5.45	25.0±11.86	40.0±13.01	80.0±14.5	100 ±11.46	25.0±13.21	40.0±15.09	75.0±16.13
C3	AVF	100 ±6.08	22.22±13.26	54.55±15.04	77.78±13.89	100 ±8.93	22.22±13.88	55.56±16.24	77.78±16.49
	V1	100 ±1.48	33.33±13.56	55.56±14.61	75.0±15.04	100 ±2.4	33.33±14.46	55.56±15.39	70.0±15.26
	V2	100 ±6.32	40.0±12.36	63.64±14.18	77.78±14.53	100 ±4.58	40.0±14.11	62.5±14.86	75.0±14.28
	V3	100 ±3.84	30.77±11.33	54.55±14.01	77.78±14.97	100 ±7.83	30.38±12.07	50.0±13.94	77.78±14.09
	V4	100 ±3.85	30.77±10.91	53.85±14.8	77.78±14.51	100 ±8.23	33.33±11.2	50.0±14.27	77.35±13.41
	V5	100 ±2.39	30.0±12.08	41.67±14.93	80.0±16.14	100 ±7.39	29.28±13.78	40.84±13.03	77.78±15.71
	V6	100 ±1.52	33.33±14.45	50.0±15.13	77.78±15.99	100 ±6.61	30.0±14.0	50.0±14.57	77.78±15.55
C4	I	100 ±4.12	33.33±10.54	53.85±13.82	83.33±15.9	100 ±6.4	30.0±10.43	54.55±14.78	80.0±17.52
	II	100 ±2.57	33.33±10.68	62.5±13.97	80.0±17.0	100 ±7.57	33.33±10.61	62.5±15.08	77.78±18.24
	III	100 ±13.04	25.0±12.69	40.0±14.92	75.0±19.53	100 ±14.59	22.22±15.56	40.0±14.73	71.43±21.44
	AVL	100 ±4.27	25.0±12.81	53.85±14.59	72.73±17.43	100 ±5.33	22.22±13.32	54.55±14.07	70.0±16.71
	AVR	100 ±5.94	30.0±13.69	50.0±14.07	81.82±15.62	100 ±10.22	28.57±13.95	50.0±14.41	80.0±15.12
	AVF	100 ±5.74	25.0±13.97	62.5±13.42	77.78±15.05	100 ±8.21	22.22±13.6	60.0±15.27	77.78±15.38
	V1	100 ±1.28	45.45±13.19	60.0±13.9	77.78±14.74	100 ±1.48	44.44±14.43	55.56±14.33	70.0±15.91
	V2	100 ±6.0	44.44±12.49	63.64±14.35	77.78±14.46	100 ±4.47	42.26±13.27	62.5±14.34	72.73±15.09
	V3	100 ±4.03	37.5±13.19	60.0±15.37	80.0±14.72	100 ±7.03	37.5±14.03	62.5±14.52	77.78±14.55
	V4	100 ±3.89	41.67±14.59	60.0±14.72	80.0±17.32	100 ±6.88	40.0±14.52	60.0±14.88	77.78±18.03
C5	V5	100 ±2.63	37.5±11.83	50.0±14.1	80.0±16.87	100 ±5.7	37.5±13.68	50.0±14.6	77.78±18.16
	V6	100 ±1.57	40.0±12.81	55.56±14.51	80.0±16.09	100 ±5.91	40.0±13.51	55.56±15.11	77.78±18.13
	I	100 ±3.36	41.67±9.35	60.0±12.69	91.67±15.89	100 ±5.47	40.0±10.04	55.56±14.21	81.82±17.7
	II	100 ±2.45	40.0±9.7	66.67±12.61	88.89±17.21	100 ±6.7	37.5±11.13	66.67±14.21	80.0±18.08
	III	100 ±12.91	30.0±14.91	50.0±15.7	80.0±20.55	100 ±14.69	25.0±16.1	50.0±17.11	75.0±22.68
	AVL	100 ±4.21	33.33±14.83	62.5±15.72	72.73±20.23	100 ±4.31	33.33±15.33	62.5±14.74	71.43±20.73
	AVR	100 ±4.71	37.5±13.57	54.55±14.58	88.89±13.21	100 ±8.55	37.5±14.34	53.85±13.68	80.0±15.9
C6	AVF	100 ±5.31	30.0±16.01	66.67±13.38	80.0±13.36	100 ±8.13	30.0±16.23	62.5±14.96	75.0±16.38
	V1	100 ±1.43	55.56±13.89	72.73±12.58	77.78±14.29	100 ±1.1	55.56±15.65	71.43±12.54	75.0±15.95
	V2	100 ±6.17	60.0±13.44	77.78±12.97	80.0±14.11	100 ±4.53	55.56±15.82	77.35±14.54	75.0±16.45
	V3	100 ±4.49	41.67±10.7	60.0±13.93	87.5±18.26	100 ±7.01	41.67±10.37	62.5±12.7	77.78±19.41
	V4	100 ±3.26	41.67±11.12	60.0±13.11	81.82±18.45	100 ±7.7	40.0±11.66	60.0±13.35	77.78±18.45
	V5	100 ±2.5	44.44±11.46	55.56±11.85	81.82±18.6	100 ±6.1	42.86±11.52	50.0±13.64	78.18±18.43
	V6	100 ±1.71	45.45±12.05	60.0±13.27	81.82±18.67	100 ±5.68	44.44±12.76	58.33±15.54	78.89±18.45
C7	I	100 ±3.39	55.56±8.82	70.0±11.3	100 ±15.81	100 ±5.93	55.56±9.88	66.67±13.74	91.67±16.54
	II	100 ±2.35	55.56±7.63	76.92±12.34	90.91±16.96	100 ±6.49	55.56±9.55	77.78±12.34	91.67±16.92
	III	100 ±13.61	44.44±16.78	60.0±11.43	88.89±19.87	100 ±13.12	44.44±17.79	60.0±13.11	88.89±20.09
	AVL	100 ±4.4	50.0±14.53	63.64±13.35	83.33±19.57	100 ±4.59	50.0±13.98	63.64±12.51	88.89±18.88
	AVR	100 ±6.69	54.55±13.73	63.64±12.78	92.31±16.35	100 ±10.07	50.0±14.89	60.0±13.29	91.29±17.1
	AVF	100 ±5.23	55.56±12.52	75.0±11.51	90.91±17.82	100 ±7.81	55.56±12.84	70.0±13.35	90.91±18.29
	V1	100 ±1.65	55.56±10.52	66.67±12.5	88.89±18.2	100 ±1.34	55.56±11.94	70.0±12.2	80.0±20.02
	V2	100 ±5.91	55.56±11.14	77.78±11.85	90.0±17.65	100 ±4.11	55.56±12.38	77.78±12.11	82.57±18.89
	V3	100 ±3.89	55.56±9.19	70.0±11.77	91.67±16.64	100 ±6.95	55.56±9.68	71.43±12.47	88.2±18.27
	V4	100 ±3.23	55.56±9.27	72.73±11.6	91.67±17.38	100 ±6.97	55.56±10.42	75.0±12.94	88.89±18.01
C8	V5	100 ±2.4	55.56±9.52	70.0±11.21	91.67±17.37	100 ±5.08	55.56±10.19	66.67±13.32	88.2±17.55
	V6	100 ±1.68	55.56±8.87	72.73±11.08	90.91±17.55	100 ±4.42	55.56±10.65	70.72±12.94	87.5±17.55

Table 24: ECG (limb) lead-reconstruction: percentage of detected R peaks in all the reconstructed leads.

Lead	%‐R (Sot‐) ↑				%‐R (Sot+) ↑				
	ECGreco	EKGAN [12]	Pix2Pix [10]	CopyPaste	ECGreco	EKGAN [12]	Pix2Pix [10]	CopyPaste	
C_I	II	100±3.14	100±2.38	100±1.51	100±2.18	100±9.64	100±8.76	100±7.22	100±8.21
	III	100±20.91	100±18.65	100±5.43	100±5.21	100±16.33	100±15.77	100±11.15	100±10.63
	AVL	100±5.56	100±12.01	91.67±12.6	100±1.17	100±5.42	100±9.52	100±11.11	100±1.45
	AVR	100±5.12	100±4.2	100±16.33	100±1.88	100±9.01	100±7.94	100±17.58	100±8.08
	AVF	100±6.47	100±6.39	100±1.48	100±6.01	100±10.57	100±10.76	100±6.84	100±9.37
	V1	100±1.78	100±1.44	100±6.69	100±1.17	100±3.86	100±1.8	100±7.47	100±1.77
	V2	100±6.34	100±6.23	100±8.18	100±3.04	100±6.18	100±5.42	100±8.87	100±4.1
	V3	100±4.33	100±4.06	100±3.96	100±2.69	100±9.36	100±8.38	100±7.97	100±6.88
	V4	100±3.64	100±4.08	100±1.71	100±2.1	100±9.45	100±8.66	100±6.73	100±7.51
	V5	100±3.65	100±2.34	100±5.06	100±1.57	100±8.76	100±8.37	100±11.23	100±7.07
	V6	100±2.33	100±2.08	100±3.97	100±1.41	100±7.33	100±6.89	100±10.18	100±5.6
C_II	I	100±4.85	100±7.36	100±7.48	100±7.38	100±7.82	100±12.94	100±13.43	100±12.83
	III	100±9.52	100±14.21	100±2.1	100±0.52	100±12.19	100±16.72	100±7.98	100±6.99
	AVL	100±4.21	100±7.63	92.31±11.13	100±0.52	100±4.74	100±8.63	90.91±11.91	100±0.87
	AVR	100±6.72	100±13.73	100±16.39	100±12.23	100±13.79	100±14.95	100±17.66	100±15.41
	AVF	100±6.78	100±7.42	100±1.05	100±0.52	100±8.72	100±9.94	100±3.33	100±3.35
	V1	100±2.11	100±3.26	100±4.58	100±1.38	100±0.96	100±1.12	100±3.63	100±0.58
	V2	100±6.36	100±7.12	100±6.38	100±5.59	100±4.49	100±4.43	100±4.73	100±3.27
	V3	100±5.08	100±5.09	100±4.59	100±4.35	100±7.8	100±8.86	100±8.22	100±8.14
	V4	100±4.47	100±5.27	100±3.07	100±3.2	100±9.27	100±10.4	100±7.63	100±8.61
	V5	100±3.19	100±4.0	100±4.47	100±2.18	100±7.65	100±10.7	100±11.05	100±8.31
	V6	100±2.48	100±2.92	100±3.23	100±1.37	100±6.14	100±9.88	100±10.44	100±6.86
C_III	I	100±4.24	100±19.79	100±5.43	100±18.97	100±7.41	100±21.26	100±8.9	100±21.52
	II	100±3.36	100±6.35	100±3.35	100±17.2	100±9.87	100±12.15	100±9.48	100±19.12
	AVL	100±8.4	100±11.82	90.0±15.82	100±15.88	100±8.13	100±13.85	88.89±14.97	100±17.02
	AVR	100±4.69	100±26.19	100±5.32	100±21.11	100±10.42	100±24.46	100±8.84	100±22.9
	AVF	100±6.0	100±11.97	100±6.16	100±17.53	100±8.15	100±17.55	100±7.26	100±18.23
	V1	100±3.58	100±14.57	100±9.78	100±16.3	100±4.37	100±17.61	100±10.61	100±16.88
	V2	100±6.9	100±14.15	100±10.07	100±17.11	100±6.02	100±16.66	100±10.49	100±17.38
	V3	100±5.42	100±14.59	100±5.28	100±17.27	100±8.6	100±17.0	100±8.22	100±18.84
	V4	100±4.27	100±11.09	100±5.32	100±17.43	100±9.17	100±15.44	100±10.37	100±19.81
	V5	100±3.74	100±11.11	100±6.31	100±17.36	100±9.15	100±15.82	100±11.25	100±19.89
	V6	100±3.37	100±11.73	100±6.9	100±17.3	100±8.42	100±15.89	100±10.14	100±19.54
C_AVL	I	100±3.12	100±13.01	100±3.82	100±13.19	100±5.82	100±15.89	100±8.62	100±15.49
	II	100±2.5	100±2.92	100±2.81	100±10.19	100±7.63	100±9.74	100±8.05	100±12.61
	III	100±7.63	100±8.83	100±12.39	100±11.24	100±11.28	100±11.46	100±12.61	100±13.53
	AVR	100±6.66	90.0±17.73	100±2.88	100±17.31	100±10.45	88.89±19.5	100±7.31	100±18.1
	AVF	100±6.71	100±6.83	100±6.61	100±11.79	100±10.21	100±10.2	100±10.21	100±12.69
	V1	100±1.28	100±4.77	90.0±11.98	100±10.22	100±2.55	100±5.91	91.67±13.22	100±8.06
	V2	100±6.35	100±6.38	100±7.41	100±11.49	100±4.78	100±4.41	100±6.93	100±8.86
	V3	100±4.47	100±6.18	100±4.36	100±10.83	100±8.55	100±9.78	100±8.04	100±11.81
	V4	100±3.66	100±4.4	100±4.54	100±10.66	100±7.81	100±10.88	100±8.97	100±13.34
	V5	100±2.39	100±3.83	100±3.05	100±10.6	100±6.56	100±11.09	100±8.44	100±13.45
	V6	100±1.48	100±2.98	100±2.65	100±10.27	100±4.9	100±10.17	100±7.66	100±13.07
C_AVF	I	100±6.92	100±4.31	100±8.85	100±3.06	100±5.75	100±6.41	100±11.82	100±6.16
	II	100±7.14	100±5.25	100±3.4	100±2.52	100±9.3	100±9.46	100±8.34	100±9.02
	III	100±21.89	100±19.46	100±6.44	100±5.47	100±16.84	100±18.14	100±10.38	100±9.98
	AVL	100±8.94	100±13.31	91.67±14.8	100±0.8	100±3.97	100±11.74	100±11.93	100±2.35
	AVF	100±8.53	100±8.93	100±7.66	100±6.79	100±10.37	100±10.07	100±9.87	100±10.07
	V1	100±6.08	100±5.6	100±10.6	100±1.29	100±2.64	100±2.44	100±8.35	100±2.14
	V2	100±8.4	100±7.87	100±9.9	100±4.54	100±4.43	100±5.1	100±9.89	100±4.6
	V3	100±8.44	100±7.43	100±6.25	100±2.53	100±8.13	100±8.3	100±8.98	100±7.01
	V4	100±6.44	100±6.42	100±4.9	100±2.63	100±8.98	100±8.61	100±8.34	100±7.85
	V5	100±5.93	100±5.06	100±6.0	100±2.18	100±8.62	100±9.48	100±11.06	100±8.86
	V6	100±6.51	100±5.57	100±6.27	100±1.94	100±7.88	100±8.23	100±11.06	100±7.28

Table 25: ECG (thoracic) lead-reconstruction: percentage of detected R peaks in all the reconstructed leads.

Lead	%‐R (Sot‐) ↑				%‐R (Sot+) ↑			
	ECGrecover	EKGAN [12]	Pix2Pix [10]	CopyPaste	ECGrecover	EKGAN [12]	Pix2Pix [10]	CopyPaste
CV ₁	I 100±7.81	100±9.52	100±8.36	100±9.62	100±13.1	100±14.85	100±14.52	100±14.3
	II 100±2.95	100±2.78	100±2.85	100±5.12	100±11.06	100±10.55	100±9.93	100±10.11
	III 100±10.36	100±5.25	100±7.63	100±6.74	100±13.57	100±12.25	100±10.64	100±9.76
	AVL 100±4.66	100±5.72	85.71±15.67	100±4.34	100±8.0	100±7.41	87.5±13.96	100±2.81
	AVR 100±12.57	100±15.68	100±14.26	100±14.62	100±16.71	100±18.66	100±16.34	100±16.47
	AVF 100±6.73	100±6.24	100±6.4	100±5.87	100±11.16	100±13.25	100±12.7	100±10.51
	V2 100±6.18	100±7.24	100±7.36	100±6.68	100±6.88	100±6.71	100±8.68	100±5.03
	V3 100±4.76	100±5.7	100±4.71	100±6.3	100±11.43	100±9.91	100±10.0	100±9.02
	V4 100±4.58	100±4.76	100±4.36	100±6.2	100±12.13	100±11.55	100±11.95	100±11.28
	V5 100±4.0	100±4.39	100±4.09	100±5.72	100±12.06	100±11.73	100±11.49	100±11.47
CV ₂	V6 100±2.68	100±3.16	100±2.94	100±5.2	100±11.56	100±11.64	100±10.83	100±10.72
	I 100±3.46	100±7.96	100±8.51	100±7.69	100±11.26	100±14.11	100±14.22	100±14.03
	II 100±2.61	100±2.8	100±2.36	100±2.33	100±9.87	100±9.75	100±9.35	100±9.54
	III 100±7.74	100±5.37	100±4.96	100±4.86	100±11.72	100±9.91	100±9.76	100±9.88
	AVL 100±4.63	100±12.87	90.0±12.96	100±0.0	100±3.2	100±9.67	90.0±12.84	100±1.33
	AVR 100±8.04	100±15.3	100±14.86	100±12.51	100±14.71	100±17.14	100±17.29	100±16.76
	AVF 100±6.05	100±6.68	100±5.68	100±6.35	100±10.34	100±9.92	100±10.07	100±10.2
	V1 100±1.38	100±1.72	100±9.53	100±1.28	100±1.61	100±1.14	100±9.44	100±0.87
	V3 100±3.57	100±4.81	100±4.77	100±3.28	100±7.07	100±8.8	100±8.74	100±8.04
	V4 100±3.8	100±4.2	100±3.71	100±3.66	100±9.72	100±11.13	100±10.55	100±10.57
CV ₃	V5 100±2.48	100±3.79	100±7.83	100±3.55	100±9.85	100±11.02	100±11.04	100±11.03
	V6 100±2.43	100±2.7	100±5.43	100±2.56	100±9.94	100±10.14	100±10.6	100±10.52
	I 100±4.95	100±5.57	100±8.55	100±5.36	100±9.8	100±12.64	100±13.64	100±12.1
	II 100±2.49	100±2.8	100±2.21	100±2.35	100±9.8	100±9.92	100±7.84	100±9.01
	III 100±13.09	100±12.73	100±5.37	100±4.94	100±13.06	100±12.79	100±9.52	100±9.53
	AVL 100±5.16	100±12.53	100±12.58	100±0.58	100±3.49	100±9.33	100±10.91	100±1.17
	AVR 100±8.26	100±11.52	100±16.25	100±7.84	100±13.48	100±15.65	100±17.56	100±13.92
	AVF 100±6.43	100±6.38	100±5.2	100±6.05	100±10.44	100±9.25	100±9.39	100±10.13
	V1 100±1.44	100±1.65	100±9.01	100±1.37	100±1.01	100±1.01	100±7.17	100±0.58
	V2 100±6.01	100±6.42	100±8.72	100±4.25	100±4.5	100±4.5	100±6.14	100±3.17
CV ₄	V4 100±3.82	100±4.07	100±2.3	100±2.84	100±8.57	100±10.21	100±8.14	100±7.4
	V5 100±2.52	100±3.89	100±5.89	100±2.82	100±8.94	100±10.87	100±9.78	100±9.19
	V6 100±2.34	100±2.53	100±4.14	100±2.13	100±8.95	100±10.21	100±10.42	100±9.14
	I 100±5.24	100±5.8	100±8.08	100±5.77	100±8.14	100±10.97	100±12.64	100±10.88
	II 100±2.85	100±2.59	100±1.66	100±2.01	100±9.05	100±9.83	100±7.75	100±8.03
	III 100±9.32	100±11.36	100±5.4	100±5.35	100±13.97	100±12.78	100±9.61	100±9.53
	AVL 100±3.3	100±6.72	100±9.26	100±0.0	100±3.14	100±6.71	100±9.82	100±0.0
	AVR 100±6.45	100±7.9	100±15.23	100±6.83	100±13.97	100±13.28	100±18.7	100±12.84
	AVF 100±6.7	100±6.36	100±1.69	100±6.37	100±10.61	100±9.81	100±7.59	100±9.75
	V1 100±1.28	100±1.28	100±4.3	100±1.28	100±3.1	100±0.82	100±4.14	100±0.58
CV ₅	V2 100±6.24	100±6.26	100±6.62	100±5.33	100±5.31	100±4.46	100±4.64	100±3.17
	V3 100±3.89	100±4.54	100±3.92	100±2.35	100±7.89	100±7.87	100±7.19	100±4.0
	V5 100±2.64	100±3.46	100±3.64	100±0.64	100±6.45	100±10.07	100±10.45	100±5.46
	V6 100±2.16	100±2.61	100±3.25	100±1.04	100±7.28	100±9.23	100±10.66	100±5.89
	I 100±5.11	100±5.98	100±7.74	100±5.74	100±9.83	100±10.64	100±12.77	100±10.39
	II 100±2.73	100±2.71	100±1.58	100±1.92	100±10.08	100±9.44	100±7.34	100±6.88
	III 100±7.41	100±9.06	100±5.16	100±5.08	100±12.66	100±14.1	100±9.09	100±8.58
	AVL 100±4.51	100±5.82	100±10.34	100±0.0	100±4.26	100±7.36	100±11.71	100±0.58
	AVR 100±7.48	100±7.5	100±15.84	100±7.23	100±12.96	100±13.44	100±17.8	100±12.83
	AVF 100±6.7	100±6.36	100±0.41	100±4.88	100±10.4	100±10.69	100±5.85	100±7.14
CV ₆	V1 100±1.41	100±1.28	100±2.72	100±0.64	100±3.6	100±3.03	100±5.16	100±0.58
	V2 100±6.23	100±6.26	100±6.35	100±5.52	100±6.89	100±6.02	100±4.67	100±3.04
	V3 100±3.57	100±4.83	100±3.94	100±3.92	100±8.29	100±8.71	100±8.41	100±6.04
	V4 100±3.82	100±4.17	100±2.18	100±2.2	100±8.88	100±9.27	100±6.82	100±4.56
	V6 100±1.76	100±2.37	100±2.91	100±0.96	100±7.57	100±8.72	100±10.49	100±4.18
	I 100±4.96	100±6.83	100±7.57	100±6.4	100±6.63	100±10.84	100±13.68	100±10.85
	II 100±2.66	100±2.66	100±1.9	100±1.55	100±8.31	100±9.64	100±7.99	100±6.86
	III 100±8.9	100±10.86	100±5.16	100±5.37	100±12.02	100±13.19	100±9.19	100±8.59
	AVL 100±2.89	100±5.73	100±10.79	100±0.0	100±3.37	100±7.05	90.91±12.61	100±0.65
	AVR 100±6.16	100±9.84	100±15.8	100±11.13	100±11.57	100±13.42	100±17.76	100±13.47
CV ₇	AVF 100±6.03	100±6.71	100±0.41	100±5.37	100±9.93	100±10.41	100±5.19	100±6.29
	V1 100±1.28	100±1.28	100±2.78	100±0.64	100±0.96	100±1.01	100±1.33	100±0.58
	V2 100±6.23	100±6.26	100±6.35	100±5.64	100±4.55	100±4.49	100±4.46	100±3.91
	V3 100±4.78	100±4.83	100±4.3	100±4.34	100±7.9	100±8.63	100±8.47	100±7.75
	V4 100±3.87	100±4.01	100±2.65	100±2.87	100±8.19	100±9.69	100±7.39	100±7.31
	V5 100±3.23	100±3.89	100±3.97	100±1.74	100±6.56	100±9.62	100±11.16	100±6.04